



**Ana Catarina Costa  
Fernandes**

**Desenvolvimento de Hidrogéis Granulares Foto-  
reticuláveis para Aplicações Biomédicas**

**Development of a Photocrosslinkable Granular  
Hydrogel for Biomedical Applications**





Universidade de Aveiro

Ano 2021

**Ana Catarina  
Costa Fernandes**

**Desenvolvimento de Hidrogéis Granulares Foto-  
reticuláveis para Aplicações Biomédicas**

**Development of a Photocrosslinkable Granular Hydrogel  
for Biomedical Applications**

Dissertação apresentada à Universidade de Aveiro para cumprimento dos requisitos necessários à obtenção do grau de Mestre em Bioquímica Alimentar realizada sob a orientação científica do Doutor Vítor Gaspar, Professor Doutor João Mano do Departamento de Química da Universidade de Aveiro



## **o júri**

### **presidente**

Prof. Doutora Rita Maria Pinho Ferreira  
Professora auxiliar da Universidade de Aveiro

### **Arguente principal**

Doutora Iola Melissa Fernandes Duarte  
Investigadora Principal da Universidade de Aveiro

### **Orientador**

Doutor Vítor Manuel Abreu Gaspar  
Investigador doutorado (nível 1) da Universidade de Aveiro



## **Acknowledgments**

Firstly, I would like to acknowledge Professor João Mano for the amazing opportunity to work in between an exceptional group of researchers, in a field that was completely new for me, and in such an interesting topic. And of course, to supervisor Dr. Vítor Gaspar, for all the guidance and support all the time. Then, I want to express my gratitude to all the COMPASS team for welcoming me so well into the group and for always offer me help when I needed it. I cannot forget, to Pedro, Luís, Maria, and Rui for always help in the different tasks during this journey.

I also want to acknowledge, all the master thesis students of our group, Inês, Elisa, Raquel, Diogo, Maria, Francisca, Ana, Ezgi, We did it, guys! It was impossible without you. A special thanks to Inês and Elisa, for the patience, and for didn't let me give up when I wanted, and for being there in the worst moments. Thanks to my roomies for all the good disposition and great memories created. I cannot forget my friends, specially Inês Silva, Filipa, and Lia to always have time for me, and give the best advice, and for most of all being an inspiration as human beings, and of course for don't let me ever give up.

Lastly, I want to mention my family that supported all this journey, especially to my parents and sister for always pretending that listened to me and understand what I was saying. Lastly my dogs always for finding somehow energy in me.

**palavras-chave**

**Micropartículas; gelatina; micropartículas interligadas, Vascularização, VEGF, Hidrogel granular.**

**resumo**

Em engenharia de tecidos e medicina regenerativa (TERM) os hidrogéis têm sido desenvolvidos como plataformas para encapsulamento e entrega de células, como tentativa de regenerar e reparar os tecidos lesionados. No entanto, apesar das diversas vantagens, as taxas de difusão de nutrientes e metabólitos celulares irrealistas, ainda se mantêm como principais limitações nestas plataformas. Hidrogéis granulares compostos pela agregação de micropartículas de hidrogel (HMPs) são propostos como solução para colmatar estas falhas. As HMPs podem ser covalentemente ligadas usando mecanismos químicos avançados formando uma plataforma porosa. Os avanços mais recentes mostram potencial para infiltração celular, e regeneração de tecidos quando comparados com hidrogéis. Nesta tese, o bio-polímero de gelatina foi modificado com grupos semelhantes hidroxifenil para a agregação das plataformas MAP, via reticulação foto- ou enzimática. Inicialmente as partículas esféricas de tamanho micro (diâmetro 76  $\mu\text{m}$ ) foram produzidas por uma emulsão sem óleos. As partículas foram ligadas por diferentes tipos de químicas o que não influenciou a rigidez do MAP. O MAP de gelatina apresentou uma elevada biocompatibilidade e habilidade para promover a adesão e proliferação de células-tronco e células precursoras de células vasculares. Adicionalmente, os resultados também mostraram a capacidade de impressão com a manutenção da integridade celular. Assim, os MAP de adesão desenvolvidos apresentaram diversas vantagens para utilização no contexto de terapias celulares para engenharia de tecidos de osso ou vascular.



**keywords**

**Gelatin, Microparticles, Photocrosslinking, Granular hydrogel  
Microporous annealed particles, Stem Cells**

**Abstract**

In the tissue engineering and regenerative medicine (TERM) field, hydrogels have been exploited for a long time as scaffolds for cells encapsulation and delivery in an attempt to functionally repair or regenerate damaged tissues. However, despite presenting several advantages the unrealistic diffusion rates of cells, nutrients and metabolites still remain key limitations found in these widespread platforms. Granular hydrogels comprised by the guided aggregation of hydrogel microparticles (HMPs) are proposed as a solution to bridge these flaws. The particles can be covalently annealed together generally using advanced chemical tools forming a microporous scaffold (MAP).

The most recent advances in MAPs indicate their potential for improving cell infiltration and tissue regeneration, when compared to regular hydrogels.

In this thesis, gelatin biopolymers were modified with pendant hydroxyphenyl-like chemical moieties for assembling MAP scaffolds via photo- or enzyme crosslinkable. Initially spherical, micro-sized gelatin microgels (ca. 76  $\mu\text{m}$ ) were produced via oil-free emulsion. Microparticles were then annealed and it was demonstrated that the different types of annealing chemistries (Photo- or enzymatic) did not significantly influenced the stiffness of the scaffold. The gelatin-based MAP presented high biocompatibility and the ability to promote stem cells and vascular precursor cells adhesion and proliferation. Additionally, the results also showed the printable features of the developed granular hydrogels with the maintenance of cell integrity.

Overall, the developed cell adhesive MAP scaffold presents several advantages for being used in the context of cell therapies and bone or vascular tissue engineering applications.



# Contents

<b>Contents .....</b>	<b><i>i</i></b>
<b>List of Figures.....</b>	<b><i>iv</i></b>
<b>List of Tables.....</b>	<b><i>ix</i></b>
<b>List of Abbreviations and Acronyms.....</b>	<b><i>x</i></b>
<b>List of Publications .....</b>	<b><i>xii</i></b>
<b>1. Introduction.....</b>	<b><i>1</i></b>
1.1. Introduction .....	<b><i>2</i></b>
1.2. Angiogenesis and Vasculogenesis.....	<b><i>3</i></b>
1.3. Tissue Engineering Strategies for Functional Repair .....	<b><i>4</i></b>
1.4. References .....	<b><i>6</i></b>
<b>2. Advanced Chemical Tools for Interlinking Granular Hydrogels .....</b>	<b><i>11</i></b>
2.1. Introduction .....	<b><i>14</i></b>
2.2. Granular hydrogels metastable behavior.....	<b><i>16</i></b>
2.3. Annealing of granular hydrogels.....	<b><i>18</i></b>
2.3.1. Non-covalent bonds.....	<b><i>19</i></b>
2.3.2. Covalent bonds .....	<b><i>20</i></b>
2.4. Functional characteristics of granular systems.....	<b><i>23</i></b>
2.5. Hydrogel microparticles production .....	<b><i>29</i></b>
2.6. MAPs Tissue Engineering Applications.....	<b><i>33</i></b>
2.6.1. Bone .....	<b><i>33</i></b>
2.6.2. Cartilage .....	<b><i>35</i></b>
2.6.3. Nervous system.....	<b><i>37</i></b>
2.6.4. Wound healing and vascularization.....	<b><i>38</i></b>
2.6.5. Other applications.....	<b><i>40</i></b>
2.7. Granular hydrogel in 3D bioprinting .....	<b><i>41</i></b>
2.8. Conclusions and further perspectives .....	<b><i>43</i></b>

2.9.	References .....	45
<b>3.</b>	<b><i>Aims</i></b> .....	<b>53</b>
<b>4.</b>	<b><i>Materials and Methods</i></b> .....	<b>54</b>
4.1.	Materials.....	54
4.2.	Methods .....	54
4.2.1.	Biomaterials chemical functionalization.....	54
4.2.2.	HMPs formation.....	56
4.2.3.	Microparticles annealing .....	58
4.2.4.	Bulk hydrogel crosslinking .....	59
4.2.5.	Characterization of the granular hydrogels.....	59
4.2.6.	Encapsulation efficiency and release.....	59
4.2.7.	Mechanical Characterization .....	60
4.2.8.	Cell culture .....	60
4.2.9.	Cell Viability.....	61
4.2.10.	3D bioprinting .....	62
4.2.11.	Statistical Analysis.....	62
4.3.	References .....	62
<b>5.</b>	<b><i>Results and Discussion</i></b> .....	<b>64</b>
5.1.	Introduction .....	67
5.2.	Materials and Methods.....	69
5.2.1.	Materials .....	69
5.2.2.	Methods.....	69
5.2.2.1.	Gelatin-hydroxyphenylpropionic acid synthesis .....	69
5.2.2.2.	Oxidized laminarin synthesis.....	70
5.2.2.3.	Hydrogel microparticles production .....	71
5.2.2.4.	HMPs annealing.....	71
5.2.2.5.	Gelatin HPA bulk hydrogel formation .....	72
5.2.2.6.	Characterization of the granular hydrogels .....	72
5.2.2.7.	Mechanical assays .....	73
5.2.2.8.	Encapsulation efficiency and release .....	73

5.2.2.9.	3D bioprinting assays .....	74
5.2.2.10.	Cell culture.....	74
5.2.2.11.	Cell Viability and morphology .....	75
5.2.2.12.	Statistical Analysis .....	75
<b>5.3.</b>	<b>Results and discussion .....</b>	<b>76</b>
5.3.1.	Gelatin-HPA synthesizes and characterization .....	76
5.3.2.	Gelatin HMPs size and distribution.....	79
5.3.3.	Release profile .....	84
5.3.4.	MAPs biological performance - Cell Compatibility and Support .....	85
5.3.5.	3D bioprinting .....	90
<b>5.4.</b>	<b>Conclusions .....</b>	<b>91</b>
<b>5.5.</b>	<b>References .....</b>	<b>91</b>
<b>5.6.</b>	<b>Supplementary information .....</b>	<b>94</b>
<b>6.</b>	<b><i>Conclusion and future perspectives.....</i></b>	<b>98</b>

# List of Figures

## Introduction

Figure 1 Schematic representation of tissue engineering foundations, the cells the materials and tissue architectures, that can be designed in combination or separately. Adapted from [6].. ..... 3

## Advanced Chemical Tools for Interlinking Granular Hydrogels

Figure 1 Categories of HMPs. HMPs can be included in different states, in a free-floating solution or even in an aerosol, in a jammed state or as a composite..... 15

Figure 2 Granular hydrogel as a bottom-up approach by choosing the polymer, and the mesh, that will influence the hydrogel microparticles. The size, of hydrogel microparticles their porosity o the bioactive factors encapsulated will affect the final structure. Finally, the interactions enable to create a larger structure, with different forms, and with innumerous particles combinations possible. .... 16

Figure 3 Influence of the packing ratio on HMPs state and interstitial fluid..... 17

Figure 4 Chemical toolbox for interlinking HMPs and ultimately assemble MAPs scaffolds. Metal complexation (e.g., iron, vanadium, aluminum, silver nanoparticles, etc) with gallol/catechol groups. Covalent bonds with photo-mediated, click-chemistry, via methacrylic groups reaction, for example. Host-Guest chemistry, via cyclodextrin interaction with norbornene, etc. Enzymatic-mediated annealing, where the Factor FXIIIa links the protein G and K..... 18

Figure 5 Multifunctionalities of Granular Hydrogels, and their properties such as their ability to high heterogeneity by combining different types of HMPs or different sizes. HMPs high injectability. The HMPs are interlinked but between them, they have porosity. .... 23

Figure 6 a) Cell spreading according to HMPs size I) HMPs with large dimensions, II) medium dimensions and smaller dimensions, III) with the higher forms of clusters on HMPs with larger dimensions. [33] b) void space area, and fraction formed with larger and small HMPs. Reproduced with permission [62] Copyright 2017, Wiley. .... 29

Figure 7 Hierarchically HMPs (MANF) formation and bone volume and bone regeneration after 8 weeks, comparatively to a non-porous hydrogel. Reproduced with permission [64] Copyright 2019, Elsevier..... 35

Figure 8 Effects of HMPs or MAP in regeneration and in promoting angiogenesis a) Representative photographs of the difference between HMPs and only cells and blood monitorization perfusion in ischemic hindlimb with fluorescence imaging. Reproduced with permission [64] Copyright 2014, PNAS. b) Schematic of patterning method pipetting a granular hydrogel on wound and the intensity profile plot of each color microgel along the cross-section was generated. Reproduced with permission [64] Copyright 2018, Wiley. c) MAP for wound closures, with cells distributed along the HMPs, comparing with a non-porous scaffold; wound closure in relation to a non-porous hydrogel and Keratin-5 staining of the basement epithelial layer outline developing hair follicles and sebaceous glands within the MAP scaffold after five days. Reproduced with permission [38] Copyright 2015, Nature. .... 40

Figure 9 Examples of HMPs on 3 D bioprinting. a) Scheme of printing a with the contraction of several layers and with precision to print a nose or an ear. Reproduced with permission [13] Copyright 2019, Royal Society of Chemistry. b) Filament of a granular ink an applications, as well as, their biocompatibility and different sizes of deposits Reproduced with permission [106] Copyright 2019, Wiley. c) Granular hydrogels as a supporting bath, with gelatin HMPs, and oxidized alginate for the cross-links. With a high ability to create complex structures, with cell biocompatibility, and structures anatomic like the bone Reproduced with permission [143] Copyright 2020, ASC. .... 44

**Materials and methods**

Figure 1 Schematic representation of the HMPs production by emulsion. .... 57

Figure 2 Schematic representation of the HMPs photo-annealing, A) in a molecular and in B) a macroscopic, overview. .... 58

**Results and discussion**

Figure 1 <sup>1</sup>H-NMR spectra of gelatin and gelatin-HPA with different degrees of substitution, low(blue) and high (red), and the peak corresponded to each hydrogen on the aromatic ring. .... 76

Figure 2 UV-visible absorption spectrum of gelatin(turquoise) and gelatin-HPA low(red) and high(blue) modified. Positive control of HPA (yellow) and negative control (purple). .... 77

Figure 3 ATR-FTIR spectra of gelatin (black) and different modifications of freeze dried gelatin-HPA (low in blue, and high in red), and the HPA (purple), at 25°C. .... 78

Figure 4 Oxidized-laminarin(oxLAM) characterization. <sup>1</sup>H-NMR spectra of native laminarin and modified laminarin, with a decrease in the peaks assigned in the green box. Spectra was acquired in deuterated water at 25°C. In the yellow sextion is evidenced the formation of hemiacetal groups. In the green section the reduction of the β-(1-6) branches. .... 79

Figure 5 HMPs diameter distribution according to different stirring speeds,A) Gelatin-HPA B) HMPs sample of the formulation at 600rpm; C) SEM image of the HMPs, D) histogram of the HMPs diameter distribution. .... 80

Figure 6 A )Low gelatin MAP scaffold annealed by UV light B) enzymatic annealed MAP scaffold; C) MAP stability in the medium and PBS. D; E; F) images acquired SEM MAP with the magnification of D) 40 times; E) 100 times F) and 500 times. G) graphic representation of the swelling ability, through 7 days; H) graphic representation of water content through 7 days..... 81

Figure 7 A)Water content of low oxLAM granular hydrogels over 7 days. B) Young's modulus of the granular hydrogels produced, without statistical significance difference C) Self-healing ability of the high granular hydrogel. D) Injectability of the granular hydrogel, and E) the filament created..... 82

Figure 8 A)Young's Modulus determined under compressive assays, of a Gelatin-HPA, end MAP scaffolds. Error bars represent standard deviation; \*\*\*\*p ≤ 0.0001. B)Scaffolds before and after the compression. C) Granular hydrogel injection; D) formation of a continuous filament of the granular hydrogel; E) continuous filament in microscopic analysis..... 83

Figure 9 MAP analysis of the area occupied by the HMPs A) surface reconstruction of a MAP; B) confocal image of a MAP. .... 84

Figure 10 Encapsulation in the HMPs a) HMPs with BSA-FITC, with the FITC groups encapsulated with fluorescence in green. .... 85

Figure 11 Live- dead assay, where alive cells are stained with green calcein, while dead cells are stained with red PI. Image hAS and HUVECs monocultures and a co-culture of both cell types. DAPI-phalloidin 3D images staining cells, the F-actin is stained in red by the phalloidin, and the nucleus with DAPI( in blue). .... 85

Figure 12 Live- dead staining, with hASC, where live cells are stained with calcein – green channel, while dead cells are with PI – red channel. A - C) Bulk hydrogels; D - F) MAPs scaffold, at day 1, 3 and 7. DAPI-phalloidin 3D confocal laser scanning reconstruction of stained cells of: (G - I) Bulk and (J – L) MAPs scaffolds. F-actin- red



channel, DAPI cell nucleus – Blue channel, at days 1, 3 and 7. M) cell viability assay through the 7 days with bulk hydrogel in green and MAP in blue. scale bar: 200µm. Data is presented as mean ± s.d., n=3, \*p<0.05. .... 87

Figure 13 Live- dead staining, with HUVECs, where live cells are stained with calcein-green channel, while dead cells are stained with PI- red channel. A-C) Bulk hydrogel, D-F) Gelatin-HPA MAPs scaffolds. DAPI-phalloidin 3D confocal laser scanning microscopy reconstruction of G) Bulk hydrogel and H) MAP, at day 1. F-actin- red channel, DAPI nuclear staining- blue channel. scale bar: 200 µm. I) AlamarBlue<sup>®</sup> Cell viability assay with bulk hydrogel in green and MAP in blue, at the course of seven days (Data is represented as mean ± s.d., n=3, \*p<0.05. .... 88

Figure 14 Live- dead staining, with co-culture, where live cells are stained with Calcein – green channel, while dead cells are stained with PI – red channel. A - C) Bulk hydrogels, D-F ) MAPs scaffolds, at days 1, 3 and 7. G-L) DAPI-phalloidin 3D confocal laser scanning reconstructed micrographs. .... 89

Figure 15 Live- dead staining, with hASC, where alive cells are stained with green calcein, while dead cells are stained with red PI. C) live dead after the printing, D) live dead on day one. where alive cells are stained with green calcein, while dead cells are stained with red. The scale bar corresponds to 200µm. .... 90

**Supplementary information**

S 1 TNBS assay. Calibration curve (blue dots), the low modified gelatin (grey dots), high modified gelatin (yellow dots) were compared to gelatin (orange dots). .... 94

S 2 HMPs distribution through the different stirrings speed, and respective histograms of HMPs diameters distribution. .... 96

S 3 Distribution of the hydrogels microparticles through different concentrations and speeds. All the groups were statistically different with p<0.0001 with exception from the ones presented with, ns non statistically different and \*\* p<0.01. Data is presented as at least 200particles. .... 96

S 4 ELISA-based quantification of VEGF release along time. Data is presented as mean ± s.d., n=2. .... 97

S 5 Live- dead staining, with a low cell density of HUVECs, where live cells are stained with calcein -channel, while dead cells are stained with PI – red channel. A-B) Bulk hydrogel and C-D) Gelatin-HPA Maps scaffolds at day 1 and 3. Scale bar : 200µm. E)

AlamarBlue®-based cell viability with bulk hydrogel and MAPs scaffolds, at day 7. Data is presented as mean  $\pm$  s.d., n=3, \*\*\*\*p<0.0001..... 97

## **List of Tables**

### **Introduction**

Table 1 Annealing process already developed and with the respective polymers and application .....	24
. Table 2 Different methodologies for HMPs production, advantages, and disadvantages of each method .....	31

### **Results and discussion**

Table 1 Different degrees of substitution of Gelatin-HPA post-synthesis. ....	77
-------------------------------------------------------------------------------	----

## List of Abbreviations and Acronyms

3D	Three dimensions
ASC	Adipose-derived mesenchymal stem cell
ATB	Antibiotic-antimycotic
BDNF	Brain-derived neurotrophic factor
BMP-2	Bone morphogenic protein 2
BSA-FITC	Albumin-fluorescein isothiocyanate conjugate
CNS	Central neuronal system
CRISP	Cysteine rich secretory protein
DAPI	4',6-diamidino-2-phenylindole, dihydrochloride
DBCO	Azide-dibenzocyclootyne
DMF	Dimethylformamide
DNA	Deoxiribonucleic acid
ECGS	Endothelial Cell Growth Supplement
ECM	Extra cellular matrix
EDC	1-ethyl- 3- (3- dimethylaminopropyl)- carbo-diimide hydrochloride
ELISA	Enzyme-Linked Immunosorbent Assay
FBS	Fetal bovine serum
FDA	Food and Drug Administration
FGF	Fibroblast growth factors
GAG	Glucosamine glycans
GelMA	Methacrylate gelatin
Gelatin-HPA	Hydroxyphenylpropionic gelatin
GF	Growth factors
HIF	Hypoxia-inducible factors
HMPs	Hydrogel microparticles
hMSC	human mesenchymal stem cells
HPA	Hydroxyphenylpropionic acid
HUVECS	Human umbilical vein endothelial cell
IL	Interleukin
MAP	Microporous annealed particles
miRNA	micro-RNA

MSC	Mesenchymal stem cells
NHS	N-Hydroxysuccinimide
OEC	Outgrowth endothelial cells
PBS	phosphate saline buffer
PCL	poly $\epsilon$ -caprolactone)
PDGF	Platelet-derived growth factor
PEG	Poly(ethylene glycol)
PEGDA	Poly(ethylene glycol) diacrylate
PEG-tet	Poly(ethylene glycol) with tetrazine
PLGA	Poly(lactic-co-glycolic acid
PNIPAm	Poly(N-isopropylacrylamide)
RGD	Tripeptide Arg-Gly-Asp
RT	Room temperature
TE	Tissue Engineering
TERM	Tissue engineering and regenerative medicine
TGF- $\beta$	Transforming growth factor $\beta$
TNBS	2,4,6-trinitrobenzene-sulfonic acid
UV	Ultra-violet radiation
VEGF	Vascular endothelial growth factor

## List of Publications

Review article entitled “**Chemical Engineering tools to Assemble Granular Hydrogels**” (Manuscript in preparation) -----11

Practical Article “**Injectable Microporous annealed particles (MAP) for cells supporting proliferation**” Manuscript in preparation-----64

**1. Introduction**

## 1.1. Introduction

Tissue engineering (TE) aims to regenerate and repair damaged tissues by applying engineering and life science methodologies, constructing artificial scaffolds that mimic the native tissues. [1] One of the purposes of tissue engineering and regenerative medicine (TERM) is to ideally fabricate a degradable construct able to recruit patients own cells to regenerate tissues or in the other end develop advanced scaffolds for promoting cell encapsulation and delivery to injured sites. [2] This first approach is highly advantageous as it will highly reduce the possible immunologic rejection from the host for instance in comparison to when cells from other donors are administered, thus facilitating the regeneration of damaged tissues. [3] TERM tools also offer the opportunity to develop advanced 3D in vitro models that are tissue mimetics and that allow pre-clinical screening of candidate therapeutics before their translation to clinical trials. [4] In essence, the foundations of TE comprises the use of key components including: (i) tissue precursor cells (e.g., embryonic, induced pluripotent or adult stem cells), and (ii) supporting scaffolds offering mechanical support for cells protection/delivery and initial proliferation upon implantation in the injury site. This strategy also benefits from the inclusion of bioactive and

bioinstructive molecules such as bioactive factors (e.g., cytokines, growth factors) to guide cells differentiation (Figure 1) [5,6]. Biomaterials have a crucial role in TE by offering a substrate for cell adhesion, proliferation and for providing important biophysical/biomechanical cues. [7] By definition, biomaterials are any material that interacts with a biological system for medical reasons, diagnosis, or clinical treatment. Ideally, these materials should be biocompatible, and ideally cost-effective, with easy manipulation. [1,7] Frequently, biomaterials are developed as an attempt to replicate the extracellular matrix, native tissues ECM features, with the objective of increasing cell differentiation and of bioinstructing/inducing specific cellular responses/phenotypes, leading to tissue formation, and at the same time, offer enough mechanical support. [4,8] However, most products in the market have low tissue integration or cell recruiting properties, generally eliciting the activation of the host immune system that culminates with the formation of a fibrous capsule around the implanted biomaterial. To increase biocompatibility and regeneration it is essential to establish natural-like interactions between the implanted scaffolds and patient tissues, as well as to assure that nutrients/oxygen and metabolites are exchanged when cell-laden biomaterials are inserted, so as to secure cells survival and increase the potential for functional tissue repair. For this purpose, ensuring the activation of endogenous angiogenesis processes and the formation of functional/perfusible vascular networks is critical for the repair process to be accelerated and to take place successfully. [3]



In tissues, nutrients and oxygen only can diffuse for 100  $\mu\text{m}$  to 200  $\mu\text{m}$  depending on tissue characteristics and metabolism, consequently, the formation of a functional/perfusible vasculature is essential to assure homeostasis. [9–11]

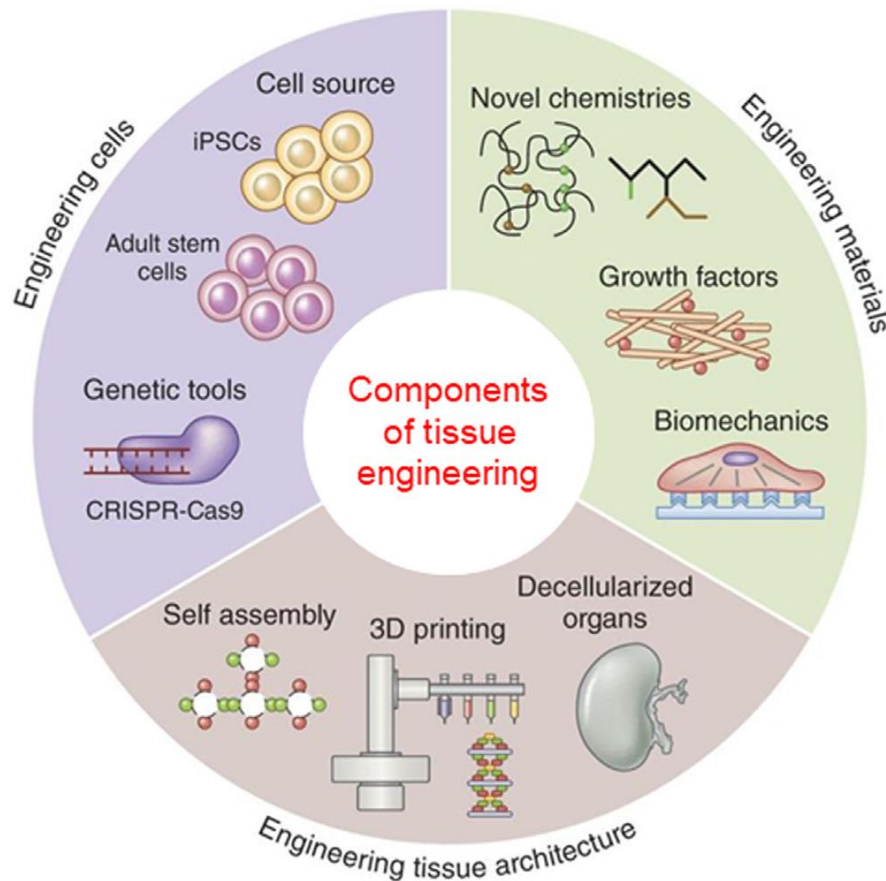


**Figure 1** Schematic representation of tissue engineering foundations, the cells the materials and tissue architectures, that can be designed in combination or separately. Adapted from.[6].

## 1.2. Angiogenesis and Vasculogenesis

In the human body, problems in assuring nutrients/metabolites/oxygen exchanges can arise from the onset of several diseases such as atherosclerosis or from trauma (e.g., critical injuries, bone fractures, aneurisms, etc). These pathologies generally create a deficit and damages to surrounding tissues with numerous medical strategies aiming to promote angiogenesis in those regions as quickly as possible. [12-15]

To understand the importance of vascular networks in the repair process it is initially necessary to comprehend and distinguish vasculogenesis and angiogenesis concepts. Vasculogenesis is characterized by the generation of the primordial blood vessels in the embryo [16–19], and it initiates with the formation of blood-like islands mainly caused by the presence of key growth factors such as fibroblast growth factor (FGF), as well as, vascular endothelial growth factor (VEGF). After the creation of the initial vessels, other blood vessels are recruited. The process of

new vessel formation by pre-existent ones is so-termed angiogenesis. [19,20] This process occurs during the lifetime of the individual owing to tissues necessity for oxygen and nutrients/metabolites exchange. In the literature two types of angiogenesis are generally described: (i) sprouting angiogenesis (discovered nearly 200 years ago - described below), and intussusceptive angiogenesis, [16,19,21] which involves the formation of blood vessels by splitting of the existent vessels. The sprouting angiogenesis can thus be divided into three main events:

1. The degradation of the basal membrane and the formation of a vascular sprout; [16,18,20,22] that promotes migration of endothelial cells; [16,18,20,22]
2. Maturation and development of the new blood vessels, and with this, the inhibition of growth factors that lead to vessel recruitment and nutrients; [16,18,20,22]
3. Initiation of the angiogenesis process by VEGF transforming growth factor  $\beta$  (TGF-  $\beta$ ) however, none of these factors alone can terminate the angiogenesis process. [23,24]

### 1.3. Tissue Engineering Strategies for Functional Repair

In TERM, hydrogels represent highly hydrated polymeric networks, that are frequently explored due to their cytocompatibility, general cell-adhesive properties and by the interesting viscoelastic features similar to those observed in native tissues ECM. [8,27] Up-to-date hydrogels have been widely used as platforms for cell encapsulation delivery and/or for the delivery of bioactive molecules (e.g., growth factors, cytokines). [28–30] Hydrogels, play a master role in cell-therapies once they offer enough stiffness for cell differentiation, cell adhesion, and are highly processable offering the possibility to generate anisotropic, spatially oriented scaffolds that further improve the regenerative potential of cell-based therapies. [4,25,26] Particularly, hydrogels comprising natural-origin biopolymers (e.g., gelatin, hyaluronan, collagen, alginate, chitosan), synthetic (e.g., PCL, PLGA, PVA) or hybrid materials have widely employed in TERM. Nonetheless, despite their recognized advantages, they still fail to reproduce natural tissues oxygen/nutrients/metabolites diffusion, especially in cell-laden hydrogel platforms with larger dimensions ( $> 500 \mu\text{m}$ ). [31] In fact, it is important to emphasize that the low diffusivity ability of most hydrogels limits cells bioavailability following encapsulation. Hence, ideally a hydrogel scaffold for TERM strategies that take advantage of native cells recruitment, and/or stem cells therapies encapsulation/delivery, should either present a high diffusion of nutrients/oxygen/metabolites to cells, or on the other hand, present suitable features for promoting angiogenesis through the bulk hydrogel volume. Yet, most the biomaterials strategies based for instance in bulk scaffolds (e.g., hydrogels, microgels, microfiber mats), fail in this step,

diminishing the potential of the scaffold to promote functional tissue repair. [12–14] These limitations create a necessity for blood vessels formation inside the hydrogel to assure cells viability and/or host cells recruitment in deep regions. [32]

Nowadays, in TERM, the induction of new vessels, i.e., neovascularization, by angiogenesis, into the scaffolds remains a challenge since cell infiltration is very slow. Hence to overcome this, various researchers are trying to develop scaffolds that improve vascularization. For that, different bioactive molecules, delivered by distinct platforms, had been shown to improve vessel recruitment. [40–43] Particularly, growth factors participating in angiogenesis are often encapsulated, one of the most widely used is VEGF, due to its important role in angiogenesis. [40,44] VEGF is able just for itself to trigger the angiogenesis mechanism. The angiogenesis process is a complex process with a large number of growth factors and cascades, but in some examples by simply delivering VEGF positive results are obtained. [11,45–47] It was shown in diabetic mouse models, that the delivery of a VEGF-loaded hydrogel increased not only the functional  $\beta$ -cells, but also the glucose tolerance by improving the insulin release. [48] The same occurred in other tissues, for example, bone, where the speed of vessel infiltration and vessel instability is crucial in regeneration. In neuronal tissues, the delivery of VEGF increased angiogenesis. [49] Adding to growth factors delivery, vascular endothelial cells collected from the umbilical cord are also often used in TERM.

Other interesting strategies for improving diffusion into hydrogel scaffolds involves the generation of pores in hydrogels structure by using different methodologies such as: (i) solvent/casting leaching,[33] (ii) freeze-drying,[34] (iii) gas forming agents,[35] (iv) 3D printing,[36] or (v) by the inclusion of leachable particles to facilitate cellular infiltration. However, most of these methodologies are not compatible with cells encapsulation and/or their degradation results in generation of cytotoxic by-products.

Gathering on this, researchers are focusing on the use of hydrogel microparticles (HMPs), and exploring them as standalone cell delivery systems, that assure cell viability after delivery, by protecting cells from the shear forces involved in injection, allowing a decrease in the number of cells required to be delivered for obtaining a therapeutic outcome. [37,50–53] HMPs have also been explored as standalone systems for the delivery of growth factors by not only increasing the life time of the growth factors, but also allowing their sustainable release in a suitable spatiotemporal window, as showed with VEGF. [40,54–57]

More importantly and interestingly, in recent years researchers became aware that jamming/compacting HMPs leads to the creation of weak interparticle interactions, these are so-called - *granular hydrogels* - and are mostly comprised by multi-particle entities. The concept of granular hydrogels is thus based on a bottom-up approach, where the HMPs are the unitary

building blocks that can be combined to generate higher order superstructures that combine together the unique features of their unit components, and also that benefit from the gain-of-function derived from their combination. These formulations present shear thinning properties, generally behaving as solid-like structures upon compaction, but under stress, their behavior resembles that of a liquid. [58–60]

Interestingly, granular hydrogels arise from weak particle-particle interactions promoted by packing/jamming, but researchers have gathered on these units and have devised methodologies to assemble them HMPs (e.g., covalent crosslinking, particle-particle adhesion, etc.), in such a way that the particles form stable and interconnected networks - microporous annealed particle (MAP) scaffolds.

MAP scaffolds represent microporous super-structures with unique diffusivity features when compared to standard hydrogels. In recent, years MAPs scaffolds assembled from covalent bonds between HMPs have particularly captivated the attention of researchers due to their unique microporous structure that enables a rapid cell infiltration and angiogenesis. [31,61,63,64] Such results led the scientific community to assume that MAPs are by themselves a proangiogenic scaffold. [31,64]. MAPs assembly strategies based on chemical tools, as well as their unique features and examples of their applications in TERM will be described in the following chapter.

### 1.4. References

1. Dhandayuthapani, B., Yoshida, Y., Maekawa, T., e Kumar, D.S. (2011) Polymeric Scaffolds in Tissue Engineering Application: A Review. *International Journal of Polymer Science*, 2011, 1–19.
2. Van Vlierberghe, S., Dubruel, P., e Schacht, E. (2011) Biopolymer-Based Hydrogels As Scaffolds for Tissue Engineering Applications: A Review. *Biomacromolecules*, 12 (5), 1387–1408.
3. Mariani, E., Lisignoli, G., Borzi, R.M., e Pulsatelli, L. (2019) Biomaterials: Foreign Bodies or Tuners for the Immune Response? *IJMS*, 20 (3), 636.
4. Shin, H., Jo, S., e Mikos, A.G. (2003) Biomimetic materials for tissue engineering. *Biomaterials*, 24 (24), 4353–4364.
5. Chandra, P.K., Soker, S., e Atala, A. (2020) Tissue engineering: current status and future perspectives, in *Principles of Tissue Engineering*, Elsevier, pp. 1–35.
6. Khademhosseini, A., e Langer, R. (2016) A decade of progress in tissue engineering. *Nat Protoc*, 11 (10), 1775–1781.
7. Williams, D.F. (2019) Specifications for Innovative, Enabling Biomaterials Based on the Principles of Biocompatibility Mechanisms. *Front Bioeng Biotechnol*, 7, 255.
8. Gaharwar, A.K., Singh, I., e Khademhosseini, A. (2020) Engineered biomaterials for in situ tissue regeneration. *Nat Rev Mater*.
9. Carmeliet, P., e Jain, R.K. (2000) Angiogenesis in cancer and other diseases. *Nature*, 407 (6801), 249–257.
10. Rouwkema, J., Koopman, B.F.J.M., Blitterswijk, C.A.V., Dhert, W.J.A., e Malda, J. (2009) Supply of Nutrients to Cells in Engineered Tissues. *Biotechnology and Genetic Engineering Reviews*, 26 (1), 163–178.
11. Quinlan, E., López-Noriega, A., Thompson, E.M., Hibbitts, A., Cryan, S.A., e O'Brien, F.J. (2017) Controlled release of vascular endothelial growth factor from spray-dried alginate microparticles in collagen-hydroxyapatite scaffolds for promoting vascularization and bone repair: Functionalized CHA scaffolds for controlled release of VEGF to enhance bone repair. *J Tissue Eng Regen Med*, 11 (4), 1097–1109.

12. Samourides, A., Browning, L., Hearnden, V., e Chen, B. (2020) The effect of porous structure on the cell proliferation, tissue ingrowth and angiogenic properties of poly(glycerol sebacate urethane) scaffolds. *Materials Science and Engineering: C*, 108, 110384.
13. Judawisastra, H., Nugraha, F.R., e Wibowo, U.A. (2020) Porous Architecture Evaluation of Silk Fibroin Scaffold from Direct Dissolution Salt Leaching Method. *Macromol. Symp.*, 391 (1), 1900187.
14. Torres, A.L., Bidarra, S.J., Vasconcelos, D.P., Barbosa, J.N., Silva, E.A., Nascimento, D.S., e Barrias, C.C. (2020) Microvascular engineering: Dynamic changes in microgel-entrapped vascular cells correlates with higher vasculogenic/angiogenic potential. *Biomaterials*, 228, 119554.
15. Moutinho, M., Simões, I., Rodrigues, S., Abreu, D., Silva, E., Sousa, P., e Fernandes, J.F. e (2019) Global Impact of Peripheral Obstructive Arterial Disease in Portugal: An Eight Year Study. *Acta Med Port*, 32 (5), 348.
16. Risau, W. (1997) Mechanisms of angiogenesis. *Nature*, 386 (6626), 671–674.
17. Risau, W. (1995) Differentiation of endothelium. *FASEB J*, 9 (10), 926–933.
18. Schmidt, A., Brixius, K., e Bloch, W. (2007) Endothelial Precursor Cell Migration During Vasculogenesis. *Circulation Research*, 101 (2), 125–136.
19. Th, A. Chapter 1 Overview of Angiogenesis, pp. 10.
20. Carmeliet, P. (2000) Mechanisms of angiogenesis and arteriogenesis. *Nat Med*, 6 (4), 389–395.
21. Burri, P.H., e Tarek, M.R. (1990) A novel mechanism of capillary growth in the rat pulmonary microcirculation. *Anat. Rec.*, 228 (1), 35–45.
22. Fuchs, S., Hofmann, A., e Kirkpatrick, C.J. (2007) Microvessel-Like Structures from Outgrowth Endothelial Cells from Human Peripheral Blood in 2-Dimensional and 3-Dimensional Co-Cultures with Osteoblastic Lineage Cells. *Tissue Engineering*, 13 (10), 2577–2588.
23. Lee, J.-H., Parthiban, P., Jin, G.-Z., Knowles, J.C., e Kim, H.-W. (2020) Materials roles for promoting angiogenesis in tissue regeneration. *Progress in Materials Science*, 100732.
24. Karamysheva, A.F. (2008) Mechanisms of angiogenesis. *Biochemistry Moscow*, 73 (7), 751–762.
25. Mano, J.F. (2015) Designing biomaterials for tissue engineering based on the deconstruction of the native cellular environment. *Materials Letters*, 141, 198–202.
26. Newsom, J.P., Payne, K.A., e Krebs, M.D. (2019) Microgels: Modular, tunable constructs for tissue regeneration. *Acta Biomaterialia*, 88, 32–41.
27. Raucci, M.G., D'Amora, U., Ronca, A., e Ambrosio, L. (2020) Injectable Functional Biomaterials for Minimally Invasive Surgery. *Adv. Healthcare Mater.*, 2000349.
28. Khojasteh, A., Fahimipour, F., Eslaminejad, M.B., Jafarian, M., Jahangir, S., Bastami, F., Tahriri, M., Karkhaneh, A., e Tayebi, L. (2016) Development of PLGA-coated  $\beta$ -TCP scaffolds containing VEGF for bone tissue engineering. *Materials Science and Engineering: C*, 69, 780–788.
29. Youngblood, R.L., Truong, N.F., Segura, T., e Shea, L.D. (2018) It's All in the Delivery: Designing Hydrogels for Cell and Non-viral Gene Therapies. *Molecular Therapy*, 26 (9), 2087–2106.
30. Chen, M.H., Chung, J.J., Mealy, J.E., Zaman, S., Li, E.C., Arisi, M.F., Atluri, P., e Burdick, J.A. (2019) Injectable Supramolecular Hydrogel/Microgel Composites for Therapeutic Delivery. *Macromol. Biosci.*, 19 (1), 1800248.
31. Dimatteo, R., Darling, N.J., e Segura, T. (2018) In situ forming injectable hydrogels for drug delivery and wound repair. *Advanced Drug Delivery Reviews*, 127, 167–184.
32. Smith, L.R., Irianto, J., Xia, Y., Pfeifer, C.R., e Discher, D.E. (2019) Constricted migration modulates stem cell differentiation. *MBoC*, 30 (16), 1985–1999.
33. Salvador, T., Oliveira, M.B., e Mano, J.F. (2020) Leachable - Free Fabrication of Hydrogel Foams Enabling Homogeneous Viability of Encapsulated Cells in Large - Volume Constructs. *Adv. Healthcare Mater.*, 9 (20), 2000543.
34. Khan, S., Chockalingam, S., Kundu, P.P., e Packirisamy, G. (2020) Fabrication of bimodal porous scaffold with enhanced mechanical properties using silanized sisal fibers for potential application in bone tissue engineering. *Materials Today Communications*, 25, 101260.
35. Johnson, K., Muzzin, N., Toufanian, S., Slick, R.A., Lawlor, M.W., Seifried, B., Moquin, P., Latulippe, D., e Hoare, T. (2020) Drug-impregnated, pressurized gas expanded liquid-processed alginate hydrogel scaffolds for accelerated burn wound healing. *Acta Biomaterialia*, 112, 101–111.
36. Zhang, J., Wehrle, E., Vetsch, J.R., Paul, G.R., Rubert, M., e Müller, R. (2019) Alginate dependent changes of physical properties in 3D bioprinted cell-laden porous scaffolds affect cell viability and cell morphology. *Biomed. Mater.*, 14 (6), 065009.
37. Li, Y., Liu, W., Liu, F., Zeng, Y., Zuo, S., Feng, S., Qi, C., Wang, B., Yan, X., Khademhosseini, A., Bai, J., e Du, Y. (2014) Primed 3D injectable microniche enabling low-dosage cell therapy for critical limb ischemia. *Proc Natl Acad Sci USA*, 111 (37), 13511–13516.

38. Golchin, A., e Farahany, T.Z. (2019) Biological Products: Cellular Therapy and FDA Approved Products. *Stem Cell Rev and Rep*, 15 (2), 166–175.
39. Begovac, P.C., Thomson, R.C., Fisher, J.L., Hughson, A., e Gällhagen, A. (2003) Improvements in GORE-TEX® vascular graft performance by Carmeda® bioactive surface heparin immobilization. *European Journal of Vascular and Endovascular Surgery*, 25 (5), 432–437.
40. Ngo, M.T., e Harley, B.A.C. (2020) Angiogenic biomaterials to promote therapeutic regeneration and investigate disease progression. *Biomaterials*, 255, 120207.
41. Nakamura, S., Kanatani, Y., Kishimoto, S., Nakamura, S., Ohno, C., Horio, T., Masanori, F., Hattori, H., Tanaka, Y., Kiyosawa, T., Maehara, T., e Ishihara, M. (2009) Controlled release of FGF-2 using fragmin/protamine microparticles and effect on neovascularization. *J. Biomed. Mater. Res.*, 91A (3), 814–823.
42. Cuchiara, M.P., Gould, D.J., McHale, M.K., Dickinson, M.E., e West, J.L. (2012) Integration of Self-Assembled Microvascular Networks with Microfabricated PEG-Based Hydrogels. *Adv. Funct. Mater.*, 22 (21), 4511–4518.
43. Gaspar, D., Peixoto, R., De Pieri, A., Striegl, B., Zeugolis, D.I., e Raghunath, M. (2019) Local pharmacological induction of angiogenesis: Drugs for cells and cells as drugs. *Advanced Drug Delivery Reviews*, 146, 126–154.
44. Wei, Z., Volkova, E., Blatchley, M.R., e Gerecht, S. (2019) Hydrogel vehicles for sequential delivery of protein drugs to promote vascular regeneration. *Advanced Drug Delivery Reviews*, 149–150, 95–106.
45. Yu, Y., Lin, X., Wang, Q., He, M., e Chau, Y. (2019) Long - term therapeutic effect in nonhuman primate eye from a single injection of anti - VEGF controlled release hydrogel. *Bioengineering & Translational Medicine*, 4 (2).
46. Rufaihah, A.J., Johari, N.A., Vaibavi, S.R., Plotkin, M., Di Thien, D.T., Kofidis, T., e Seliktar, D. (2017) Dual delivery of VEGF and ANG-1 in ischemic hearts using an injectable hydrogel. *Acta Biomaterialia*, 48, 58–67.
47. Bible, E., Qutachi, O., Chau, D.Y.S., Alexander, M.R., Shakesheff, K.M., e Modo, M. (2012) Neovascularization of the stroke cavity by implantation of human neural stem cells on VEGF-releasing PLGA microparticles. *Biomaterials*, 33 (30), 7435–7446.
48. Linn, T., Schmitz, J., Hauck-Schmalenberger, I., Lai, Y., Bretzel, R.G., Brandhorst, H., e Brandhorst, D. (2006) Ischaemia is linked to inflammation and induction of angiogenesis in pancreatic islets. *Clin Exp Immunol*, 144 (2), 179–187.
49. Nih, L.R., Gojgini, S., Carmichael, S.T., e Segura, T. (2018) Dual-function injectable angiogenic biomaterial for the repair of brain tissue following stroke. *Nature Mater*, 17 (7), 642–651.
50. Isozaki, A., Nakagawa, Y., Loo, M.H., Shibata, Y., Tanaka, N., Setyaningrum, D.L., Park, J.-W., Shirasaki, Y., Mikami, H., Huang, D., Tsoi, H., Riche, C.T., Ota, T., Miwa, H., Kanda, Y., Ito, T., Yamada, K., Iwata, O., Suzuki, K., Ohnuki, S., Ohya, Y., Kato, Y., Hasunuma, T., Matsusaka, S., Yamagishi, M., Yazawa, M., Uemura, S., Nagasawa, K., Watarai, H., Di Carlo, D., e Goda, K. (2020) Sequentially addressable dielectrophoretic array for high-throughput sorting of large-volume biological compartments. *Sci. Adv.*, 6 (22), eaba6712.
51. Kamperman, T., Henke, S., van den Berg, A., Shin, S.R., Tamayol, A., Khademhosseini, A., Karperien, M., e Leijten, J. (2017) Single Cell Microgel Based Modular Biinks for Uncoupled Cellular Micro- and Macroenvironments. *Adv. Healthcare Mater.*, 6 (3), 1600913.
52. Yao, L., Phan, F., e Li, Y. (2013) Collagen microsphere serving as a cell carrier supports oligodendrocyte progenitor cell growth and differentiation for neurite myelination in vitro. *Stem Cell Res Ther*, 4 (5), 109.
53. Jiang, J., Liu, A., Chen, C., Tang, J., Fan, H., Sun, J., e Fan, H. (2020) An efficient two-step preparation of photocrosslinked gelatin microspheres as cell carriers to support MC3T3-E1 cells osteogenic performance. *Colloids and Surfaces B: Biointerfaces*, 188, 110798.
54. Patel, Z.S., Ueda, H., Yamamoto, M., Tabata, Y., e Mikos, A.G. (2008) In Vitro and In Vivo Release of Vascular Endothelial Growth Factor from Gelatin Microparticles and Biodegradable Composite Scaffolds. *Pharm Res*, 25 (10), 2370–2378.
55. Nourbakhsh, M., Zarrantaj, P., Jafari, S.H., Hosseini, S.M., Aliakbari, S., Pourbadie, H.G., Naderi, N., Zibaii, M.I., Gholizadeh, S.S., Ramsey, J.D., Thomas, S., Farokhi, M., e Saeb, M.R. (2020) Fabricating an electroactive injectable hydrogel based on pluronic-chitosan/aniline-pentamer containing angiogenic factor for functional repair of the hippocampus ischemia rat model. *Materials Science and Engineering: C*, 117, 111328.

56. Lee, A., Hudson, A.R., Shiwardski, D.J., Tashman, J.W., Hinton, T.J., Yerneni, S., Bliley, J.M., Campbell, P.G., e Feinberg, A.W. (2019) 3D bioprinting of collagen to rebuild components of the human heart. *Science*, 365 (6452), 482–487.
57. Kleinheinz, J., Jung, S., Wermker, K., Fischer, C., e Joos, U. (2010) Release kinetics of VEGF165 from a collagen matrix and structural matrix changes in a circulation model. *Head Face Med*, 6 (1), 17.
58. Ramola, K., e Chakraborty, B. (2016) Disordered contact networks in jammed packings of frictionless disks. *J. Stat. Mech.*, 2016 (11), 114002.
59. Baumgarten, K., e Tighe, B.P. (2017) Viscous forces and bulk viscoelasticity near jamming. *Soft Matter*, 13 (45), 8368–8378.
60. Bauman, E., Granja, P.L., e Barrias, C.C. (2018) Fetal bovine serum-free culture of endothelial progenitor cells-progress and challenges. *J Tissue Eng Regen Med*, 12 (7), 1567–1578.
61. Nih, L.R., Sideris, E., Carmichael, S.T., e Segura, T. (2017) Injection of Microporous Annealing Particle (MAP) Hydrogels in the Stroke Cavity Reduces Gliosis and Inflammation and Promotes NPC Migration to the Lesion. *Adv. Mater.*, 29 (32), 1606471.
62. Koh, J., Griffin, D.R., Archang, M.M., Feng, A.-C., Horn, T., Margolis, M., Zalazar, D., Segura, T., Scumpia, P.O., e Carlo, D.D. (2019) Enhanced In Vivo Delivery of Stem Cells using Microporous Annealed Particle Scaffolds. 10.
63. Xin, S., Gregory, C., e Alge, D.L. (2019) Interplay Between Degradability and Integrin Signaling on Mesenchymal Stem Cell Function within Poly(ethylene glycol) Based Microporous Annealed Particle Hydrogels. *Acta Biomaterialia*, S1742706119307494.
64. Griffin, D.R., Weaver, W.M., Scumpia, P.O., Di Carlo, D., e Segura, T. (2015) Accelerated wound healing by injectable microporous gel scaffolds assembled from annealed building blocks. *Nature Mater*, 14 (7), 737–744.
65. Fang, J., Koh, J., Fang, Q., Qiu, H., Archang, M.M., Hasani - Sadrabadi, M.M., Miwa, H., Zhong, X., Sievers, R., Gao, D., Lee, R., Di Carlo, D., e Li, S. (2020) Injectable Drug - Releasing Microporous Annealed Particle Scaffolds for Treating Myocardial Infarction. *Adv. Funct. Mater.*, 2004307.
66. Cheng, W., Zhang, J., Liu, J., e Yu, Z. (2020) Granular hydrogels for 3D bioprinting applications. *View*, 20200060.
67. Levato, R., Jungst, T., Scheuring, R.G., Blunk, T., Groll, J., e Malda, J. (2020) From Shape to Function: The Next Step in Bioprinting. *Adv. Mater.*, 32 (12), 1906423.
68. Gungor-Ozkerim, P.S., Inci, I., Zhang, Y.S., Khademhosseini, A., e Dokmeci, M.R. (2018) Bioinks for 3D bioprinting: an overview. *Biomater. Sci.*, 6 (5), 915–946.
69. Moroni, L., Boland, T., Burdick, J.A., De Maria, C., Derby, B., Forgacs, G., Groll, J., Li, Q., Malda, J., Mironov, V.A., Mota, C., Nakamura, M., Shu, W., Takeuchi, S., Woodfield, T.B.F., Xu, T., Yoo, J.J., e Vozzi, G. (2018) Biofabrication: A Guide to Technology and Terminology. *Trends in Biotechnology*, 36 (4), 384–402.
70. Groll, J., Burdick, J.A., Cho, D.-W., Derby, B., Gelinsky, M., Heilshorn, S.C., Jüngst, T., Malda, J., Mironov, V.A., Nakayama, K., Ovsianikov, A., Sun, W., Takeuchi, S., Yoo, J.J., e Woodfield, T.B.F. (2018) A definition of bioinks and their distinction from biomaterial inks. *Biofabrication*, 11 (1), 013001.
71. Zhu, X., Li, H., Huang, L., Zhang, M., Fan, W., e Cui, L. (2020) 3D printing promotes the development of drugs. *Biomedicine & Pharmacotherapy*, 131, 110644.
72. Highley, C.B., Rodell, C.B., e Burdick, J.A. (2015) Direct 3D Printing of Shear-Thinning Hydrogels into Self-Healing Hydrogels. *Adv. Mater.*, 27 (34), 5075–5079.
73. Xin, S., Chimene, D., Garza, J.E., Gaharwar, A.K., e Alge, D.L. (2019) Clickable PEG hydrogel microspheres as building blocks for 3D bioprinting. *Biomaterials Science*, 7 (3),.
74. Xin, S., Wyman, O.M., e c, D.L. (2018) Assembly of PEG Microgels into Porous Cell-Instructive 3D Scaffolds via Thiol-Ene Click Chemistry. *Adv. Healthcare Mater.*, 7 (11), 1800160.
75. Xie, D., Sun, Y., Wang, L., Li, X., Zang, C., Zhi, Y., e Sun, L. (2016) Ultraviolet light-emitting diode irradiation-induced cell death in HL-60 human leukemia cells in vitro. *Molecular Medicine Reports*, 13 (3), 2506–2510.
76. Highley, C.B., Song, K.H., Daly, A.C., e Burdick, J.A. (2019) Jammed Microgel Inks for 3D Printing Applications. *Adv. Sci.*, 6 (1), 1801076.
77. Kudva, A.K., Dikina, A.D., Luyten, F.P., Alsborg, E., e Patterson, J. (2019) Gelatin microspheres releasing transforming growth factor drive in vitro chondrogenesis of human periosteum derived cells in micromass culture. *Acta Biomaterialia*, 90, 287–299.
78. Blocki, A., Löper, F., Chirico, N., Neffe, A.T., Jung, F., Stamm, C., e Lendlein, A. (2017) Engineering of cell-laden gelatin-based microgels for cell delivery and immobilization in regenerative therapies. *CH*, 67 (3–4), 251–259.

## *INTRODUCTION*

---

79. Buie, T., McCune, J., e Cosgriff-Hernandez, E. (2020) Gelatin Matrices for Growth Factor Sequestration. *Trends in Biotechnology*, S0167779919303002.
80. Echave, M.C., Sánchez, P., Pedraz, J.L., e Orive, G. (2017) Progress of gelatin-based 3D approaches for bone regeneration. *Journal of Drug Delivery Science and Technology*, 42, 63–74.



## **2. Advanced Chemical Tools for Interlinking Granular Hydrogels**

### **Subchapter**

This subchapter is based on the review article entitled “Chemical Tools for Interlinking Granular Hydrogels”

Manuscript in preparation

**Advanced Chemical Tools for Interlinking Granular Hydrogels**

Ana Fernandes, Vítor M. Gaspar, João F. Mano

Dr. V.M. Gaspar

Department of Chemistry

CICECO - Aveiro Institute of Materials University of Aveiro

Campus Universitário de Santiago 3810-193, Aveiro, Portugal

vm.gaspar@ua.pt

Prof. J.F. Mano

Department of Chemistry

CICECO - Aveiro Institute of Materials University of Aveiro

Campus Universitário de Santiago 3810-193, Aveiro, Portugal

jmano@ua.pt

### **Abstract**

Granular hydrogel scaffolds formed by the jamming of hydrogel microparticle blocks are unique bottom-up assembled platforms that present numerous advantages for diverse biomedical applications. Owing to their modular nature arising from their microparticle unit blocks, granular hydrogels can be assembled into stable inter-connected particle macro-structures. Such hierarchic platforms, so termed microporous annealed scaffolds (MAPs), exhibit highly desirable features for being explored as bioactive, cell-bioinstructive and cell recruiting platforms upon implantation. To take advantage of the full potential, heterogeneity and modularity of such platforms the use of cell-compatible assembly chemistries is a key requirement. Herein, we showcase the most recent advances on granular hydrogels interlinking technologies with an emphasis on the chemical tools that can be exploited for their autonomous or guided assembly into higher order microporous annealed structures. The most recent advances on granular hydrogels for tissue regeneration applications are also presented and discussed in light of their advantages, limitations and envisioned future prospects. Holistically, such multifunctional materials with micro-to-macro features unlock the opportunity to recapitulate and stimulate functional tissue repair and future advances are expected to further accelerate their applicability in a wide range of scenarios.

**Keywords:** Granular hydrogels, Chemical Tools, Bottom-up assembly, Microporous Annealed Particles

## 2.1. Introduction

Conventional hydrogels represent a versatile scaffold by replicating the native extracellular matrix (ECM) due to the high-water content. To date, hydrogels have already proven to be suitable as cell culture substrates or vehicles for bioactive molecule delivery. [1–3] However, usually hydrogels are crosslinked into large volumes (bulk hydrogel structures) at a macro-meter scale, which presents some disadvantages. In fact, large structures (>500-800  $\mu\text{m}$ ) fail in nutrient diffusion and gas exchange, leading to a decrease of cell viability, and failure in recreating tissues bifunctional heterogeneity. [4,5] To overcome these limitations microporosity can be introduced in bulk hydrogels by different techniques such as: (i) solvent/proven leaching [6], (ii) freeze-drying, gas forming agents [7], (iii) 3D printing[8], or (iv) by the inclusion of leachable particles, that are the removed to facilitate cellular infiltration. However, in most cases, these techniques are not cell friendly and/or involve subsequent cell seeding top-down strategies that encompass low cell attachment yield.

Seeking to overcome this, hydrogels with smaller dimensions are presented as a solution, namely hydrogel microparticles (HMPs). They can be used as single entities or in an aggregation state to form modular superstructure. The HMPs can be presented in dispersion, or even in a composite, or in a granular hydrogel, Figure 1. Granular hydrogels are also known as jammed hydrogels, are formed with the packing ratio increase, providing a solid-like structure. HMPs usually have a size between 1 and 1000  $\mu\text{m}$  and can be made from biological-origin, synthetic or hybrid biomaterials. [9–11]

Frequently, HMPs are used for drug, cell [12], or proteins [13] delivery, allowing a spatiotemporally controlled release of biomolecules [14], and these characteristics can be used on granular hydrogels to create heterogeneity and to increase their bifunctionality.

HMPs are the building blocks for granular hydrogels, as a bottom-up approach. The combination of multiple HMPs confers much more control of the finished scaffold, allowing the creation of heterogeneity and complexity like those observed in tissues. Granular hydrogels with different chemistries, stiffnesses, polymers, or even different types of loaded biomolecules can be produced (Figure 2). Nonetheless, until now, the heterogeneous systems developed so far are still very simple, with changes in HMPs density [15] or polymers composition. [16]

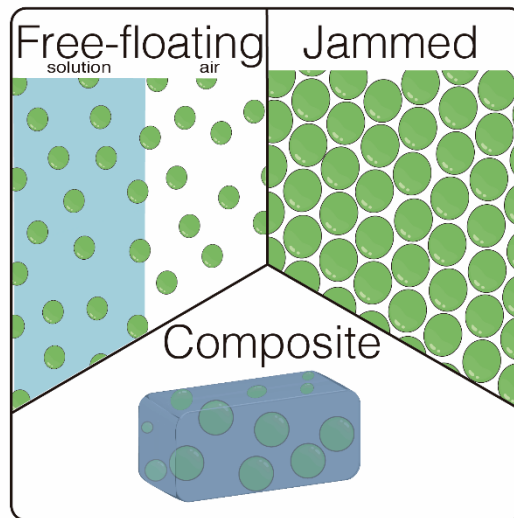


**Figure 1** Categories of HMPs. HMPs can be included in different states, in a free-floating solution or even in an aerosol, in a jammed state or as a composite.

The properties of the HMPs in a jammed state confer them interesting characteristics in comparison to standard a bulk hydrogel. The small size of HMPs allows them to be injected through needles or catheters, and the interactions between the HMPs allow a shear-thinning behavior giving rise to a more solid-like structure that can be readily disrupted upon subjected to a force – shear-thinning. [17–19] The void spaces created between the HMPs upon jamming ensure nutrients and gas exchanges, enabling the construction of larger scaffolds, overcoming one of the main constraints presented in bulk hydrogels. Nevertheless, by varying the void spaces sizes (i.e., by controlling packing ratio) affects cells infiltration into scaffold as will be discussed below [20,21]. To maintain the scaffold conformation HMPs can be annealed, forming microporous annealed particles (MAP) scaffolds, with the same advantages as their granular hydrogels sub-units, but with the gain of function of creating a hierarchic microporous scaffold with a higher length scale (e.g., millimeter-to-centimeter size). [22,23]

This review will discuss the recent advances in granular hydrogels and MAPs. First, by distinguishing and clarifying the granular hydrogel characteristics as well as their metastable behavior. Later, the interactions between the HMPs in granular hydrogels and MAPs, as well as other chemistries already developed and others to be explored will be discussed. Finally, their applications in tissue engineering will be showcases. The overall goal is to show the recent advances and the clinic applicability of these scaffolds, as well

as provide advice and guiding principles to create evermore bioactive and functional scaffolds, either for cell recruitment or for cells delivery.

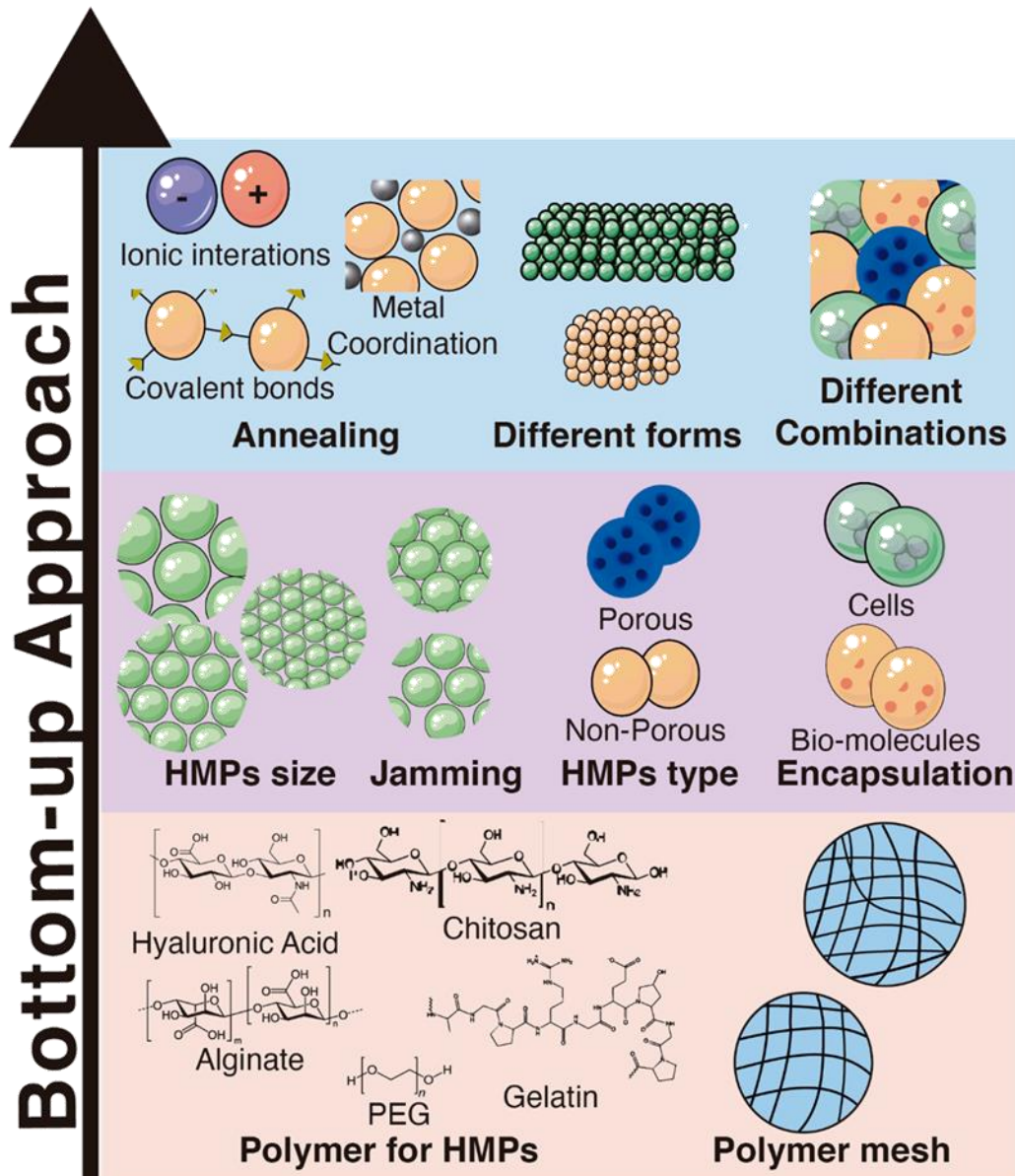


**Figure 2** Granular hydrogel as a bottom-up approach by choosing the polymer, and the mesh, that will influence the hydrogel microparticles. The size, of hydrogel microparticles their porosity o the bioactive factors encapsulated will affect the final structure. Finally, the interactions enable to create a larger structure, with different forms, and with innumerable particles combinations possible.

## 2.2. Granular hydrogels metastable behavior

In granular hydrogels, HMPs are jammed/in an agglomerated state. Upon reaching a pre-determined threshold of particle-to-volume fraction obligates HMPs to establish inter-particle interactions, e.g., Van der Walls forces or hydrogen bonds, with one

another. [24–26] The jamming transition is achieved by increasing particles-to-volume fraction ( $\phi \approx 0.58$ ), in proper conditions of stress and temperature, namely random loose packing. In random loose, packing the particles are minimally jammed. However, by increasing packing, with particle-to-volume to  $\sim 0.64$ , the interstitial fluid between particles is minimal. Increasing more the packing, to particle-to-volume  $\phi \rightarrow 1$  leads to the collapse of the interstitial space and HMPs in the granular hydrogel crush. In this last case, the HMPs deformations are not reversible, Figure 3. [5,27]

The metastability in granular hydrogels in a thermodynamic sense is far-from-

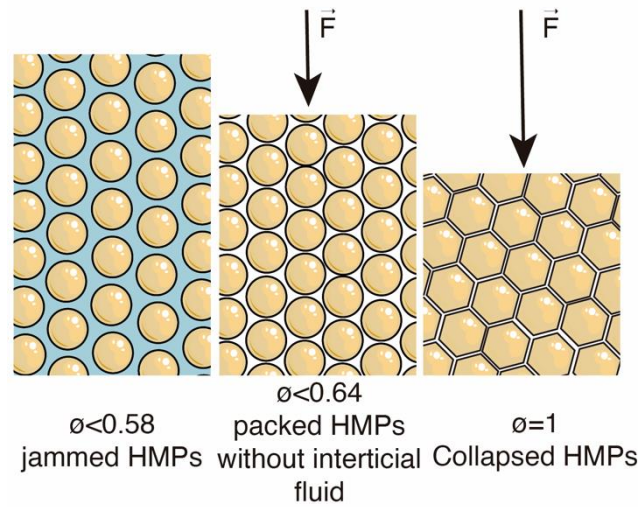


**Figure 3** Influence of the packing ratio on HMPs state and interstitial fluid.

equilibrium once by non-zero applied stresses, the system is jammed, but by external applying forces the jamming state is disrupted. [24,24,25,28] Un-jamming occurs when local constraints can no longer be satisfied due to the density and/or shear stress reached the limit. Otherwise, the weak interactions, under a stress force break, and the granular hydrogel acquire liquid behavior. [10,20,29,30] Herewith, for the forces to establish static mechanical equilibrium is necessary to assure the Coulomb condition restriction (charge), force balance, and torque balance (static equilibrium). Once in a jammed state, the force balance and torque are satisfied by every HMP in a network, which means that is dependent on the polymer constitution. [24–26,28,31]

The HMPs, the building blocks of the granular hydrogel, have a direct influence on the properties of the final structure. For example, the swell ability is more limited than in bulk hydrogel, once is limited of each HMPs to swell. Otherwise, with the increase of the void spaces, the interactions between HMPs decrease, and the structure are deconstructed. [27,32]

Furthermore, the weak interactions in granular hydrogels lead to a fast accommodation of the imposed stresses, due to the HMPs ability to rearrange their interactions to form a more stable structure. [33] They show lower stiffnesses that can be increased with the diminution of the void spaces area due to the improvement of the interaction between HMPs. The establishment of covalent bonds between the HMPs, forming a MAP, provides more stability to the structure from a thermodynamic point of view similar to a porous hydrogel. [15,34]

### 2.3. Annealing of granular hydrogels

The formation of granular hydrogels occurs by modulating the jammed state of HMPs. This step, in most cases, occurs using centrifugation or vacuum filtration. After that, a granular hydrogel is formed, able to be injected or printed in a single filament or even form a supporting bath for 3D bio-printing. [35,36] Nevertheless, to increase the stiffness of the constructs is added a linkage between the HMPs forming a MAP, Table 1. Several interactions could be implemented on granular hydrogels to increase the storage modulus, those can be by form by covalent bonds, forming a MAP or non-covalent bonds Figure 4.

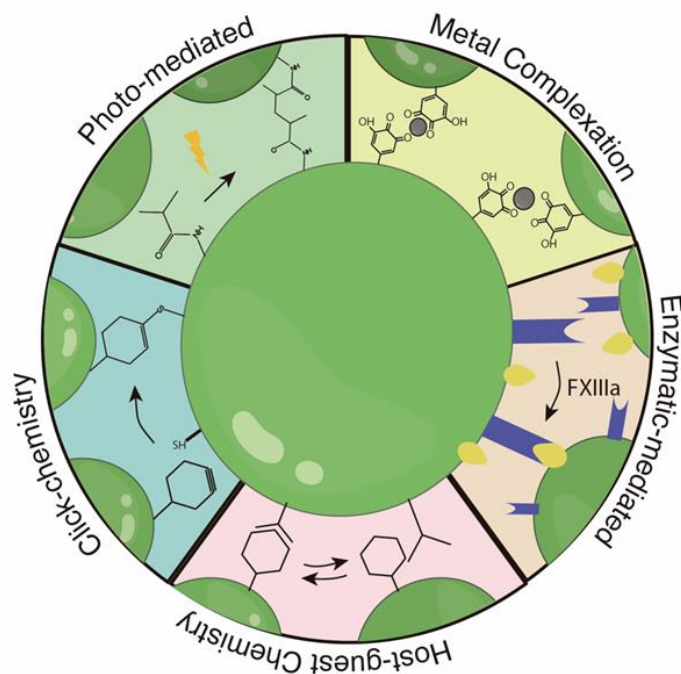


**Figure 4** Chemical toolbox for interlinking HMPs and ultimately assemble MAPs scaffolds. Metal complexation (e.g., iron, vanadium, aluminum, silver nanoparticles, etc) with gallol/catechol groups. Covalent bonds with photo-mediated, click-chemistry, via methacrylic groups reaction, for example. Host-Guest chemistry, via cyclodextrin interaction with norbornene, etc. Enzymatic-mediated annealing, where the Factor FXIIIa links the protein G and K.



### 2.3.1. Non-covalent bonds

In hydrogels several ways can be explored to promote the crosslinking of the precursor solution, including changes in temperature solution, pH, ionic, hydrophobic interactions, etc. However, only a few of those can be easily implemented in granular hydrogels interlinking into MAPs scaffolds, mainly due to the complexity and multifarious nature of the established interactions when multi-component systems are involved.

#### **Thermal annealing**

Recently hydrogels were the temperature-triggered liquid to gel transition captivate the attention of regenerative medicine. It would be interesting to see these technologies applied to granular hydrogels. However, these interactions are difficult to transpose into granular hydrogels. Thermo gels are formed by amphiphilic polymers that are surrounded by cage-like structure. However, exceeding transition temperature, the interactions are destabilized, leading to structure collapse, losing the solid form. [37–39] To transpose this technology to granular hydrogels, the HMPs would need to be in an ultra-packed state to form a cage-like structure, which would annul the granular hydrogel advantages. Lastly, the polymer chosen would need to have a transition temperature below 40°C, which in these types of cross-linking is not common for example, poly(N-isopropylacrylamide) (PNIPAm) temperature transition is 32 °C. Nevertheless, these polymers can be used however to produce the HMPs. [40]

#### **pH dependent annealing**

In TE hydrogels sensitive to pH fluctuations are captivating more interest, principally because of the ability of ionization of the different groups on the polymeric chain dependent on pH, which leads to the creation of repulsive or attractive faces leading to reversible cross-linking. [41] This stimuli is widely used for drug delivery system once they can release the drug depending on the pH.. [42,43] However, annealing dependent on pH is not very stable and can fluctuate with the evolution of numerous biological processes such as those mediating inflammation.

The complexity of pH-mediated annealing process increases due to the short window of the biological pH, which explains the difficulty of translation to granular hydrogels. In one of the approaches already developed, HMPs were coated with boronic acid-alginate. In this, the elastic and storage modulus are pH-dependent and thus the interparticle

adhesive ability. At physiological pH, the boronic acid is deprotonated, increasing the ability to form hydrogen bonds, which increases the interactions with ECM, conferring to the scaffold adhesive ability. [44] Nevertheless, it is expected that more granular hydrogels with this type of chemistry, will be developed in the near future, for instance taking advantage of other pH responsive groups (e.g., imidazole, hydrazine, etc.).

### **Ionic interactions**

Ionic cross-linking is a reversible method for bulk hydrogels fabrication but can also be adapted to granular hydrogels manufacture. In this strategy, multivalent ions or small molecules charged are used. [45] It is an easy methodology, yet the reaction kinetic is hard to control, especially *in situ*. The metal used can provide other properties to the granular hydrogels, such as electromagnetism conductivity. [35] Frequently are necessary phenolic compounds from a chelate complex with the metal. The phenolic groups increase the adhesion with the surrounding tissue. An example of this is the use of gallol groups that belong to the quinones family. They can complex with silver nanoparticles, creating conductive, and self-healing granular hydrogels with a storage modulus of 129.8 Pa. [35] This granular hydrogel could also be complexed with metal, providing several applications, showing the ability to conduct an electric stimulus. Nevertheless, the multivalent ions need to be carefully chosen to prevent toxicity and evaluated their stability in a metabolic environment.

### **Self-assembled peptides**

Self-assembled peptides are derivatives from protein structural motifs, where the amino-acid chains present polar or charged domains. This characteristic allows the assembly of larger structures by hydrogen bonds, ionic bonds, hydrophobic interaction, or even Van der Waals interactions. [46] As a protein derivative, they show not toxic, non-immunogenic characteristics, as degradability due to the easy metabolization, and non-thrombogenic characteristics that support their utilization. They revealed to promote angiogenesis and anti-inflammatory characteristics. [47] This methodology is already translated to colloidal gels, to the nanoparticle's assembly,[48] and could be easily transposed to granular hydrogels.

#### **2.3.2. Covalent bonds**

### **Free-radical reaction**

Annealing the HMPs by photo-mediated reactions is an easy way to increase the storage modulus and scaffold stability of these multi-particle systems. In these reactions, radiation triggers the formation of radical species by degradation of the photo-initiator, which initiates the series reaction that anneals HMPs, forming a MAP. This type of annealing methodology is generally fast, though such exposure under high radiation may lead to cell damage and must be carefully controlled. [49] This chemistry is very promising once the HMPs cross-linking can be simultaneous with the annealing, as shown with methacrylate gelatin, GelMA, HMPs. [50,51]

However, the HMPs can also be first crosslinked and then annealed, such as demonstrated with GelMA HMPs. In this example first, the HMPs were crosslinked with via an amide bond and then annealed by using UV radiation. [52] Polymers with norbornene groups [53], or thiol groups [11,54,55], also showed suitable for granular hydrogels photo cross-linking or even poly(ethylene glycol) diacrylate, PEGDA. [36]

This annealing is often used in 3D bioprinting due to the simplicity of the quick procedure. However, it is necessary to increase the packing state with vacuum filtration to produce a printable ink. As already showed using hyaluronic acid modified with norbornene motifs and PEGDA, revealing printability and high structure fidelity. [36]

The annealing mediated by UV-light shows some drawbacks once they can damage cellular DNA, and the cross-linking is dependent on a lamp, precluding their utilization *in situ* by a minimum procedure, due to low penetrative ability because of their higher frequency. [56]

### **Click-Chemistry based annealing**

The annealing by click-chemistry is generally highly selective, but is slower than that occurring via UV, leading to more HMPs compaction caused by the gravitational force, creating a lower void fraction (between 11- 15%). [16,21] The HMPs are more compacted (lower particle-to-volume ratio), which leads to a higher Young's modulus (4533 Pa). [34] In these strategies for example, HMPs with tetrazine or norbornene developed as a gene delivery system, revealing high biocompatibility. [16] This strategy was also used on a MAP for injection in a stroke exhibiting high biocompatibility and possibility of administration via minimally invasive procedures. [34]

Nevertheless, this methodology is more compatible with *in situ* annealing than the photo-cross-linking one.

### **Host-Guest annealing**

Another option already demonstrated is host-guest chemistry for granular hydrogels dynamic interlinking. This approach is already very used for the formation of bulk hydrogels *in situ*. [57] For granular hydrogels using adamantane-norbornene motifs in hyaluronic acid and cyclodextrin-hyaluronic acid revealed an optimal combination for 3D bioprinting. This biomaterial ink showed the ability to have fluid-like behavior by upon being subjected to compressive forces, also demonstrating high recoverability and solid-like features when in resting state. [58] This self-healing ability is highly suitable and desirable for *in vivo* applications. However, the inherent reversibility of this chemistry does not provide the generation of MAPs platforms with suitable mechanical properties such as those observed with other totally covalent strategies. Nevertheless, the metastable behavior of such granular hydrogels can in the future be explored.

### **Enzymatic annealing**

Enzymatic annealing occurs by enzyme action, usually, a transglutaminase that links proteins that are in HMPs composition. This annealing occurs, usually, at 37°C for 90 min, being highly suitable for *in situ* annealing, following injection via minimally invasive procedures. [59,60]

Usually, transglutaminase is used in these strategies, for example, Factor XIII (FXIIIa) or/and plasminogen crosslinks G and K proteins. The polymers mostly used in this approach are hyaluronic acid [23,61] and PEG [62,63], which are generally with these functional proteins prior to any coupling. This system is frequently conjugated with RDG, a peptide sequence - arginine-glycine-aspartic acid, to increase cell adhesion and vascularization formation due to the lack of adhesion motifs in PEG. Metalloproteases are commonly introduced, increasing the degradation of HMPs. [22] Comparing enzymatically annealed MAPs with a granular hydrogel with the same HMPs in their constitution indicates that MAPs present 13-fold higher Young's modulus, corroborating the advantages of this approach. [23,62,64]

The void space fraction varies between 11 to 15% and is lower than in reactions activated by UV light, but similar to the ones in click-chemistry. The enzyme-mediated is slower than UV-mediated annealing leading to more time for HMPs to deposit, increasing higher packings. [64] The high concentrations of the enzyme can reveal

negative effects on cell proliferation; however, it did not present a problem in the MAPs developed.

The annealing should be chosen according to the desired tissue application to increase cell differentiation. Another factor in a count is the polymer used, once some polymers such as alginate chitosan or synthetic polymers do not have binding motifs reducing the cell compatibility. Otherwise, mechanical properties can provide an enormous advantage.

## 2.4.Functional characteristics of granular systems

HMPs have a high potential for TE due to the vast range of applications, from to cell delivery, drug delivery, or even gene therapy. [67] These characteristics are easily transposed to granular hydrogels and augmented considering their modular nature. [50,62] Granular hydrogels' functional properties confer several vantages when compared to other scaffolds in the TE field, providing new approaches, including scaffold modulation, controllable microporosity, improved cell proliferation/infiltration by providing a 3D environment with higher complexity than bulk hydrogels, Figure 5

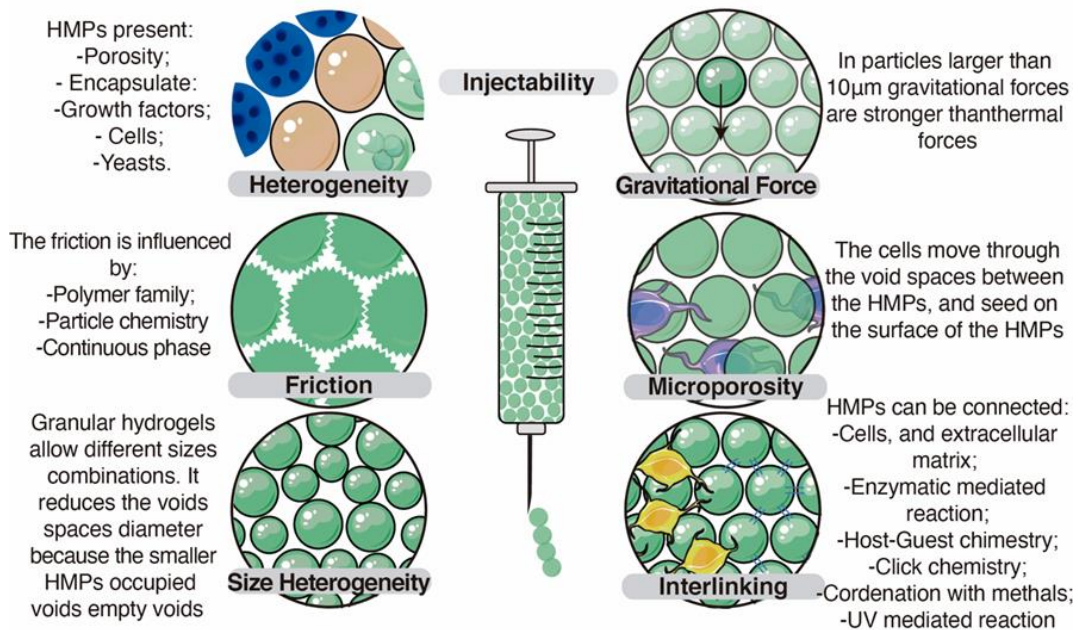


**Figure 5** Multifunctionalities of Granular Hydrogels, and their properties such as their ability to high heterogeneity by combining different types of HMPs or different sizes. HMPs high injectability. The HMPs are interlinked but between them, they have porosity

*INTRODUCTION*

**Table 1 Annealing process already developed and with the respective polymers and application**

Annealing process:	Polymers used	Utilization:
UV mediated	Methacrylate gelatin	-Porous HMPs increased the bone regeneration;[52] -Bead-based scaffold, for cell seeding with higher cell ability to penetrate the MAP than a bulk hydrogel. [50]
	PEG-dithiol PEG- norbornene	-3D Bioprinting ink;[11] -Scaffold cross-linking influence on cell adhesion and rheological properties. [54,55]
	Hyaluronic acid -norbornene or PEGDA	-3D Bioprinting ink. [36]
	Norbornene hyaluronic acid	-Scaffold for delivery of human platelet lysates and as a ink for 3D bioprinting. [65]
Click chemistry mediated	Hyaluronic acid PEG-tetrazine	-Injected into the stroke area with cellular infiltration and reduction of the glial formation; [34] -Stiffness, void space size, and adhesion properties impact cell proliferation, cell spreading, and gene transfer assays. [16]
	PEG-DBCO+ azide	-Evaluation of the effects of different sizes of HMPs on cell proliferation. [21]
Guest-host interaction	Adamantane - norbornene - Hyaluronic acid Andcyclodextrin -hyaluronic acid	-Self-healing properties for injection on myocardial infarction, with an increase of cell infiltration. [58]
Enzymatic (Q and K peptides, FXIIIa transglutaminase)	Hyaluronic acid 4 arm-PEG	-Injected in a stroke area for regeneration, and cellular infiltration; [23,60] -Wound healing, with an increase in wound closure; [62] -Cell delivery system. [22]
Metal coordination	Gallol methacrylate hyaluronic acid Ag nanoparticles	-Injectable granular hydrogel conductive properties and self-healing for muscle. [35]
Hydrogen bonds	Methacrylate hyaluronic acid and boronic acid alginate	-Tissue adhesive granular hydrogel, self-heling ability. [44]
	Polyvinyl alcohol and chitosan methacrylate	-Bioprinting ink. [66]

### **Heterogeneity**

The heterogeneity allowed by the HMPs enables the creation of complex granular hydrogels, with multifactorial able to reproduce the ECM characteristics. First, the granular hydrogels could have HMPs with multi-compartmentalized [68,69] or by different layers [70], or diverse polymers [59]. Granular hydrogels were also developed for growth factors (GF) delivery. [18,65] The different layers or particles enables the release in distinct times,[71]and provides a specific stimulus during the different phases of the tissue regeneration. Then, more simply granular hydrogels can combine different HMPs creating more heterogeneity for the scaffold by changing polymer, charge, composition. [30,63] This heterogeneity can even be achieved by different HMPs populations combinations and then mixing until they are uniformly distributed, [63] such as shown by Eben Alsberg and his team by producing gelatin HMPs with TGF- $\beta$ 1 and hydroxyapatite HMPs loaded bone morphogenetic protein 2, BMP-2, and this mixture increased the proliferation of hMSC. [72]

The heterogeneity could be as simple as switching the chirality of the peptides in the polymer. [73] This simple combination led to an activation increase in the innate adaptive immune system, essential to tissue regeneration. The HMPs can lead to several applications, since drug delivery to rheologic properties, diffusion rates, cell infiltration, or even HMPs interactions. For example, mixing HMPs with different stiffness cross-linking degrees leads to cell responses specific for each region. [63] This ability to create modular scaffolds is essential in TE, with a principal impact on complex structures, where the stiffness or biochemical properties vary inside the tissue.

### **Bioactive molecules delivery**

The HMPs are frequently designed for drug delivery, allowing the diverse combinations of drugs with combinations of different HMPs, or HMPs with distinct layers [74], assuring minimum invasion procedures and a more controllable release. However, only a few granular hydrogels or MAPs are used as a delivered system. [63,71,75] The utilization of growth factors, GF, is essential for tissue regeneration, once GFs present cells with the necessary clues to recruit other cells or induce cells into differentiation and in matrix production. [10] However, the short half-life of GF and high price lead to some constraints in their utilization. [76] Biomaterials are frequently used to increase the encapsulation GF, namely HMPs. The GF encapsulation increases stability

leading to longer half-times and controlled release. [77] This leads to the expectation of more granular systems as biomolecules release systems. For example, MAPs were already used for human blood platelet lysates encapsulation, showing a sustainable release, and increasing vascularization. [65] It is expected the combination of different HMPs loaded with distinct biomolecules into the granular hydrogels, to promote a differentiated and faster regeneration. It is also anticipated that the release to be controlled by varying the sizes of HMPs, size, polymer, or even polymer mesh to release that follows the tissue regeneration, Figure 2. [78–80] The release is influenced by the interactions between the drug or growth factor with the granular hydrogel polymer, or polymer cross-linking, which can delay the release accordantly with the biomolecule-polymer affinity, enabling a release in line with the regeneration. [78,79] Recently, the incorporation of nanoparticles loaded with drugs myocardial infarction into HMPs to build an into MAP showed to increase the angiogenesis, reducing the fibrotic scar as well as the inflammatory response. [18]

### **Rheological properties**

The rheological properties of HMPs in a jammed state are useful in several investigations to predict and optimize the mechanical properties of granular hydrogels. [81] The mechanical properties of granular hydrogels are dependent on the interaction between the HMPs, and the individual mechanical properties of each HMP. This last is dependent on density, polymer type, and concentration, as well as the cross-linking between the polymer chains as explained above. [29] By studying the HMP rearrangement, concedes more knowledge and accuracy on the mechanical comportment of jammed hydrogels. [82] The HMPs can decrease the friction simulating a separation layer and sliding through surfaces, Figure5. However, this is dependent on the HMPs amount, size, and surface. The low friction coefficient is obtained by diminishing the surface-surface interaction between the HMPs. [31,64] Increasing HMPs size, the number of HMPs, or individual particle stiffness, decreases the surface interaction, HMPs deformity, with an easy rollover of the surfaces in the jammed system. [27] It was already demonstrated that in a linear response deformation, above the jamming transition concentration, the elastic modulus of jammed HMPs, follows the same scaling laws as continuous hydrogels. [82] Thus, as expected, the HMPs, in a granular hydrogel, have a shear at a rate higher than a cross over shear rate, do not have time to restore their shape



and pass to the adjacent HMPs. These deformations seem to have a correlation with polymer chain diffusive motion but also seem to depend on how fast the fluid in the voids spaces is drained. [82] However, most of the studies of granular hydrogel characteristics are performed with hard HMPs such as Carbopol due to the more stable properties with different temperatures. [83,84] Nevertheless, soft HMPs with polymers like gelatin, where the mechanical properties fluctuate with temperature, leading to worst previsions. Leading to a necessity to study the rheological and mechanical properties of softer HMPs.

### **Injectability**

The high injectability ability allows minimally invasive procedures not being necessary, open surgeries, which is time-consuming, with the need for more resources and people management. Although hydrogels can be injected as a precursor solution, it leads to constraints on the cross-linking methods once they are difficult to control *in situ*. [4,59,63,85] In high pressures, tissues are difficult to combine with injection due to the fluid return or turbulent flow in the needle. Granular hydrogels are easily injectable due to the HMPs nature and reduced size. [3,5,62] The HMPs jammed inside of the syringe minimizes the turbulent flows that can occur, leading to and reduction of the dispersion after the injection, and allow controlled and continuous delivery of the amount of the HMPs, and promptly fill the cavity space due to their fast ability to adapt to different shapes. The interaction between HMPs with electrostatic or non-covalent forces, permitting their injectability, Figure 5. [11,54]

However, in MAP, because of irreversible covalent bonds established between HMPs, when broken and cannot be reestablished, functioning like a highly porous hydrogel. However, the covalent bonds can be established *in situ*, injecting as a granular hydrogel and then becoming a MAP. [23,60,62]

Nevertheless, in the granular hydrogel, after a force application, the granular hydrogel shows compartment similar to a liquid. When force ceases, the interactions between HMPs are reestablished, and the granular hydrogel show compartment solid-like. The capacity to recover the form confers to the granular hydrogel's self-healing ability. [29] The self-healing behavior enables prior injection, the cell seeding into the particles. Then the delivery by a minimum invasive procedure once they can restore the connection after injection.

Nonetheless, in tissues with high motility like muscles, or the heart, the HMPs have to be annealed after injection to prevent dislodging. [51] The same should occur with high-pressure regions, such as fluid-filled stroke cavities where HMPs are annealed to prevent the backflow after the removal of the syringe. [60,63] In this last example, it is necessary to point some exceptions to the covalent bond formation, such as the system chelate linkages. As demonstrated using hyaluronic HMPs modified gallol groups that were interlinked by silver nanoparticles. [35,86] Depending on the metal coordination with different groups can be enough to assure the HMPs placement.

### **Void Spaces**

As mentioned before, the void spaces in granular hydrogels and MAP exhibit considerable advantages in comparison with a bulk hydrogel. In granular hydrogels, the cells show the ability to move through the void spaced between HMPs. [25,87] This compartment is essential for successful cell infiltration and faster absorption. The cell movement between the void spaces on jammed hydrogels does not lead to HMPs movement in granular hydrogels, assuring the localization of each HMP, but was also showed that cells move faster in small pores, yet if the pores are too small, they start to damage cellular length-scale. [88] The porosity, also, influences cell differentiation and behavior. [89] Lastly, the porosity created by the void spaces increases the permeability, fluid-flow, mass transport, and cell infiltration, similar to a natural recovery of tissues, increases the absorption rates of the scaffold. [21,62,90] As expected, comparing a bulk hydrogel with a granular hydrogel, the blood vessel infiltration and formation is much higher in the last scaffold. [22,51,62] If cells are inside of the HMPs, the spherical form of the hydrogel assures the higher ratio between the surface and the HMP volume, this way, it ensures the highest exchanges rates with the environment leading to an enhancing of cell viability and biochemistry activity, as well as, less inflammation. [62] The cell infiltration and movement were revealed that void spaces with a larger diameter had more cell infiltration, with more proliferative cells with a higher spreading behavior and more actin fibers produced, Figure 6a. [21] However, by changing the HMPs sizes, the void

space volume does not present significant differences, but the void space diameter increases with larger HMPs, [10,16,21,90] Figure 6b.

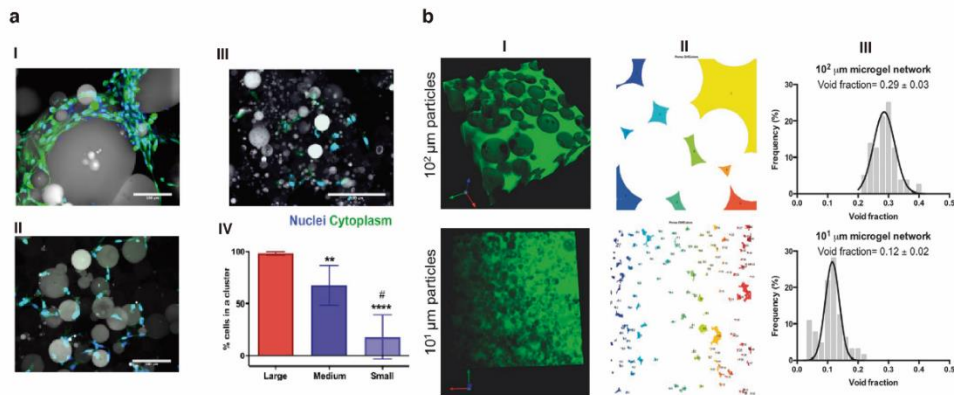


**Figure 6** a) Cell spreading according to HMPs size I) HMPs with large dimensions, II) medium dimensions and smaller dimensions, III) with the higher forms of clusters on HMPs with larger dimensions. Reproduced with permission [16] Copyright Acta Biomaterialia. b) void space area, and fraction formed with larger and small HMPs. Reproduced with permission [21], Copyright 2017, Wiley.

## 2.5. Hydrogel microparticles production

HMPs can be produced by different techniques including microfluidics, batch emulsions, electrodynamic spraying, mechanical fragmentation, photolithography, and spray-drying. The different fabrication techniques have benefits and constraints and should be chosen accordantly with the desired, polymer characteristics or rheological, behavior, and cross-linking, or the final application. all of these techniques are summarized in Table 2. [29]

Microfluidics technique is compatible with multi-compartmentalized particles,[12] allowing cell encapsulation,[53] as well as, the incorporation of small molecules, drugs, or proteins [91,92] inside the HMP. By changing simple aspects, such as, the flow, or the angle between the channels is possible to produce HMPs with different sizes and shapes, and by easily increasing the microfluidic channels length is possible to modulate the cross-linking and stiffness of the HMP. [93] However, once the precursor solutions pass through narrow microchannels at low pressures, is necessary that these solutions have low viscosity[29], and at the same time form stable HMPs otherwise they will clump the microfluidic chip. [94] Recently, several multichannel dispositive are being designed, to maximize and diminished the time necessary to produce HMPs at a large scale. However, in most commercial devices are still time-consuming, especially with low HMPs

diameters, and with low yields. [16] However, from all the techniques this one is the most promising, due to all the alterations possible in the dispositive. Nevertheless, this methodology also allows the production of different physicochemical gradients by coupling distinctive precursors solution on the microchannels and alternating the flow rates. [95] This approach simplifies the creation of gradients making the process much faster and simple, which can trigger different cellular responses. [15] This technique not only can produce HMPs, but allow cell encapsulation, and de separation of the ones that are encapsulated and the ones that are not, it also allows the production of microfibers. [93, p. 2020,96]

An alternative to microfluidics, and very used, is electrodynamic spraying. This technique involves the extrusion of the hydrogel precursor solution through a syringe where a high voltage is applied to the needle tip. In the tip, due to the high voltage, the surface tension is outstripped for the surface tension, leading to the formation of a jet of spherical droplets. [11,97,98] The HMPs are then collected in a substrate or emulsion for subsequent cross-linking. The size of HMPs can be optimized by varying the nozzle size, the applied voltage, the polymer flow rate, and the distance between the needle and the substrate or solution to collect HMPs (distance to collector). [99] The HMPs size is generally more polydisperse than the ones obtained via microfluidics but is less time-consuming. However, to diminish the polydispersity the HMPs are frequently sieved. [55] Similarly, to microfluidic techniques, the polymers used in the electrodynamic spraying must have a low viscosity to pass through the needle. A huge advantage of this technique is the compatibility with cell encapsulation.

The batch emulsion is one of the most widely used techniques, with a huge variety of protocols already optimized. [100,101] Usually the emulsion is created between an oil phase and an aqueous hydrogel precursor, by mechanical mixing. [102,103] The droplets are then crosslinked, the oil phase removed by a series of washing, centrifugation, and filtration steps. This is an easy and fast technique and does not require specific equipment to produce oil in water emulsion. However, the HMPs that are fabricated have polydisperse diameters and need an additional sieving step, on the other hand, a large number of HMPs are produced. This technique also allows cell encapsulation,[104] as well as the incorporation of small molecules or proteins. [105,106]

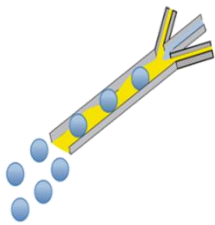
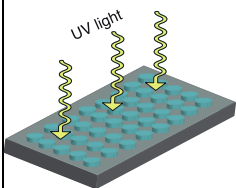
Alternatively, HMPs can also be produced by breaking a previously formed hydrogel by forcing the hydrogel to pass through a fine steel mesh or using a rotational blender.

[107] This methodology is quite simple permitting the production of many HMPs, though the size distribution is difficult to be controlled, and the form non-spherical, for this is barely used in HMPs production.

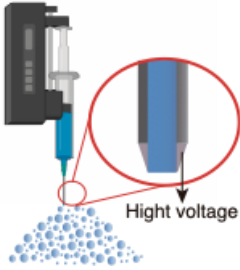
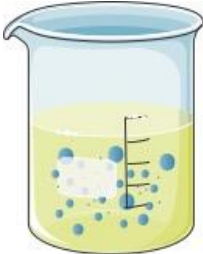
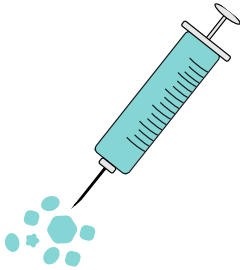
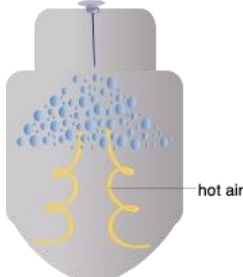
In lithography, the hydrogel precursor is loaded in a negative mold or using a photomask to cross-link the hydrogel, and lastly, a photomask is applied to a flowing hydrogel precursor. [108,109] This technique allows the production of different shapes and with monodisperse HMPs but has a low particles throughput and is more time consuming of all the techniques, and with more labor. [110]

The spray drying method is less used than the other techniques discussed above. This methodology is mainly used for drug encapsulation by producing small particles. [111] Herein, the hydrogel precursor is dispersed by an atomizer or a spray nozzle through a vertical tower in which hot gas passes downwards. This technique allows a lower polydispersity but its potential or cell encapsulation is debatable

. **Table 2** Different methodologies for HMPs production, advantages, and disadvantages of each method.

Methodology	Representation	Advantage and Disadvantages	Cited by:
Microfluidic Chips		<p>Advantages:</p> <ul style="list-style-type: none"> <li>-Permits the formation of a huge range of sizes with high control;</li> <li>-Monodisperse HMPs;</li> <li>-Allows the incorporation of cells inside of bead, as well as small molecules and proteins;</li> <li>- Different shapes and multi- compartmentalized HMPs.</li> </ul> <p>Disadvantages:</p> <ul style="list-style-type: none"> <li>-Require an oil phase that can be toxic to the cells;</li> <li>-Is a slow method;</li> <li>-Low viscosity from the microgels precursor solution is required.</li> <li>-Minimum size produced is <math>\sim 5\mu\text{m}</math></li> </ul>	[15,23,35, 50,58,62, 93– 95,112]
Lithography		<p>Advantages:</p> <ul style="list-style-type: none"> <li>-Allows the formation of regular different forms;</li> <li>-Particles cross-linking is generally fast;</li> <li>-Monodisperse particles.</li> </ul> <p>Disadvantages:</p> <ul style="list-style-type: none"> <li>-Low throughput and particles production.</li> <li>Minimum size produced <math>&lt;1\mu\text{m}</math></li> </ul>	

## INTRODUCTION

<p>Electrodynamic spraying</p>		<p>Advantages:</p> <ul style="list-style-type: none"> <li>- Fast methodology;</li> <li>-High production yield;</li> <li>-Consents the incorporation of cells inside the produced spherical particles;</li> <li>-Small molecules, or proteins can be incorporated inside the HMPs/microgels.</li> </ul> <p>Disadvantages:</p> <ul style="list-style-type: none"> <li>-The particles are collected in an oil phase, or in a surface requiring further recovery steps;</li> <li>-Formation of a polydisperse particles, and sometimes without a spherical phase;</li> <li>-Low viscosity from the microgels precursor solution is required.</li> </ul> <p>Minimum size produced is 5<math>\mu</math>m</p>	<p>[11,54,55, 97– 99,113]</p>
<p>Emulsion</p>		<p>Advantages:</p> <ul style="list-style-type: none"> <li>-Easy methodology,</li> <li>-Compatible with cell encapsulation;</li> <li>-Small molecules, or proteins can be incorporated inside HMPs or microgels.</li> </ul> <p>Disadvantages:</p> <ul style="list-style-type: none"> <li>- The particles produced have wide size ranges;</li> <li>-Generally, the particles are fabricated in a water oil emulsion, that includes an oil phase which can destabilize the cellular membrane.</li> </ul> <p>Minimum size produced ~1<math>\mu</math>m</p>	<p>[16,71,72, 101,103,104,106,114,115]</p>
<p>Hydrogel-breaking</p>		<p>Advantages:</p> <ul style="list-style-type: none"> <li>-Fast methodology;</li> <li>-Does not have an oil phase;</li> <li>-Formation of a large number of HMPs/microgels.</li> </ul> <p>Disadvantages:</p> <ul style="list-style-type: none"> <li>-Irregular forms are created;</li> <li>-Cell incorporation not tested.</li> </ul> <p>Minimum size produced ~20-50<math>\mu</math>m</p>	<p>[66,107]</p>
<p>Spray drying</p>		<p>Advantages:</p> <ul style="list-style-type: none"> <li>-Small molecules can be produced;</li> <li>-Large size of HMPs production.</li> </ul> <p>Disadvantages:</p> <ul style="list-style-type: none"> <li>-High HMPs polydispersity;</li> <li>-Expensive equipment;</li> <li>-Thermolabile polymers cannot be used.</li> </ul>	<p>[111]</p>

## 2.6. MAPs Tissue Engineering Applications

### 2.6.1. Bone

Bone fracture is one of the most common traumatic injuries, usually heals by cartilaginous callus formation. However, in elderly individuals or in extensive damages, the bone cannot properly heal. In these cases, the golden standard to improve bone regeneration is the utilization of autografts. [31,116,117] During the years, TE has presented an alternative to bone graft, one of the most commercialized is a collagen sponge with bone morphogenic protein (BMP-2), a growth factor that enhances bone formation, commercially called INFUSE™. However, this approach releases BMP-2 in a short period, leading to some constraints, such as immunologic diseases, heterotopic bone formation, that lead to chronic pain. [118]

In different trials with collagen HMPs was showed that the release of BMP-2 is affected by the cross-linking. The release was more sustainable in higher crosslinked HMPs. It was also demonstrated that larger HMPs sizes present a higher initial burst release comparing to the small ones, revealing that BMP-2 is not only dependent on diffusion. [119] Changing the polymer or the cross-linkers affects the growth factor release. For gelatin crosslinked with genipin, the BMP-2 is only released by the cell interaction with the HMPs. [120] The properties of individual HMPs are translated into a granular hydrogel once they are the unit on the bottom up-approach. With this, the cell interactions, different cross-linking degrees, sizes, or the encapsulation of specific bone proteins enabling a heterogeneous scaffold comparatively to a bulk hydrogel, leads promising future by implementing granular hydrogels with those optimizations.

As shown on hydrogel larger pore sizes have a better osteogenic differentiation than smaller ones. [121] This was applied to MAPs, where hierarchical nanofibrous HMPs, were injected into a bone defect. In this last example, the release of bioactive molecules was modulated with heparin interactions. [120,122] The larger pores on the HMPs increases cell infiltration leading to an increase of specific osteogenic gene expression, as well as cell viability, proliferation, as neovascularization. [52] In hierarchical annealed HMPs, large pores between the HMPs associated with the porosity created by the fibers that constituted the HMPs, showed a coadjuvant effect in increasing the cell migration with angiogenesis promotion. This scaffold also revealed useful as a cell delivery system once cells were protected from the shear forces inside the HMPs, once the HMPs act as a

Noah's Ark for cells, providing an adherence during the delivery in the bone cavity. [123,124] However, for this annealed system by UV light was necessary an open surgery due to the low penetration ability, which could be avoided with other annealing methodologies.

A determinant factor in bone regeneration is vascularization however, in most approaches, this factor is not pondered. [125] Simply, by VEGF incorporation in collagen–hydroxyapatite HMPs, the new vessel formation was improved, promoting the recruitment of pro-osteogenic cells and their differentiation. This combination associated with large pores could be easily adapted to granular hydrogels. Nevertheless, MAP had revealed a pro-angiogenic activity in other tissues. [126] Inducing mechanical stimulus during the healing process associated with cells, combined with transforming growth factor  $\beta$ 1 (TGF- $\beta$ 1), also a pro-angiogenic growth factor, encapsulated in gelatin microspheres in a granular system proved to increase the production of collagen type I, II, and X, that is essential to osteoregeneration. [114] Hierarchical HMPs annealed by UV light were implanted in a calvaria defect, increasing 83% of the bone volume comparatively to gelatin HMPs it was revealed also a neovascularization ability due to the blood vessel formation. [52]

Granular hydrogels can present several advances on bone TE due to their vascular recruitment ability, as cell penetration into the scaffold, increasing the regeneration process. However, for bone regeneration it is expected that larger HMPs be more effective than small ones, due to larger voids spaces because large porosity reveals better results. [127] The void spaces of granular hydrogels already showed to increase differentiation on osteocytes and regeneration because of the large, interconnected pores created, Figure 7. [31] It is expected the development of a granular hydrogel able to recruit not only osteoprogenitor cells but also vascular cells, due to the possibility of different growth factors combination. On the other hand, the stiffness of the granular hydrogels already developed are much lower than the ones founded on the bone, which could represent an inconvenience for cell differentiation.



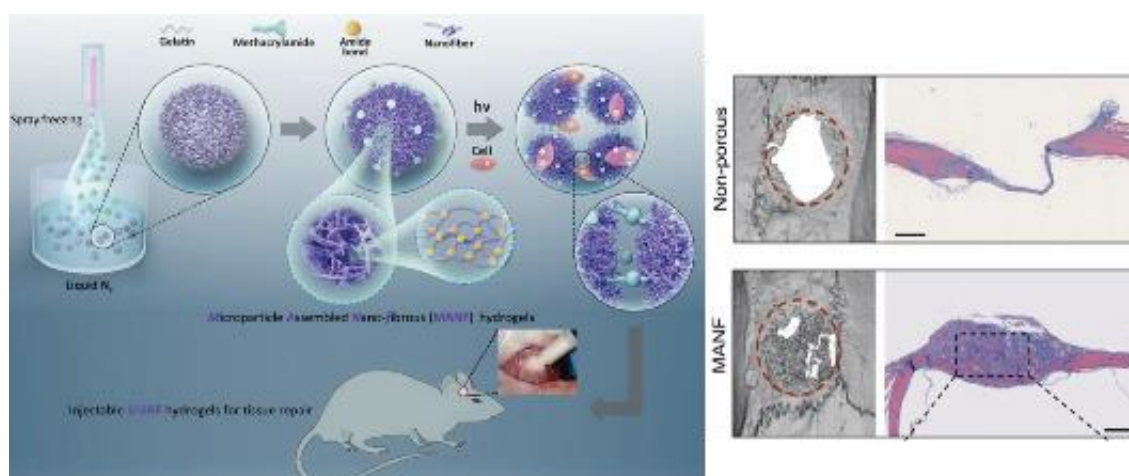


**Figure 7** Hierarchically HMPs (MANF) formation and bone volume and bone regeneration after 8 weeks, comparatively to a non-porous hydrogel. Reproduced with permission [31] Copyright 2019, Elsevier.

### 2.6.2. Cartilage

Articular cartilage can suffer severe damage due to traumas, inflammatory causes, or even age, and diseases such as osteoarthritis effects are caused by cartilage damage. The lack of vascularization, high cell density cartilage, and low chondrocyte proliferation, and low metabolic activity limits cartilage regeneration, and it represents an enormous challenge in TE. [128,129] In this term, HMPs developed as a growth factor delivery for chondrocyte differentiation, such as TGF- $\beta$ 1 showed an increase of cartilage formation. This work showed that HMPs can stimulate mesenchymal stem cells (MSC) into chondrocyte differentiation, due to the more controlled release of the factor, as well as, to increase the extracellular matrix such as glycosaminoglycans (GAG) deposition, preventing the formation of fibrous cartilage. [130]

The amount delivering the GF is also relevant for TE. Recently, the same amount of TGF- $\beta$ 1 deliver by a reduced number and a high number of HMPs revealed better results in the high number of HMPs. It could be explained by the higher diffusion rates between a larger number of HMPS as the larger structure is created with more places for cells to adhere. [130] As in the bone, the cross-linking is crucial, in HMPs with low cross-linking revealed an increase of GAG and collagen type II, the most common collagen in cartilage deposition particularly if loaded with TGF- $\beta$ 1. [105] This result was explained by the ease of degradation of HMPs and the fast release of TGF- $\beta$ 1, which play a crucial role in cartilaginous differentiation. The fast degradation of the HMPs provided empty spaces to

cell GAG deposition. [130] These principles could be later translated into a granular hydrogel by using softer and easily degradable HMPs.

Interestingly, HMPs produced with decellularized cartilage HMPs combined with collagen increased cell infiltration comparing with decellularized cartilage by itself due to their high dense native tissue, increasing proteoglycan production. [131] It would be intriguing to produce HMPs with decellularized cartilage for a granular hydrogel, once are expected great results.

Nevertheless, the complexity of the extracellular matrix, for modifications may difficult the process as well as the decellularization process, that may lead to protein denaturation or growth factors loss that would decrease the benefits of using a decellularized matrix. With gelatin HMPs, loaded with TGF- $\beta$ 1 combined with hMSC cultured in customized agarose wells to form a tube. The hMSC produced enough GAG to assemble the HMPs with the cells and form a ring, with stiffness adequate to handle it with tweezers. [106] In this approach to granular hydrogels, where the cells are responsible for maintaining the HMPs together. In this model, was able to resist axial plane compression with an improvement of neocartilage formation. With this would be interesting to combine extracellular matrix, ECM, HMPs with TGF- $\beta$  to see if they have a cooperative effect on cartilage formation

MAPs were also adapted for cartilage regeneration by assembling with PEG of gelatin HMPs with cells encapsulated. In this, cells were able to migrate to the surface of the HMPs and deposit ECM between the void spaces, showing an increase of viability and GAG deposition. [53] The delivery of MSC by HMPs, compared with bulk hydrogels or as cells in pallet, increased viability once it preserves the cell integrity and, at the same time, higher diffusion rates with the medium. Curiously, the cell-mediated assembled microgel produced more ECM to improve the interaction between microgels to increase the support. Recently, a cell encapsulated in HMPs, annealed *in situ*, increased cell viability after injection, *in vitro*, and *in vivo*. After 28 days after 28 days, the MAP scaffold had more cartilaginous matrix uniformly distributed across the whole construct, with a matrix deposition with higher quality than bulk hydrogels. [132] With this, it would be interesting to develop a jammed system that combined the delivery of GF as well as the cells. It will increase the differentiation to chondrocytes and accelerate the ECM deposition, which could be helpful in the clinic.

### 2.6.3. Nervous system

Neuronal damage, by stroke or traumatic injuries, is responsible long-term for disability worldwide, to solve that regenerative medicine has been trying to replace the lost neurons and re-establishing the ECM, or as well, create in vitro models to predict the evolution of these situations, to understand better the brain plasticity. [133] One of most difficulties is on hippocampal neural precursor cells (NPC) seeding, once they quickly reach confluency rapidly and went to a spontaneous differentiation, and form clusters, proving a poor control to the investigators. Recently, heparin HMPs were revealed to be useful, once they allowed the cell culture for later injection without differentiation and enabling the trypsinization. [134]

After damage in the neuronal system, the microglia start a reparation, though, due to the low neuron regeneration, it usually results in a glial scar formation, this is one of the major difficulties for the regeneration of a neuronal system. It was already showed that porous structures increase neuron viability and axonal infiltration. [135] Using non-spherical jammed HMPs, on a spinal cord injury was previously showed an improvement in the regeneration and remodeling of an injury by facilitating cell invasion and myelination by increasing the activated macrophages in the damaged area. [136] Cell encapsulation and delivery are other popular approaches, such as oligodendrocytes progenitor cells seeded in collagen HMPs these cells recruit white and grey matter to the injury area. [137] However, GF encapsulations also showed positive results. [77]

The encapsulation of VEGF on PLGA particles and inject them into a stroke cavity of a rat revealed an increase epithelial cells recruitment, which lead to hypervascularization. Nevertheless, around the stroke area, the formation of an astrocyte scar limited the cellular penetration and axon invasion. [77] The injection in CNS of brain-derived neurotrophic factor (BDNF) on PLGA particles. The sustainable release of particles proved to trigger TrkB receptors, responsible for neuronal survival and differentiation. [138]

The MAP injection into a stroke area by a minimum invasive procedure proved to be suitable for the neuronal system. The scaffold did not cause brain swelling or deformations, being able to fill the stroke cavity after five days. Comparing the MAP with nanoporous hydrogel or even without any hydrogels revealed a glial scar six times smaller. It also showed the ability of astrocyte infiltration of an average length of 279  $\mu\text{m}$  compared with 42  $\mu\text{m}$  of the nanoporous hydrogel. It has also revealed a proangiogenic on the peri-infarct environment, with 22% of vessels 3.6 higher than other conditions.

More interestingly, it allowed the neuronal stem cells infiltration into the granular hydrogel occupying 3.75% of the scaffold area only after ten days. [23]

Different types of annealing were tested on a stroke model, such as enzymatic or by guest-host. HMPs annealed by guest-host annealing chemistry revealed glial scar thickness reduction similar to the ones with FXIIIa, and a decrease of inflammatory monocytes (CD11+). [61] These examples of MAP injected into a stroke area are an excellent contribution to the treatment and recovery of a stroke. The HMPs used on these scaffolds could be heterogeneous with different rates of stiffness and injected, forming different layers as already shown in a stroke cavity. [60]

These examples of MAP injected into a stroke area are an excellent contribution to the treatment and recovery of a stroke. The HMPs used on these scaffolds could be heterogeneous with different rates of stiffness and injected, forming different layers as already shown in a stroke cavity. [60] It is expected growth factors or even cells to increase vascularization and cell recruitment in further studies. Long term studies would also reveal the benefits of using a MAP to verify the improvement axonal invasion of the granular area, and brain connections restoration as the lost abilities. The functionalization of HMPs for the MAP would probably present higher axon infiltration and is expected an immense evolution in this sense once MAP by itself already exhibits great results.

#### **2.6.4. Wound healing and vascularization**

Vascularization is crucial for damaged tissue regeneration, once is responsible for providing nutrients and gas exchange, mainly because the diffusion only is possible 100 to 200 $\mu$ m thickness [126], the vasculature formation remains a challenge for tissue engineering. [139] HMPs provide not only high diffusion rates but also allow the encapsulation of GF or pre-vascular cells. [76] HMPs have already been shown to increase factors the half-live time, as well as provide them controlled release, a 3D environment similar to reality. [18,65,77] The use of methacrylate gelatin HMPs injected with human umbilical vein endothelial cells, HUVECs promotes high capillaries formation than if only injected cells. The results were even better if the HUVECs were modified to produce higher VEGF quantities.

HMPs can also be used as a cell carrier to ischemic models was showed that only by delivery of  $10^6$  or  $10^7$  cells in an ischemic limb would have therapeutic effects it occurs

because only ~5% would survive. However, the encapsulations of a lower amount of MSCs niches ( $10^5$  cells) in gelatin had better results than an injection of MSC, with a blood flow similar to the non-ischemic limb, Figure 8a. [140] Encapsulating MSC and outgrowth endothelial cells(OEC) was observed a contraction of the HMPs, and then by testing without GF and in a hypoxic environment, usual conditions of ischemia revealed that the  $O_2$  and GF are essential to the vessels formations but not crucial to their maintenance. [141] In chick eggs, implantation demonstrated that the *in vitro* maturation with GF and regular levels of  $O_2$  were favorable to the migratory and invasive ability of the entrapped cells. A posterior study with a similar aggregate presented positive regulation of cell migration. [142] *In vivo* assays showed an endothelial cell network resembles capillary structures at seven days, and at 15 showed several bold vessels profusion. It would be interesting to develop an annealing process triggered by the reactive oxygen species, especially for vasculature. In the same perspective, a granular hydrogel able to deliver cells would theoretically increase de reparation and lead to vessel formation.

In wound healing, the HMPs developed, as in the other tissues, can deliver growth factors, and revealing an improvement of viability and wound closure. However, the skin was the first tissue where MAP was developed with an enzymatic cross-linking. Like in brain tests, granular hydrogels could be injected with different layers into the wound Figure 8b. [60] The void spaces on granular hydrogels facilitate the cell infiltration, increasing cell spreading after two days. [64] A granular hydrogel showed impressive results after 90 minutes, with the cell spreading markers are already present, with 93% of cell viability Figure 8c. [62] More interesting, this scaffold allowed the formation of new blood vessels, increasing not only the wound closure by epithelium formation but also with formation of small hair follicles after only five days, as well as small vessels. As expected, the annealed granular hydrogel injection decreased the peripheric inflammation, which will reduce the scar formation, however, the adhesiveness of this scaffold is not reported.

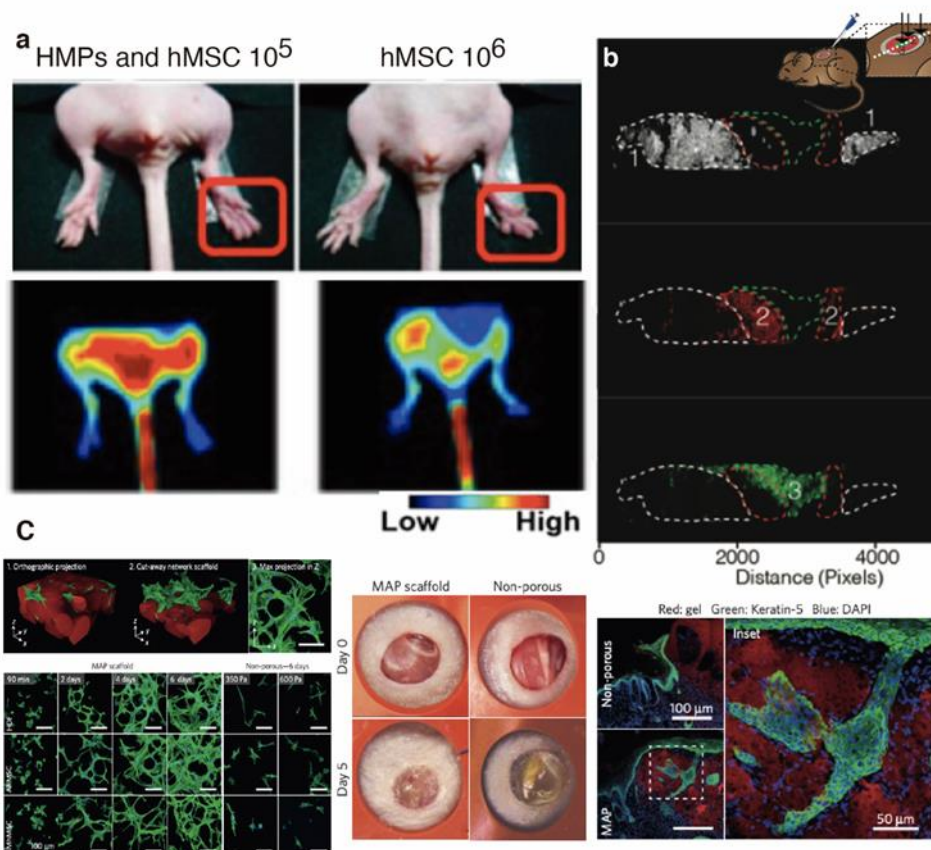


**Figure 8** Effects of HMPs or MAP in regeneration and in promoting angiogenesis a) Representative photographs of the difference between HMPs and only cells and blood monitorization perfusion in ischemic hindlimb with fluorescence imaging. Reproduced with permission [140] Copyright 2014, PNAS. b) Schematic of patterning method pipetting a granular hydrogel on wound and the intensity profile plot of each color microgel along the cross-section was generated. Reproduced with permission [60] Copyright 2018, Wiley. c) MAP for wound closures, with cells distributed along the HMPs, comparing with a non-porous scaffold; wound closure in relation to a non-porous hydrogel and Keratin-5 staining of the basement epithelial layer outline developing hair follicles and sebaceous glands within the MAP scaffold after five days. Reproduced with permission [62] Copyright 2015, Nature.

### 2.6.5. Other applications

Recently, conductive granular hydrogels were developed to this HMPs of hyaluronic acid modified with gallol groups were crosslinked by chelate with silver nanoparticles. [35] In this, the granular hydrogels showed connectivity, and it was five times higher *in situ* than in the *in-situ* bulk hydrogel with the same polymer. It was explained by the higher amount of silver in granular hydrogels due to their higher surface area. This granular hydrogel also provides muscle contractibility. This characteristic would be

useful for muscle lesions but also as a patch for cardiac tissue. This example shows the innumerable applications of granular hydrogels this and combining other HMPs with cells could be possible to increase the regeneration of tissues with low regeneration rates.

Granular hydrogels can use for drug or cell delivery or even as a scaffold, but some HMPs developed can also work as a simple diagnosis mechanism. For example, HMPs can be developed to detect DNA or miRNA faster than using microarrays or quantitative reverse chain. [109] Recently, a MAP produced using peptides with different chirality showed different immunologic responses. D peptides showed more recruitment of IL-33 and type 2 myeloid cells, which promoted more regeneration in wound healing, which revealed more follicles. [20] This simple approach by modified the chirality of the peptide to modulate the immune response is also a way to control the response to granular hydrogels. In the same point of view, MAP was also developed as a gene transfer. [16]

### **2.7. Granular hydrogel in 3D bioprinting**

3D bioprinting is a relatively recent technique in TE, it allows the scaffolds to manufacture with bio-functional components, as the extracellular matrix, drugs, or even cells. This technique allows personalized medicine by printing using a layer-by-layer approach to obtain 3D constructs of a specific device or scaffold, allowing a patient-specific treatment. Exits several types of 3D bioprinting such as microextrusion, inkjet, laser-assisted, or stereolithographic, though the last ones are not compatible with HMPs as the main constituent of the ink. [143,143,144] One of the main difficulties for 3D bioprinting is the ink composition, once it needs to be extrudable, forms a continuous filament during printing, needs to be able to build a multilayer structure, and at the same time, assure cytocompatibility, and ideally improve cell differentiation and proliferation. Most inks fail in building a multilayer structure, where the scaffold collapses due to the lack of physical strain, or sometimes the extrudability of the inks do not form a regular filament that will affect precision by the printing time. [144,145]

The granular hydrogels in a jammed state are a suitable candidate for ink constitution. They show extrudability, with high elasticity and low tensions, with the ability to form a continuous filament across needle transactions. The granular hydrogels are available to build several layers with high resolution. The printed resolution is affected by HMPs

sizes. The annealing increases the construct stability and can be procedure after or during the printing. [15,36]

HMPs annealed by click-chemistry enabled the printing of different multi-layers structures with high precision. This chemistry allowed complex anatomical structures construction, such as a nose or ears, Figure 9a. [11] The construct stability was increased by cross-linking the HMPs with UV light providing long-term stability and revealing high cellular viability. A microfluidic device directly connected bioprinter permits a faster process and by modifying the microfluidic flux, print with different types and densities HMPs, and facilitating the maintenance of sterile conditions. [15]

Generally, cells are mixed with HMPs, but these systems allow the encapsulation decreasing the shear strengths between the cells during printing, and because of this, increasing cell viability. To print cells in the HMPs is only necessary to maintain the sterile conditions, such as shown previously, with norbornene hyaluronic acid HMPs with fibroblasts encapsulated, Figure 9b. [36] The HMPs will be the main component for bioink production, most of the jamming procedures will lead to an increase of shear-thinning and self-healing proprieties [145] and unlimited combinations. Simple constructs, for example, a meniscus, are easily printed using PCL with PLGA HMPs encapsulating growth factors. [146] This composite ink tries to reproduce the meniscus complexity and to increase the differentiation on to cartilaginous cells. This scaffold had high cell biocompatibility, with chondrogenic markers expression when implemented on a goat knee. The seeded cells revealed a similar to a native meniscus with zonal expression collagen type I and II, and the goats could walk easily than the control group. Nonetheless, the PCL was melted to be printable of which is not compatible with cells encapsulation.

One of the most common 3D printing approaches is the utilization of a support bath. And a granular bath was revealed to be able to print complex structures with success. The HMPs sizes determine the printing precision. [147] For example, using a supporting bath with Carbopol HPMs avoided the surface tension, and at the same time, it does not require an interstitial fluid for the contrition, allowing the needle regression of the needle without composition or properties alteration. [83,147] By using chitosan, with non-spherical gelatin HMPs, this compromised the reliability of the filaments and precision,[107] but this problem was solved by using spherical and with low dispersity. [148] The actualized system allowed reliability until 20  $\mu\text{m}$  in diameter by contrast with 250  $\mu\text{m}$  in the mean



diameter of the non-spherical particle bath. [107] In this work, they were even able to print a tri-leaflet heart, with constructability ability, low regurgitation, and that resistance to high pressures. It was also possible to build with collagen in a neonatal-scale human heart, with high precision, and as expected the ink, revealed high cytocompatibility and even increased the formation of matrix and small vessels. [148] Recently a composite was used with gelatin HMPs immersed oxidized alginate. This way, by printing carbonyldiimidazole-modified gelatin, the ink crosslinked when contacted with the alginate in the bath, and the HMPs allowed support for the construction, Figure 9c. [149] With this, is expected the HMPs in the support bath acquire more functions, for example by releasing factors or nutrients for cells, and the support bath act as a bio stimulator for cell growth and differentiation. A cell spheroid supporting bath was already developed where a vessel was printed in between to assure the nutrients. In this example, an unlike approach provided the supporting bath a function besides the support and could be adapted to granular hydrogels if the supporting bath, for example, cells encapsulate. [150] The same could be applied to other tissues to replicate better tissue complexity, leading the encapsulated cells to provide the other cells with bioactive cues for their differentiation. This approach would open a new way to evaluate cell pathways on differentiation or even cancer and that may not be fully understood.

### **2.8. Conclusions and further perspectives**

We have mentioned characteristics of granular hydrogels can be modulated by several factors, since the HMPs properties or the annealing characteristics. Their ability to conjugate the TE foundations, cells, growth factors, and scaffold makes granular hydrogels a promising scaffold. These characteristics associated with injectability, porosity, modular design confers them a vast range of applications. In all the areas mentioned before is expected that granular hydrogels improve, especially in the different combinations of HMPs that can be delivered to the tissues.

To a better design of jammed HMPs, it is crucial to develop computational models that allow the preview of the mechanical properties of granular hydrogels, as well as biocompatibility. The computational modulation will provide information on how mechanical loading will affect granular hydrogels and more approaches that can be used to improve the granular hydrogels without consuming reagents's time, so in the future, the models will be indispensable to the development of most scaffolds.

With the rapid advance with drug designing technologies and stem cells, the functionality of HMPs applications will grow, as well as the granular hydrogels. They are presented as controlling and localized for gene therapy such as CRISP-Cas9 *in vivo* or even to localized drug delivery for cancer. In this last example form, a layer around the tumor is to deliver an antimetabolic agent. [151,152] The HMPs also likely to be developed with native tissue properties, by the inclusion of ECM, by controlled motion that can induce static or dynamic interparticle cross-linking, and this can improve a lot of cell differentiation.

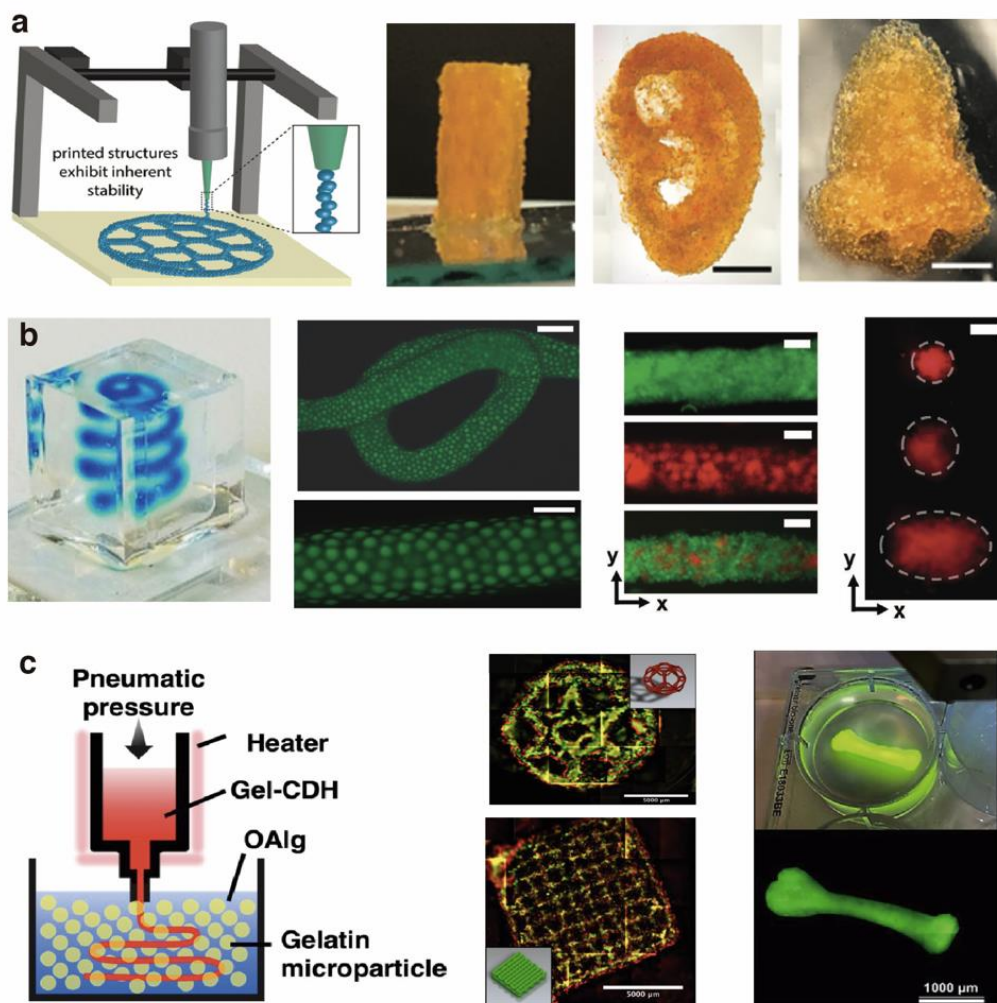


**Figure 9** Examples of HMPs on 3 D bioprinting. **a)** Scheme of printing a with the contraction of several layers and with precision to print a nose or an ear. Reproduced with permission [11] Copyright 2019, Royal Society of Chemistry. **b)** Filament of a granular ink an applications, as well as, their biocompatibility and different sizes of deposits Reproduced with permission [36] Copyright 2019, Wiley. **c)** Granular hydrogels as a supporting bath, with gelatin HMPs, and oxidized alginate for the cross-links. With a high ability to create complex structures, with cell biocompatibility, and structures anatomic like the bone Reproduced with permission [149] Copyright 2020, ASC.

The granular hydrogels are a portion of TE that has a large possibility to develop. The most recent jammed hydrogels solve injectability as diffusion of bulk hydrogels. Their transversal ability since drug delivery, to the ink composition, make these scaffolds an area with more interest, and investment, which will lead to new biomedical applications.

## 2.9. References

1. Mano, J.F. (2015) Designing biomaterials for tissue engineering based on the deconstruction of the native cellular environment. *Materials Letters*, 141, 198–202.
2. Kamata, H., Li, X., Chung, U., and Sakai, T. (2015) Design of Hydrogels for Biomedical Applications. *Adv. Healthcare Mater.*, 4 (16), 2360–2374.
3. Wang, L.-S., Chung, J.E., Pui-Yik Chan, P., and Kurisawa, M. (2010) Injectable biodegradable hydrogels with tunable mechanical properties for the stimulation of neurogenesis differentiation of human mesenchymal stem cells in 3D culture. *Biomaterials*, 31 (6), 1148–1157.
4. Hsu, R., Chen, P., Fang, J., Chen, Y., Chang, C., Lu, Y., and Hu, S. (2019) Adaptable Microporous Hydrogels of Propagating NGF - Gradient by Injectable Building Blocks for Accelerated Axonal Outgrowth. *Advanced Science*, 6 (16), 1900520.
5. Riley, L., Schirmer, L., and Segura, T. (2019) Granular hydrogels: emergent properties of jammed hydrogel microparticles and their applications in tissue repair and regeneration. *Current Opinion in Biotechnology*, 60, 1–8.
6. Judawisastra, H., Nugraha, F.R., and Wibowo, U.A. (2020) Porous Architecture Evaluation of Silk Fibroin Scaffold from Direct Dissolution Salt Leaching Method. *Macromol. Symp.*, 391 (1), 1900187.
7. Johnson, K., Muzzin, N., Toufanian, S., Slick, R.A., Lawlor, M.W., Seifried, B., Moquin, P., Latulippe, D., and Hoare, T. (2020) Drug-impregnated, pressurized gas expanded liquid-processed alginate hydrogel scaffolds for accelerated burn wound healing. *Acta Biomaterialia*, 112, 101–111.
8. Zhang, J., Wehrle, E., Vetsch, J.R., Paul, G.R., Rubert, M., and Müller, R. (2019) Alginate dependent changes of physical properties in 3D bioprinted cell-laden porous scaffolds affect cell viability and cell morphology. *Biomed. Mater.*, 14 (6), 065009.
9. Adhirajan, N., Shanmugasundaram, N., and Babu, M. (2007) Gelatin microspheres crosslinked with EDC as a drug delivery system for doxycycline: Development and characterization. *Journal of Microencapsulation*, 24 (7), 659–671.
10. Caldwell, A.S., Aguado, B.A., and Anseth, K.S. (2019) Designing Microgels for Cell Culture and Controlled Assembly of Tissue Microenvironments. *Adv. Funct. Mater.*, 1907670.
11. Xin, S., Chimene, D., Garza, J.E., Gaharwar, A.K., and Alge, D.L. (2019) Clickable PEG hydrogel microspheres as building blocks for 3D bioprinting. *Biomaterials Science*, 7 (3), ..
12. Correia, C.R., Sher, P., Reis, R.L., and Mano, J.F. (2013) Liquified chitosan–alginate multilayer capsules incorporating poly( L -lactic acid) microparticles as cell carriers. *Soft Matter*, 9 (7), 2125–2130.
13. Du, J., Du, P., and Smyth, H.D. (2013) Hydrogels for controlled pulmonary delivery. *Therapeutic Delivery*, 4 (10), 1293–1305.
14. Shahin, H.I., Vinjamuri, B.P., Mahmoud, A.A., Shamma, R.N., Mansour, S.M., Ammar, H.O., Ghorab, M.M., Chougule, M.B., and Chablani, L. (2019) Design and evaluation of novel inhalable sildenafil citrate spray-dried microparticles for pulmonary arterial hypertension. *Journal of Controlled Release*, 302, 126–139.
15. Xin, S., Dai, J., Gregory, C.A., Han, A., and Alge, D.L. (2020) Creating Physicochemical Gradients in Modular Microporous Annealed Particle Hydrogels via a Microfluidic Method. *Adv. Funct. Mater.*, 30 (6), 1907102.
16. Truong, N.F., Kurt, E., Tahmizyan, N., Leshner-Pérez, S.C., Chen, M., Darling, N.J., Xi, W., and Segura, T. (2019) Microporous annealed particle hydrogel stiffness, void space size, and adhesion properties impact cell proliferation, cell spreading, and gene transfer. *Acta Biomaterialia*, 94, 160–172.
17. Xue, C., Xie, H., Eichenbaum, J., Chen, Y., Wang, Y., den Dolder, F.W., Lee, J., Lee, K., Zhang, S., Sun, W., Sheikhi, A., Ahadian, S., Ashammakhi, N., Dokmeci, M.R., Kim, H., and Khademhosseini, A. (2020) Synthesis of Injectable Shear - Thinning Biomaterials of Various Compositions of Gelatin and Synthetic Silicate Nanoplatelet. *Biotechnol. J.*, 1900456.

18. Fang, J., Koh, J., Fang, Q., Qiu, H., Archang, M.M., Hasani - Sadrabadi, M.M., Miwa, H., Zhong, X., Sievers, R., Gao, D., Lee, R., Di Carlo, D., and Li, S. (2020) Injectable Drug - Releasing Microporous Annealed Particle Scaffolds for Treating Myocardial Infarction. *Adv. Funct. Mater.*, 2004307.
19. Alzanbaki, H., Moretti, M., and Hauser, C.A.E. (2021) Engineered Microgels—Their Manufacturing and Biomedical Applications. *Micromachines*, 12 (1), 45.
20. Newsom, J.P., Payne, K.A., and Krebs, M.D. (2019) Microgels: Modular, tunable constructs for tissue regeneration. *Acta Biomaterialia*, 88, 32–41.
21. Caldwell, A.S., Campbell, G.T., Shekiri, K.M.T., and Anseth, K.S. (2017) Clickable Microgel Scaffolds as Platforms for 3D Cell Encapsulation. *Adv. Healthcare Mater.*, 6 (15), 1700254.
22. Koh, J., Griffin, D.R., Archang, M.M., Feng, A.-C., Horn, T., Margolis, M., Zalazar, D., Segura, T., Scumpia, P.O., and Carlo, D.D. (2019) Enhanced In Vivo Delivery of Stem Cells using Microporous Annealed Particle Scaffolds. 10.
23. Nih, L.R., Sideris, E., Carmichael, S.T., and Segura, T. (2017) Injection of Microporous Annealing Particle (MAP) Hydrogels in the Stroke Cavity Reduces Gliosis and Inflammation and Promotes NPC Migration to the Lesion. *Adv. Mater.*, 29 (32), 1606471.
24. Behringer, R.P., and Chakraborty, B. (2019) The physics of jamming for granular materials: a review. *Rep. Prog. Phys.*, 82 (1), 012601.
25. Ramola, K., and Chakraborty, B. (2016) Disordered contact networks in jammed packings of frictionless disks. *J. Stat. Mech.*, 2016 (11), 114002.
26. Bi, D., and Chakraborty, B. (2009) Rheology of granular materials: dynamics in a stress landscape. *Proc. R. Soc. A*, 367 (1909), 5073–5090.
27. Rudge, R.E.D., van de Sande, J.P.M., Dijksman, J.A., and Scholten, E. (2020) Uncovering friction dynamics using hydrogel particles as soft ball bearings. *Soft Matter*, 16 (15), 3821–3831.
28. Jiang, J., Liu, A., Chen, C., Tang, J., Fan, H., Sun, J., and Fan, H. (2020) An efficient two-step preparation of photocrosslinked gelatin microspheres as cell carriers to support MC3T3-E1 cells osteogenic performance. *Colloids and Surfaces B: Biointerfaces*, 188, 110798.
29. Daly, A.C., Riley, L., Segura, T., and Burdick, J.A. (2019) Hydrogel microparticles for biomedical applications. *Nat Rev Mater*.
30. Arimura, H., Ouchi, T., Kishida, A., and Ohya, Y. (2005) Preparation of a hyaluronic acid hydrogel through polyion complex formation using cationic polylactide-based microspheres as a biodegradable cross-linking agent. *Journal of Biomaterials Science, Polymer Edition*, 16 (11), 1347–1358.
31. Khojasteh, A., Fahimipour, F., Eslaminejad, M.B., Jafarian, M., Jahangir, S., Bastami, F., Tahriri, M., Karkhaneh, A., and Tayebi, L. (2016) Development of PLGA-coated  $\beta$ -TCP scaffolds containing VEGF for bone tissue engineering. *Materials Science and Engineering: C*, 69, 780–788.
32. Wyss, C.S., Karami, P., Bourban, P.-E., and Pioletti, D.P. (2020) Hybrid granular hydrogels: combining composites and microgels for extended ranges of material properties. *Soft Matter*, 16 (15), 3769–3778.
33. Baumgarten, K., and Tighe, B.P. (2017) Viscous forces and bulk viscoelasticity near jamming. *Soft Matter*, 13 (45), 8368–8378.
34. Darling, N.J., Xi, W., Sideris, E., Anderson, A.R., Pong, C., Carmichael, S.T., and Segura, T. (2020) Click by Click Microporous Annealed Particle (MAP) Scaffolds. *Adv. Healthcare Mater.*, 1901391.
35. Shin, M., Song, K.H., Burrell, J.C., Cullen, D.K., and Burdick, J.A. (2019) Injectable and Conductive Granular Hydrogels for 3D Printing and Electroactive Tissue Support. *Advanced Science*, 1901229.
36. Highley, C.B., Song, K.H., Daly, A.C., and Burdick, J.A. (2019) Jammed Microgel Inks for 3D Printing Applications. *Adv. Sci.*, 6 (1), 1801076.
37. Kurzbach, D., Junk, M.J.N., and Hinderberger, D. (2013) Nanoscale Inhomogeneities in Thermoresponsive Polymers. *Macromol. Rapid Commun.*, 34 (2), 119–134.
38. Drozdov, A.D., and Christiansen, J. deClaville (2020) Equilibrium swelling of thermo-responsive copolymer microgels. *RSC Adv.*, 10 (70), 42718–42732.
39. Hirokawa, Y., and Tanaka, T. Volume phase transition in a non - ionic gel. 7.
40. Chaudhary, G., Ghosh, A., Bharadwaj, N.A., Kang, J.G., Braun, P.V., Schweizer, K.S., and Ewoldt, R.H. (2019) Thermoresponsive Stiffening with Microgel Particles in a Semiflexible Fibrin Network. *Macromolecules*, 52 (8), 3029–3041.
41. Hoang Thi, T.T., Sinh, L.H., Huynh, D.P., Nguyen, D.H., and Huynh, C. (2020) Self-Assemblable Polymer Smart-Blocks for Temperature-Induced Injectable Hydrogel in Biomedical Applications. *Front. Chem.*, 8, 19.

42. Ferreira, L., Vidal, M.M., and Gil, M.H. (2000) Evaluation of poly(2-hydroxyethyl methacrylate) gels as drug delivery systems at different pH values. *International Journal of Pharmaceutics*, 194 (2), 169–180.
43. Kim, S., and Jung, S. (2020) Biocompatible and self-recoverable succinoglycan dialdehyde-crosslinked alginate hydrogels for pH-controlled drug delivery. *Carbohydrate Polymers*, 250, 116934.
44. Hong, S.H., Shin, M., Park, E., Ryu, J.H., Burdick, J.A., and Lee, H. (2019) Alginate - Boronic Acid: pH - Triggered Bioinspired Glue for Hydrogel Assembly. *Adv. Funct. Mater.*, 1908497.
45. Berger, J., Reist, M., Mayer, J.M., Felt, O., Peppas, N.A., and Gurny, R. (2004) Structure and interactions in covalently and ionically crosslinked chitosan hydrogels for biomedical applications. *European Journal of Pharmaceutics and Biopharmaceutics*, 57 (1), 19–34.
46. Koutsopoulos, S. (2016) Self-assembling peptide nanofiber hydrogels in tissue engineering and regenerative medicine: Progress, design guidelines, and applications: Self-Assembling Peptides in Tissue Engineering and Regeneration. *J. Biomed. Mater. Res.*, 104 (4), 1002–1016.
47. Lovett, M., Lee, K., Edwards, A., and Kaplan, D.L. *Vascularization Strategies for Tissue Engineering*. 24.
48. Shanbhag, B.K., Liu, C., Haritos, V.S., and He, L. (2018) Understanding the Interplay between Self-Assembling Peptides and Solution Ions for Tunable Protein Nanoparticle Formation. *ACS Nano*, 12 (7), 6956–6967.
49. Xie, D., Sun, Y., Wang, L., Li, X., Zang, C., Zhi, Y., and Sun, L. (2016) Ultraviolet light-emitting diode irradiation-induced cell death in HL-60 human leukemia cells in vitro. *Molecular Medicine Reports*, 13 (3), 2506–2510.
50. Sheikhi, A., de Rutte, J., Haghniaz, R., Akouissi, O., Sohrabi, A., Di Carlo, D., and Khademhosseini, A. (2019) Microfluidic-enabled bottom-up hydrogels from annealable naturally-derived protein microbeads. *Biomaterials*, 192, 560–568.
51. Sheikhi, A., de Rutte, J., Haghniaz, R., Akouissi, O., Sohrabi, A., Di Carlo, D., and Khademhosseini, A. (2019) Modular microporous hydrogels formed from microgel beads with orthogonal thermo-chemical responsivity: Microfluidic fabrication and characterization. *MethodsX*, 6, 1747–1752.
52. Hou, S., Niu, X., Li, L., Zhou, J., Qian, Z., Yao, D., Yang, F., Ma, P.X., and Fan, Y. (2019) Simultaneous nano- and microscale structural control of injectable hydrogels via the assembly of nanofibrous protein microparticles for tissue regeneration. *Biomaterials*, 223, 119458.
53. Li, F., Truong, V.X., Fisch, P., Levinson, C., Glattauer, V., Zenobi-Wong, M., Thissen, H., Forsythe, J.S., and Frith, J.E. (2018) Cartilage tissue formation through assembly of microgels containing mesenchymal stem cells. *Acta Biomaterialia*, 77, 48–62.
54. Xin, S., Wyman, O.M., and c, D.L. (2018) Assembly of PEG Microgels into Porous Cell-Instructive 3D Scaffolds via Thiol-Ene Click Chemistry. *Adv. Healthcare Mater.*, 7 (11), 1800160.
55. Xin, S., Gregory, C., and Alge, D.L. (2019) Interplay Between Degradability and Integrin Signaling on Mesenchymal Stem Cell Function within Poly(ethylene glycol) Based Microporous Annealed Particle Hydrogels. *Acta Biomaterialia*, S1742706119307494.
56. Nakajima, S., Lan, L., Kanno, S., Takao, M., Yamamoto, K., Eker, A.P.M., and Yasui, A. (2004) UV Light-induced DNA Damage and Tolerance for the Survival of Nucleotide Excision Repair-deficient Human Cells. *Journal of Biological Chemistry*, 279 (45), 46674–46677.
57. Ren, P., Wang, F., Bernaerts, K.V., Fu, Y., Hu, W., Zhou, N., Dai, J., Liang, M., and Zhang, T. (2020) Self-Assembled Supramolecular Hybrid Hydrogels Based on Host–Guest Interaction: Formation and Application in 3D Cell Culture. *ACS Appl. Bio Mater.*, 3 (10), 6768–6778.
58. Mealy, J.E., Chung, J.J., Jeong, H.-H., Issadore, D., Lee, D., Atluri, P., and Burdick, J.A. (2018) Injectable Granular Hydrogels with Multifunctional Properties for Biomedical Applications. *Advanced Materials*, 30 (20), 1705912.
59. Dimatteo, R., Darling, N.J., and Segura, T. (2018) In situ forming injectable hydrogels for drug delivery and wound repair. *Advanced Drug Delivery Reviews*, 127, 167–184.
60. Darling, N.J., Sideris, E., Hamada, N., Carmichael, S.T., and Segura, T. (2018) Injectable and Spatially Patterned Microporous Annealed Particle (MAP) Hydrogels for Tissue Repair Applications. *Adv. Sci.*, 5 (11), 1801046.
61. Darling, N.J., Xi, W., Sideris, E., Anderson, A., Pong, C., Carmichael, S.T., and Segura, T. (2019) Click by Click Microporous Annealed Particle (MAP) Scaffolds.
62. Griffin, D.R., Weaver, W.M., Scumpia, P.O., Di Carlo, D., and Segura, T. (2015) Accelerated wound healing by injectable microporous gel scaffolds assembled from annealed building blocks. *Nature Mater*, 14 (7), 737–744.

63. de Rutte, J.M., Koh, J., and Di Carlo, D. (2019) Scalable High - Throughput Production of Modular Microgels for In Situ Assembly of Microporous Tissue Scaffolds. *Adv. Funct. Mater.*, 29 (25), 1900071.
64. Sideris, E., Griffin, D.R., Ding, Y., Li, S., Weaver, M., Carlo, D.D., Hsiai, T., and Segura, T. (2016) Particle hydrogels based on hyaluronic acid building blocks. 23.
65. Mendes, B.B., Daly, A.C., Reis, R.L., Domingues, R.M.A., Gomes, M.E., and Burdick, J.A. (2020) Injectable hyaluronic acid and platelet lysate-derived granular hydrogels for biomedical applications. *Acta Biomaterialia*, S1742706120306383.
66. Zhang, H., Cong, Y., Osi, A.R., Zhou, Y., Huang, F., Zaccaria, R.P., Chen, J., Wang, R., and Fu, J. (2020) Direct 3D Printed Biomimetic Scaffolds Based on Hydrogel Microparticles for Cell Spheroid Growth. *Adv. Funct. Mater.*, 30 (13), 1910573.
67. Farris, E., Brown, D.M., Ramer-Tait, A.E., and Pannier, A.K. (2017) Chitosan-zein nano-microparticles capable of mediating in vivo transgene expression following oral delivery. *Journal of Controlled Release*, 249, 150–161.
68. Yoo, C.Y., Seong, J.S., and Park, S.N. (2016) Preparation of novel capsosome with liposomal core by layer-by-Layer self-assembly of sodium hyaluronate and chitosan. *Colloids Surf B Biointerfaces*, 144, 99–107.
69. Chen, X.Y., Butt, A.M., and Mohd Amin, M.C.I. (2019) Molecular Evaluation of Oral Immunogenicity of Hepatitis B Antigen Delivered by Hydrogel Microparticles. *Mol. Pharmaceutics*, 16 (9), 3853–3872.
70. Shi, F., Tian, X., McClements, D.J., Chang, Y., Shen, J., and Xue, C. (2021) Influence of molecular weight of an anionic marine polysaccharide (sulfated fucan) on the stability and digestibility of multilayer emulsions: Establishment of structure-function relationships. *Food Hydrocolloids*, 113, 106418.
71. Kozłowska, J., Stachowiak, N., and Sionkowska, A. (2018) Collagen/Gelatin/Hydroxyethyl Cellulose Composites Containing Microspheres Based on Collagen and Gelatin: Design and Evaluation. *Polymers*, 10 (4), 456.
72. Herberg, S., Varghai, D., Cheng, Y., Dikina, A.D., Dang, P.N., Rolle, M.W., and Alsberg, E. (2018) High-density human mesenchymal stem cell rings with spatiotemporally-controlled morphogen presentation as building blocks for engineering bone diaphyseal tissue. *Nanotheranostics*, 2 (2), 128–143.
73. Griffin, D.R., Archang, M.M., Kuan, C.-H., Weaver, W.M., Weinstein, J.S., Feng, A.C., Ruccia, A., Sideris, E., Ragkousis, V., Koh, J., Plikus, M.V., Di Carlo, D., Segura, T., and Scumpia, P.O. (2020) Activating an adaptive immune response from a hydrogel scaffold imparts regenerative wound healing. *Nat. Mater.*
74. Secret, E., Crannell, K.E., Kelly, S.J., Villancio-Wolter, M., and Andrew, J.S. (2015) Matrix metalloproteinase-sensitive hydrogel microparticles for pulmonary drug delivery of small molecule drugs or proteins. *J. Mater. Chem. B*, 3 (27), 5629–5634.
75. Taz, M., Makkar, P., Imran, K.M., Jang, D.W., Kim, Y.-S., and Lee, B.-T. (2019) Bone regeneration of multichannel biphasic calcium phosphate granules supplemented with hyaluronic acid. *Materials Science and Engineering: C*, 99, 1058–1066.
76. Nakamura, S., Kanatani, Y., Kishimoto, S., Nakamura, S., Ohno, C., Horio, T., Masanori, F., Hattori, H., Tanaka, Y., Kiyosawa, T., Maehara, T., and Ishihara, M. (2009) Controlled release of FGF-2 using fragmin/protamine microparticles and effect on neovascularization. *J. Biomed. Mater. Res.*, 91A (3), 814–823.
77. Bible, E., Qutachi, O., Chau, D.Y.S., Alexander, M.R., Shakesheff, K.M., and Modo, M. (2012) Neo-vascularization of the stroke cavity by implantation of human neural stem cells on VEGF-releasing PLGA microparticles. *Biomaterials*, 33 (30), 7435–7446.
78. Nguyen, A.H., McKinney, J., Miller, T., Bongiorno, T., and McDevitt, T.C. (2015) Gelatin methacrylate microspheres for controlled growth factor release. *Acta Biomaterialia*, 13, 101–110.
79. Solorio, L.D., Dhami, C.D., Dang, P.N., Vieregge, E.L., and Alsberg, E. (2012) Spatiotemporal Regulation of Chondrogenic Differentiation with Controlled Delivery of Transforming Growth Factor- $\beta$ 1 from Gelatin Microspheres in Mesenchymal Stem Cell Aggregates. *STEM CELLS Translational Medicine*, 1 (8), 632–639.
80. Benoit, M.-A., Baras, B., and Gillard, J. (1999) Preparation and characterization of protein-loaded poly( $\epsilon$ -caprolactone) microparticles for oral vaccine delivery. *International Journal of Pharmaceutics*, 184 (1), 73–84.
81. Timm, K., Myant, C., Spikes, H.A., and Grunze, M. (2011) Particulate lubricants in cosmetic applications. *Tribology International*, 44 (12), 1695–1703.

82. Bhattacharjee, T., Kabb, C.P., O'Bryan, C.S., Urueña, J.M., Sumerlin, B.S., Sawyer, W.G., and Angelini, T.E. (2018) Polyelectrolyte scaling laws for microgel yielding near jamming. *Soft Matter*, 14 (9), 1559–1570.
83. Jin, Y., Compaan, A., Bhattacharjee, T., and Huang, Y. (2016) Granular gel support-enabled extrusion of three-dimensional alginate and cellular structures. *Biofabrication*, 8 (2), 025016.
84. Cheng, W., Zhang, J., Liu, J., and Yu, Z. (2020) Granular hydrogels for 3D bioprinting applications. *View*, 20200060.
85. Jin, J., Wang, J., Lu, Y., Fan, Z., Huang, N., Ma, L., and Yu, H. (2019) Platelet-Derived Microparticles: A New Index of Monitoring Platelet Activation and Inflammation in Kawasaki Disease. *Indian J Pediatr*, 86 (3), 250–255.
86. Gan, D., Xing, W., Jiang, L., Fang, J., Zhao, C., Ren, F., Fang, L., Wang, K., and Lu, X. (2019) Plant-inspired adhesive and tough hydrogel based on Ag-Lignin nanoparticles-triggered dynamic redox catechol chemistry. *Nature Communications*, 10 (1).
87. Morley, C.D., Ellison, S.T., Bhattacharjee, T., O'Bryan, C.S., Zhang, Y., Smith, K.F., Kabb, C.P., Sebastian, M., Moore, G.L., Schulze, K.D., Niemi, S., Sawyer, W.G., Tran, D.D., Mitchell, D.A., Sumerlin, B.S., Flores, C.T., and Angelini, T.E. (2019) Quantitative characterization of 3D bioprinted structural elements under cell generated forces. *Nat Commun*, 10 (1), 3029.
88. Bhattacharjee, T., and Angelini, T.E. (2019) 3D T cell motility in jammed microgels. *J. Phys. D: Appl. Phys.*, 52 (2), 024006.
89. Smith, L.R., Irianto, J., Xia, Y., Pfeifer, C.R., and Discher, D.E. (2019) Constricted migration modulates stem cell differentiation. *MBoC*, 30 (16), 1985–1999.
90. Caldwell, A.S., Rao, V.V., Golden, A.C., and Anseth, K.S. (2020) Porous bio-click microgel scaffolds control hMSC interactions and promote their secretory properties. *Biomaterials*, 232, 119725.
91. Liu, Q., Zhao, M., Mytnyk, S., Klemm, B., Zhang, K., Wang, Y., Yan, D., Mendes, E., and van Esch, J.H. (2019) Self-Orienting Hydrogel Micro-Buckets as Novel Cell Carriers. *Angew. Chem. Int. Ed.*, 58 (2), 547–551.
92. Kamperman, T., Henke, S., van den Berg, A., Shin, S.R., Tamayol, A., Khademhosseini, A., Karperien, M., and Leijten, J. (2017) Single Cell Microgel Based Modular Bioinks for Uncoupled Cellular Micro- and Macroenvironments. *Adv. Healthcare Mater.*, 6 (3), 1600913.
93. Xu, Y., Jacquat, R.P.B., Shen, Y., Vigolo, D., Morse, D., Zhang, S., and Knowles, T.P.J. (2020) Microfluidic Templating of Spatially Inhomogeneous Protein Microgels. *Small*, 2000432.
94. Jans, A., Lölsberg, J., Omidinia-Anarkoli, A., Viermann, R., Möller, M., De Laporte, L., Wessling, M., and Kuehne, A.J.C. (2019) High-Throughput Production of Micrometer Sized Double Emulsions and Microgel Capsules in Parallelized 3D Printed Microfluidic Devices. *Polymers*, 11 (11), 1887.
95. Swieszkowski, W., Dokmeci, M.R., and Khademhosseini, A. (2020) Microfluidics in biofabrication. *Biofabrication*, 12 (3), 030201.
96. Isozaki, A., Nakagawa, Y., Loo, M.H., Shibata, Y., Tanaka, N., Setyaningrum, D.L., Park, J.-W., Shirasaki, Y., Mikami, H., Huang, D., Tsoi, H., Riche, C.T., Ota, T., Miwa, H., Kanda, Y., Ito, T., Yamada, K., Iwata, O., Suzuki, K., Ohnuki, S., Ohya, Y., Kato, Y., Hasunuma, T., Matsusaka, S., Yamagishi, M., Yazawa, M., Uemura, S., Nagasawa, K., Watarai, H., Di Carlo, D., and Goda, K. (2020) Sequentially addressable dielectrophoretic array for high-throughput sorting of large-volume biological compartments. *Sci. Adv.*, 6 (22), eaba6712.
97. Choi, Y.H., Kim, S.-H., Kim, I.-S., Kim, K., Kwon, S.K., and Hwang, N.S. (2019) Gelatin-based micro-hydrogel carrying genetically engineered human endothelial cells for neovascularization. *Acta Biomaterialia*, 95, 285–296.
98. Xu, Y., Peng, J., Richards, G., Lu, S., and Eglin, D. (2019) Optimization of electrospray fabrication of stem cell-embedded alginate–gelatin microspheres and their assembly in 3D-printed poly( $\epsilon$ -caprolactone) scaffold for cartilage tissue engineering. *Journal of Orthopaedic Translation*, 18, 128–141.
99. Naqvi, S.M., Vedicherla, S., Gansau, J., McIntyre, T., Doherty, M., and Buckley, C.T. (2016) Living Cell Factories - Electrosprayed Microcapsules and Microcarriers for Minimally Invasive Delivery. *Adv. Mater.*, 28 (27), 5662–5671.
100. García Cruz, D.M., Sardinha, V., Escobar Ivirico, J.L., Mano, J.F., and Gómez Ribelles, J.L. (2013) Gelatin microparticles aggregates as three-dimensional scaffolding system in cartilage engineering. *J Mater Sci: Mater Med*, 24 (2), 503–513.
101. Kudva, A.K., Dikina, A.D., Luyten, F.P., Alsberg, E., and Patterson, J. (2019) Gelatin microspheres releasing transforming growth factor drive in vitro chondrogenesis of human periosteum derived cells in micromass culture. *Acta Biomaterialia*, 90, 287–299.

102. Adhirajan, N., Thanavel, R., Naveen, N., Uma, T.S., and Babu, M. (2014) Functionally modified gelatin microspheres as a growth factor's delivery system: development and characterization. *Polym. Bull.*, 71 (4), 1015–1030.
103. Seong, Y.-J., Lin, G., Kim, B.J., Kim, H.-E., Kim, S., and Jeong, S.-H. (2019) Hyaluronic Acid-Based Hybrid Hydrogel Microspheres with Enhanced Structural Stability and High Injectability. *ACS Omega*, 4 (9), 13834–13844.
104. Blocki, A., Löper, F., Chirico, N., Neffe, A.T., Jung, F., Stamm, C., and Lendlein, A. (2017) Engineering of cell-laden gelatin-based microgels for cell delivery and immobilization in regenerative therapies. *CH*, 67 (3–4), 251–259.
105. Solorio, L.D., Vieregge, E.L., Dhimi, C.D., Dang, P.N., and Alsberg, E. (2012) Engineered cartilage via self-assembled hMSC sheets with incorporated biodegradable gelatin microspheres releasing transforming growth factor- $\beta$ 1. *Journal of Controlled Release*, 158 (2), 224–232.
106. Dikina, A.D., Strobel, H.A., Lai, B.P., Rolle, M.W., and Alsberg, E. (2015) Engineered cartilaginous tubes for tracheal tissue replacement via self-assembly and fusion of human mesenchymal stem cell constructs. *Biomaterials*, 52, 452–462.
107. Hinton, T.J., Jallerat, Q., Palchesko, R.N., Park, J.H., Grodzicki, M.S., Shue, H.-J., Ramadan, M.H., Hudson, A.R., and Feinberg, A.W. (2015) Three-dimensional printing of complex biological structures by freeform reversible embedding of suspended hydrogels. *Sci. Adv.*, 1 (9), e1500758.
108. Jung, I.Y., Kim, J.S., Choi, B.R., Lee, K., and Lee, H. (2017) Hydrogel Based Biosensors for In Vitro Diagnostics of Biochemicals, Proteins, and Genes. *Adv. Healthcare Mater.*, 6 (12), 1601475.
109. Roh, Y.H., Lee, H.J., Moon, H.J., Kim, S.M., and Bong, K.W. (2019) Post-synthesis functionalized hydrogel microparticles for high performance microRNA detection. *Analytica Chimica Acta*, 1076, 110–117.
110. Du, H., Cont, A., Steinacher, M., and Amstad, E. (2018) Fabrication of Hexagonal-Prismatic Granular Hydrogel Sheets. *Langmuir*, 34 (11), 3459–3466.
111. Cunha, L., Rodrigues, S., Rosa da Costa, A.M., Faleiro, L., Buttini, F., and Grenha, A. (2019) Inhalable chitosan microparticles for simultaneous delivery of isoniazid and rifabutin in lung tuberculosis treatment. *Drug Development and Industrial Pharmacy*, 45 (8), 1313–1320.
112. Liu, H.-Y., Korc, M., and Lin, C.-C. (2018) Biomimetic and enzyme-responsive dynamic hydrogels for studying cell-matrix interactions in pancreatic ductal adenocarcinoma. *Biomaterials*, 160, 24–36.
113. Davidson, M.D., Ban, E., Schoonen, A.C.M., Lee, M., D'Este, M., Shenoy, V.B., and Burdick, J.A. (2019) Mechanochemical Adhesion and Plasticity in Multifiber Hydrogel Networks. *Adv. Mater.*, 1905719.
114. McDermott, A.M., Herberg, S., Mason, D.E., Collins, J.M., Pearson, H.B., Dawahare, J.H., Tang, R., Patwa, A.N., Grinstaff, M.W., Kelly, D.J., Alsberg, E., and Boerckel, J.D. (2019) Recapitulating bone development through engineered mesenchymal condensations and mechanical cues for tissue regeneration. *Science Translational Medicine*, 11 (495), eaav7756.
115. Kim, S.-N., Choi, B.H., Kim, H.K., and Choy, Y.B. (2019) Poly(lactic-co-glycolic acid) microparticles in fibrin glue for local, sustained delivery of bupivacaine. *Journal of Industrial and Engineering Chemistry*, 75, 86–92.
116. Sheehy, E.J., Kelly, D.J., and O'Brien, F.J. (2019) Biomaterial-based endochondral bone regeneration: a shift from traditional tissue engineering paradigms to developmentally inspired strategies. *Materials Today Bio*, 3, 100009.
117. Pina, S., Oliveira, J.M., and Reis, R.L. (2015) Natural-Based Nanocomposites for Bone Tissue Engineering and Regenerative Medicine: A Review. *Adv. Mater.*, 27 (7), 1143–1169.
118. Donos, N., Dereka, X., and Calciolari, E. (2019) The use of bioactive factors to enhance bone regeneration: A narrative review. *J Clin Periodontol*, 46, 124–161.
119. Mumcuoglu, D., de Miguel, L., Jekhmane, S., Siverino, C., Nickel, J., Mueller, T.D., van Leeuwen, J.P., van Osch, G.J., and Kluijtmans, S.G. (2018) Collagen I derived recombinant protein microspheres as novel delivery vehicles for bone morphogenetic protein-2. *Materials Science and Engineering: C*, 84, 271–280.
120. Solorio, L., Zwolinski, C., Lund, A.W., Farrell, M.J., and Stegemann, J.P. (2010) Gelatin microspheres crosslinked with genipin for local delivery of growth factors. *J Tissue Eng Regen Med*, 4 (7), 514–523.
121. Pereira, H.F., Cengiz, I.F., Silva, F.S., Reis, R.L., and Oliveira, J.M. (2020) Scaffolds and coatings for bone regeneration. *J Mater Sci: Mater Med*, 31 (3), 27.
122. Ma, C., Jing, Y., Sun, H., and Liu, X. (2015) Hierarchical Nanofibrous Microspheres with Controlled Growth Factor Delivery for Bone Regeneration. 10.



123. Wei, D.-X., Dao, J.-W., and Chen, G.-Q. (2018) A Micro-Ark for Cells: Highly Open Porous Polyhydroxyalkanoate Microspheres as Injectable Scaffolds for Tissue Regeneration. *Advanced Materials*, 30 (31), 1802273.
124. Hossain, K.M.Z., Patel, U., Kennedy, A.R., Macri-Pellizzeri, L., Sottile, V., Grant, D.M., Scammell, B.E., and Ahmed, I. (2018) Porous calcium phosphate glass microspheres for orthobiologic applications. *Acta Biomaterialia*, 72, 396–406.
125. Hernández-González, A.C., Téllez-Jurado, L., and Rodríguez-Lorenzo, L.M. (2020) Alginate hydrogels for bone tissue engineering, from injectables to bioprinting: A review. *Carbohydrate Polymers*, 229, 115514.
126. Quinlan, E., López-Noriega, A., Thompson, E.M., Hibbitts, A., Cryan, S.A., and O'Brien, F.J. (2017) Controlled release of vascular endothelial growth factor from spray-dried alginate microparticles in collagen-hydroxyapatite scaffolds for promoting vascularization and bone repair: Functionalized CHA scaffolds for controlled release of VEGF to enhance bone repair. *J Tissue Eng Regen Med*, 11 (4), 1097–1109.
127. Liu, F., Ran, Q., Zhao, M., Zhang, T., Zhang, D.Z., and Su, Z. (2020) Additively Manufactured Continuous Cell-Size Gradient Porous Scaffolds: Pore Characteristics, Mechanical Properties and Biological Responses In Vitro. *Materials*, 13 (11), 2589.
128. Leong, W., Lau, T.T., and Wang, D.-A. (2013) A temperature-cured dissolvable gelatin microsphere-based cell carrier for chondrocyte delivery in a hydrogel scaffolding system. *Acta Biomaterialia*, 9 (5), 6459–6467.
129. Wei, W., Ma, Y., Yao, X., Zhou, W., Wang, X., Li, C., Lin, J., He, Q., Leptihn, S., and Ouyang, H. (2021) Advanced hydrogels for the repair of cartilage defects and regeneration. *Bioactive Materials*, 6 (4), 998–1011.
130. Dang, P.N., Solorio, L.D., and Alsberg, E. (2014) Driving Cartilage Formation in High-Density Human Adipose-Derived Stem Cell Aggregate and Sheet Constructs Without Exogenous Growth Factor Delivery. 13.
131. Novak, T., Seelbinder, B., Twitchell, C.M., Voytik-Harbin, S.L., and Neu, C.P. (2016) Dissociated and Reconstituted Cartilage Microparticles in Densified Collagen Induce Local hMSC Differentiation. *Adv. Funct. Mater.*, 26 (30), 5427–5436.
132. Li, F., Levinson, C., Truong, V.X., Laurent-Applegate, L.A., Maniura-Weber, K., Thissen, H., Forsythe, J.S., Zenobi-Wong, M., and Frith, J.E. (2020) Microencapsulation improves chondrogenesis in vitro and cartilaginous matrix stability in vivo compared to bulk encapsulation. *Biomater. Sci.*, 8 (6), 1711–1725.
133. George, J., Hsu, C.-C., Nguyen, L.T.B., Ye, H., and Cui, Z. (2019) Neural tissue engineering with structured hydrogels in CNS models and therapies. *Biotechnology Advances*, S073497501930045X.
134. Newland, B., Ehret, F., Hoppe, F., Eigel, D., Pette, D., Newland, H., Welzel, P.B., Kempermann, G., and Werner, C. (2019) Macroporous heparin-based microcarriers allow long-term 3D culture and differentiation of neural precursor cells. *Biomaterials*, 119540.
135. Broguiere, N., Husch, A., Palazzolo, G., Bradke, F., Madduri, S., and Zenobi-Wong, M. (2019) Macroporous hydrogels derived from aqueous dynamic phase separation. *Biomaterials*, 200, 56–65.
136. Chedly, J., Soares, S., Montebault, A., von Boxberg, Y., Veron-Ravaille, M., Mouffle, C., Benassy, M.-N., Taxi, J., David, L., and Nothias, F. (2017) Physical chitosan microhydrogels as scaffolds for spinal cord injury restoration and axon regeneration. *Biomaterials*, 138, 91–107.
137. Yao, L., Phan, F., and Li, Y. (2013) Collagen microsphere serving as a cell carrier supports oligodendrocyte progenitor cell growth and differentiation for neurite myelination in vitro. *Stem Cell Res Ther*, 4 (5), 109.
138. Kandalam, S., Sindji, L., Delcroix, G.J.-R., Violet, F., Garric, X., André, E.M., Schiller, P.C., Venier-Julienne, M.-C., des Rieux, A., Guicheux, J., and Montero-Menei, C.N. (2017) Pharmacologically active microcarriers delivering BDNF within a hydrogel: Novel strategy for human bone marrow-derived stem cells neural/neuronal differentiation guidance and therapeutic secretome enhancement. *Acta Biomaterialia*, 49, 167–180.
139. Howell, D.W., Peak, C.W., Bayless, K.J., and Gaharwar, A.K. (2018) 2D Nanosilicates Loaded with Proangiogenic Factors Stimulate Endothelial Sprouting. *Adv. Biosys.*, 2 (7), 1800092.
140. Li, Y., Liu, W., Liu, F., Zeng, Y., Zuo, S., Feng, S., Qi, C., Wang, B., Yan, X., Khademhosseini, A., Bai, J., and Du, Y. (2014) Primed 3D injectable microniches enabling low-dosage cell therapy for critical limb ischemia. *Proc Natl Acad Sci USA*, 111 (37), 13511–13516.
141. Torres, A.L., Bidarra, S.J., Pinto, M.T., Aguiar, P.C., Silva, E.A., and Barrias, C.C. (2018) Guiding morphogenesis in cell-instructive microgels for therapeutic angiogenesis. *Biomaterials*, 154, 34–47.

142. Torres, A.L., Bidarra, S.J., Vasconcelos, D.P., Barbosa, J.N., Silva, E.A., Nascimento, D.S., and Barrias, C.C. (2020) Microvascular engineering: Dynamic changes in microgel-entrapped vascular cells correlates with higher vasculogenic/angiogenic potential. *Biomaterials*, 228, 119554.
143. Davoodi, E., Sarikhani, E., Montazerian, H., Ahadian, S., Costantini, M., Swieszkowski, W., Willerth, S.M., Walus, K., Mofidfar, M., Toyserkani, E., Khademhosseini, A., and Ashammakhi, N. (2020) Extrusion and Microfluidic - Based Bioprinting to Fabricate Biomimetic Tissues and Organs. *Adv. Mater. Technol.*, 1901044.
144. Levato, R., Jungst, T., Scheuring, R.G., Blunk, T., Groll, J., and Malda, J. (2020) From Shape to Function: The Next Step in Bioprinting. *Adv. Mater.*, 32 (12), 1906423.
145. Highley, C.B., Rodell, C.B., and Burdick, J.A. (2015) Direct 3D Printing of Shear-Thinning Hydrogels into Self-Healing Hydrogels. *Adv. Mater.*, 27 (34), 5075–5079.
146. Sun, Y., You, Y., Jiang, W., Wu, Q., Wang, B., and Dai, K. (2020) Generating ready-to-implant anisotropic menisci by 3D-bioprinting protein-releasing cell-laden hydrogel-polymer composite scaffold. *Applied Materials Today*, 18, 100469.
147. Bhattacharjee, T., Zehnder, S.M., Rowe, K.G., Jain, S., Nixon, R.M., Sawyer, W.G., and Angelini, T.E. (2015) Writing in the granular gel medium. *Sci. Adv.*, 1 (8), e1500655.
148. Lee, A., Hudson, A.R., Shiwarski, D.J., Tashman, J.W., Hinton, T.J., Yerneni, S., Bliley, J.M., Campbell, P.G., and Feinberg, A.W. (2019) 3D bioprinting of collagen to rebuild components of the human heart. *Science*, 365 (6452), 482–487.
149. Heo, D., Alioglu, M., Wu, Y., Ozbolat, V., Ayan, B., Dey, M., Kang, Y., and Ozbolat, I. (2020) 3D Bioprinting of carbohydrazide-modified gelatin into microparticle-suspended oxidized alginate for fabrication of complex-shaped tissue constructs. *ACS Appl. Mater. Interfaces*, acsami.0c05096.
150. Skylar-Scott, M.A., Uzel, S.G.M., Nam, L.L., Ahrens, J.H., Truby, R.L., Damaraju, S., and Lewis, J.A. (2019) Biomanufacturing of organ-specific tissues with high cellular density and embedded vascular channels. *Sci. Adv.*, 5 (9), eaaw2459.
151. Husman, D., Welzel, P.B., Vogler, S., Bray, L.J., Träber, N., Friedrichs, J., Körber, V., Tsurkan, M.V., Freudenberg, U., Thiele, J., and Werner, C. (2019) Multiphasic microgel-in-gel materials to recapitulate cellular mesoenvironments in vitro. *Biomater. Sci.*, 10.1039.C9BM01009B.
152. Zhu, H., Zhang, L., Tong, S., Lee, C.M., Deshmukh, H., and Bao, G. (2019) Spatial control of in vivo CRISPR–Cas9 genome editing via nanomagnets. *Nat Biomed Eng*, 3 (2), 126–136.

### 3. Aims

In this master thesis, the main objective was to produce a personalized photo-crosslinkable granular hydrogel, capable of supporting cells adhesion /proliferation. For that, different MAPs with different annealing chemistries, namely light-based, enzyme based and Schiff-based are aimed to be developed. Gelatin was the biopolymer selected for hydrogel microparticles that will comprise granular hydrogel, due to its high biocompatibility and cell adhesive properties, easy manipulation, and affordable price. This backbone was then modified with chemical groups or combined with other biopolymers to give rise to microporous annealed particle scaffolds (MAPs). Thus, the specific aims of this master thesis were the following:

- Gelatin backbone modification with HPA and physicochemical characterization;
- Oxidation of laminarin (ox-LAM) for Schiff-base conjugation with gelatin;
- Synthesis and characterization of gelatin-HPA and gelatin microparticles with a size range between 60-200 $\mu$ m;
- Gelatin-HPA HMPs annealing to form a MAP via different chemistries: enzymatically-mediated, UV-light mediated or Schiff-base mediated by combination with laminarin;
- MAPs physicochemical and mechanical characterization;
- MAP *in vitro* degradability, cell adhesion properties and biocompatibility characterization;
- Processing of via additive manufacturing techniques – Extrusion 3D bioprinting.

## 4. Materials and Methods

### 4.1. Materials

Gelatin from porcine skin type A, Pluronic-F127, dimethylformamide (DMF) Tyrosinase, phosphate saline buffer (PBS), Albumin-fluorescein isothiocyanate conjugate (BSA-FITC), cell medium M199, fetal bovine serum (FBS), Antibiotic-antimycotic (ATB), ECGS, ethylene glycol, sodium periodate, from Sigma Aldrich (St. Louis, Missouri, EUA). 1-ethyl-3-(3-dimethylaminopropyl)-carbodiimide hydrochloride (EDC), Hydroxyphenylpropionic acid (HPA), were acquired from TCI Chemicals (Tokyo, Japan). DAPI (4',6-diamidino-2-phenylindole, dihydrochloride), 2,4,6-trinitrobenzene-sulfonic acid (TNBS),  $\alpha$ -MEM, Alamar Blue, from Thermo Fisher Scientific. Arabic gum supplied by Enzymatic, S.A., Ruthenium kit from Cell Systems, VEGF from STEM CELL Technologies, and heparin from BioChemica. Sodium chloride provided from Lab Chem. VEGF ELISA KIT and. Flash Phalloidin™ Red 594 from BioLegend (San Diego, CA, EUA) Laminarin 5000 Da, Carbosynth (UK), LOT YL0242. Dialysis membrane Spectra/Por 3, Spectrum Labs.

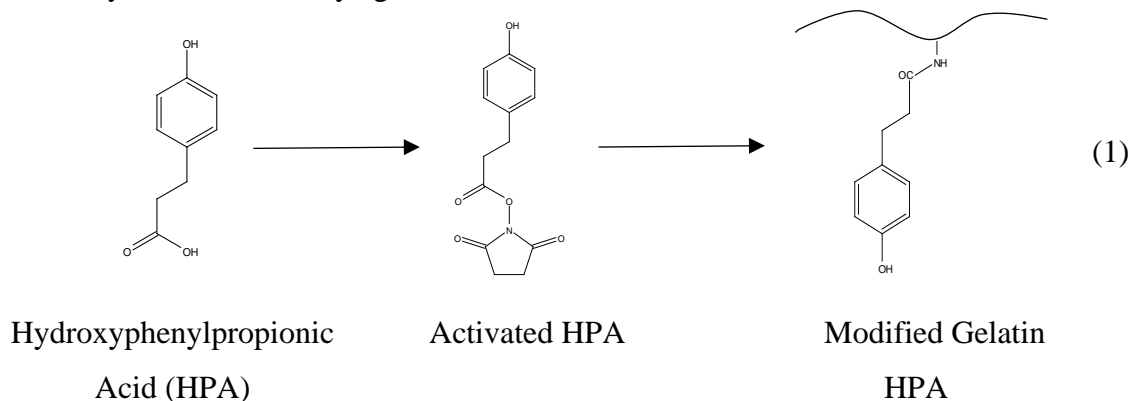
### 4.2. Methods

#### 4.2.1. Biomaterials chemical functionalization

##### Gelatin-HPA synthesis

Gelatin is an affordable and easy modifiable polymer and since it is a native collagen derivative, it possesses inherent cytocompatibility and cell adhesive properties. [1] Gelatin-HPA (Gelatin-HPA) is a widely used gelatin derivative that is highly processable and crosslinkable by a number of different stimuli including enzymes and/or light. [2–4] In this work, we aimed to produce hydrogel microparticles and use hydroxyphenylpropionic group for the annealing step. Several reports describe different degrees of Gelatin-HPA cross-linking. However, usually, this is provided by higher enzymatic concentrations or extended cross-linking times. [5,6] Herein different degrees of HPA substitution of gelatin backbone were evaluated. This synthesis occurs by a carbodiimide/active ester mediated coupling reaction. [5,7] The highest degree of substitution was obtained by dissolving 20 mmol HPA in 250 mL in a mixture of 3:2 of

distilled water and N, N-dimethylformamide (DMF) and then HPA was activated with 20 mmol of 1-ethyl-3-(3-dimethylaminopropyl)-carbo-diimide hydrochloride (EDC) and 27.8 mmol N-hydroxy-succinimide (NHS). This activation occurs for 5 hours at a pH of 4.7. Then, 150 mL of gelatin 6.5% (w/v), previously dissolved in distilled water, were added into the mixture, and the reaction occurred at 40 °C, overnight. Then, the solution was transferred to dialysis tubes of 3.5 kDa. Initially, the dialysis occurs against 100 mM of sodium chloride in the first day and then against distilled water maintained at 37 °C. In the low substitution degree, the reaction was performed at ca. 20 °C, instead of 40°C. For that, 20 mmol HPA was dissolved, in 250 mL in a mixture of 3:2 of distilled water and DMF and add then 20mmol of (EDC) and 27.8 mmol NHS, the reaction also occurs for 5 hours at a pH of 4.7. Then, 150 mL of gelatin 6.5% (w/v) was added. To the mixture. Both formulations were then dialyzed in a 3.5 kDa Repligen (132724) dialysis membrane for 5 -7 days and the first day against NaCl, 150 mM.



### Oxidized laminarin synthesis

The oxidized laminarin was obtained as previously explained and optimized in our group. [8] In a sodium periodate - based oxidation procedure, the hydroxyls in the laminarin structure were remodeled into aldehyde groups. To an intermediate degree of oxidation, the laminarin (500 mg, 0.617 mmol monomer) from *Eisenia Bicyclis* was dissolved in 5 mL of ultra-pure water in 30mL glass vials. Then, was added 440 mg (2.06 mmol) of sodium periodate (> 99.8%). The resulting mixture was flushed with N<sub>2</sub> before reacting for 5 h at RT, under moderate magnetic stirring. To stop the reaction, after 5 hours, 120 µL of ethylene glycol (2.2 mmol) was added into the solution to quench the oxidation process. This last reagent is in excess to assure the end of the reaction. The reaction mixture was transferred to a dialysis bag (molecular weight cutoff: 3500 Da) and

dialyzed for a week with distilled water. Then the solution was frozen at  $-80^{\circ}\text{C}$  and freeze-dried (LyoQuest Plus, Telstar) for 5 days.

### **Polymer Characterization**

The modification of Gel-HPA was confirmed by using proton Nuclear Magnetic Resonance technology  $^1\text{H-NMR}$ , at  $37^{\circ}\text{C}$  in 300 MHz spectrometer. Acquisition was performed with 512 scans 2 Dummy-scans and 15s of relaxation delay. In addition, further characterization was performed by attenuated total reflectance furrier transformed infrared spectroscopy (ATR-FTIR), in Bruker Tensor 27 spectrometer. Atmospheric air was used as background control, and all the samples spectra were recorded at  $4\text{ cm}^{-1}$  resolution in the spectral with of  $4000\text{-}350\text{ cm}^{-1}$  in a total of 256 scans. The obtained data were processed on OPUS software. The absorbance, of the modified gelatin was measured in a plate reader (Synergy HTX microplate reader) in a quartz plate between 250-700nm at the concentration of 1 mg/mL and compered with distilled water, 0.2 mg/mL of HPA solution, and 1 mg/mL of gelatin solution.

The substitution degree was calculated by free amines by, 2,4,6-trinitrobenzene-sulfonic acid, TNBS, which react with primary amino groups. [9] For these assays the gelatin-HPA and gelatin, as a control, were separately dissolved in sodium bicarbonate buffer (pH 8.5, 0.1M) at a concentration of 1.6 mg/ml. Then 0.5mL of TNBS (0.01% in bicarbonate buffer) was add 0.5 mL of each solution in a proportion of 1:1 with the samples. The sample solutions were the incubated at  $37^{\circ}\text{C}$  for 2 hours. Then, 0.5 mL of 10 % (w/v) of sodium dodecyl sulfate and, 250 mL were added to stop the creation and the absorbance was measured at 335nm. The molar concentration of primary amino groups in each gelatin solution was determined by comparative with glycol standard solutions at 0, 0.8, 8 16, 32, and 64  $\mu\text{g/mL}$ , that pass through the same procedure.

The oxLAM modification was confirmed using Nuclear Magnetic Resonance technology  $^1\text{H-NMR}$  at RT at 300 MHz with 512 scans 2 Dummy-scans and 15s of relaxation delay.

#### **4.2.2. HMPs formation**

The gelatin-HPA microparticles were produced according to FRESH methodology with some alterations. [10] Initially, 13 mL of ethanol (7 5% v/v), and 4.5 mL of water were heated until  $37^{\circ}\text{C}$ . Then 2.5 mL of 10 mg/mL Arabic gum was added to solution

followed 2.5 mL by 2 mM by Pluronic F-127, over different stirrings. Then 1 mL gelatin-HPA was slowly added over the different stirrings to the previous solution and left at 37 °C for 10 minutes and the pH at 6.25. Then the temperature was slowly dropped to 28 °C and added EDC and NHS at a concentration of 0.025 mol/mL, for 2 hours. Then the emulsion was centrifuged at 300g for 5 min to separate the microparticles, and washed 3 times in distilled water, to wash the excess reagents. To increase hydrogel microparticles were again crosslinked on a 50 mM concentration and then washed once then was washed 4 times in PBS maintaining the 300 g for 5 min. Lastly, to compact the particles, they were centrifuged for 1000 g for 10 min and stored.

To obtain gelatin HMPs a water-water emulsion similar to gel-HPA HMPs. Firstly ethanol (75% v/v) was heated, at 40 °C in a beaker. The intermedium phasis was created by adding 0.25 % of Pluronic<sup>®</sup> and 0.1 % (w/v) Arabic gum dissolved in an aqueous solution, to a final concentration of 50:50 water-ethanol. The process was optimized through different stirrings speeds, and by using different gelatin concentrations (10% and 20% w/v). After 10 minutes, the temperature was turned off and the solution was cooled to room temperature. During this procedure, the beaker was sealed to minimize ethanol evaporation. The resulting emulsion was then separated into Falcons and centrifuged at 300 g for 5 min to separate the gelatin microparticles from the supernatant. Then the microparticles were washed on distilled water three times, to remove the ethanol and Pluronic<sup>®</sup> F-127, 3 times and then washed twice in PBS. In the washing, steps particles were centrifuged at 300g, for 5 min. Lastly, to remove the excess of PBS the microparticles were centrifuged at 1000g for 10 min, and then the microparticles were then stored at 4°C.

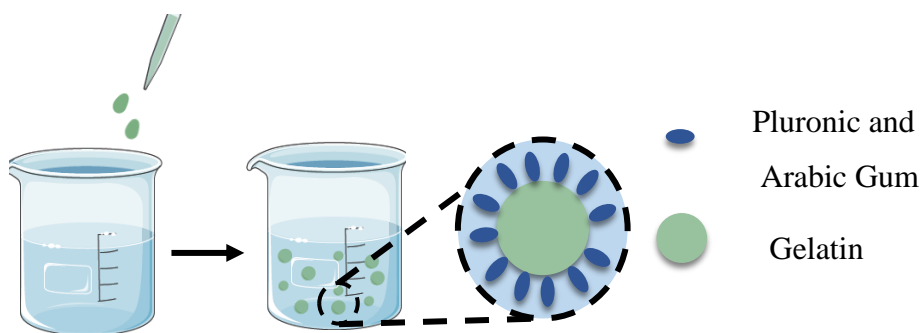


**Figure 1** Schematic representation of the HMPs production by emulsion.

### 4.2.3. Microparticles annealing

The gelatin- HPA HMPs annealing using photopolymerization by exposition to UV light procedure. Ruthenium as absorption spectra on a wavelength between 400-450 nm. With this, 2  $\mu\text{L}$  of ruthenium solution and sodium peroxide at a concentration of 37.4 mg/mL and 119 mg/mL in PBS, respectively were added into 100  $\mu\text{L}$  of HMPs. Then, the mixture was centrifuged at 300g for 5 min, and the supernatant was excreted. Then the HMPs were placed on a circular mold and crosslinked for 2 min under UV light at 3.27 mW/cm<sup>2</sup>.

In the enzymatic crosslinking of gelatin-HPA, tyrosinase was added into the solution at a concentration of 2 kU/mL. Then the mixture was centrifuged, the supernatant was removed, and the solution was transferred to a PMDS mold, and left at 37°C for 4 hours.

For the gelatin-oxLAM MAPs the oxLAM solution were prepared at 10% w/v (high oxLAM) and 5% w/v (low oxLAM) on PBS. Then, 1 mL of oxLAM, 3mL was added for the granular hydrogel production.

The hydrogel microparticles were resuspended for 3 hours, under stirring. Then the solution was centrifuged at 300g for 5 min, and the excess of laminarin was removed with a micropipette. Then, the granular hydrogel was introduced on circular molds of PBS with 6 mm of diameter and left at 37°C, for 1 hour, washed on PBS, and used as an ink or for injectability experiments.

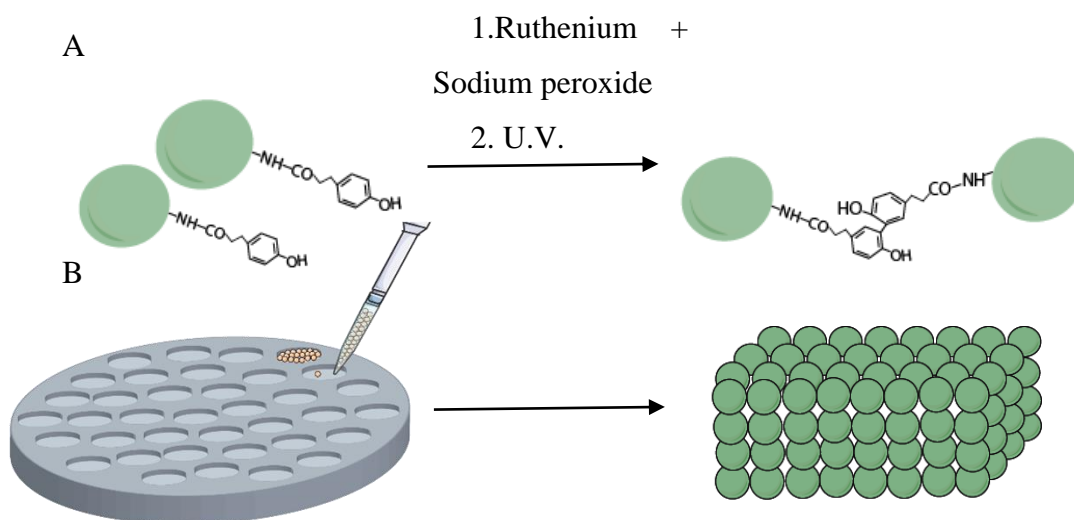


**Figure 2** Schematic representation of the HMPs photo-annealing, A) in a molecular and in B) a macroscopic, overview.



#### **4.2.4. Bulk hydrogel crosslinking**

In the bulk hydrogel, gelatin-HPA was dissolved in PBS, and crosslinked as well at 3.27 mW/cm<sup>2</sup>. In the end, the bulk hydrogel was emersed on a solution of EDC/NHS in PBS 50mM for 2 hours. Before cell culture, the hydrogels were stylized under UV light for 20 min and washed with PBS over-night.

#### **4.2.5. Characterization of the granular hydrogels**

The water uptake assays were performed as in previous protocols. [2] To study the water uptake was calculated using equation 2. For that, the mass of granular hydrogel was measured at the time point t=0 and then incubated on PBS at 37°C, for 1, 3 6, and 7 days. Then, the sample masses were measured, with the care to remove excess water by wiping with a paper towel any surrounding fluids. The water content was determined by using

(2)

$$\text{Water content} = \frac{\text{weight of swollen hydrogel} - \text{freeze} - \text{dried weight}}{\text{weight of swollen hydrogel}} \times 100$$

equation 3, to that the samples were incubated at 37°C in PBS, then the weighted and then freeze-dried. In this  $n=3$  samples were used.

In addition, the area occupied by HMPs in a given volume was determined by using fluorescence micrographs acquired in laser scanning confocal microscopes (LSM 510 Meta, and LSM 880Aryscan, Carl Zeiss, Germany) and treated with the function of object analyzer in Huygens Essential.

#### **4.2.6. Encapsulation efficiency and release**

To evaluate the encapsulation ability, BSA-FITC was used to mimic the VEGF due to the fluorescence properties. This way, using fluorescence easily confirmed the encapsulation of this protein. With this, 1000 µg/mL of BSA-FITC was included in the gelatin precursor solution and the emulsion procedure as described above. The efficacy of encapsulation was evaluated by measuring the fluorescence of the supernatant with excitation at  $\lambda=485\text{nm}$  and measuring the emission at  $\lambda=528\text{nm}$  in microplate reader by using a 96-well black-clear bottom plate (VWR, CN: CORN3915). To assure that BSA-

FITC was encapsulated we observed the HMPs in fluorescence microscopy. A calibration graph with different concentrations was used to determine the calibration line to calculate the concentration on a supernatant, and then in the releasing. The efficiency was calculated as presented in equation 4. By encapsulating 1000 µg/ mL of BSA-FITC the efficiency of encapsulation decreased to 85%.

$$\text{Encapsulation efficiency(\%)} = \frac{\text{Protein encapsulated} - \text{Protein detected}}{\text{Protein encapsulated}} \times 100$$

The same procedure was tested for VEGF, however, no VEGF was detected. As an alternative, HMPs were immersed on a VEGF solution (2 µg/mL), and then the HMPs were crosslinked with EDC/NHS. The release profile was determined after microparticles annealing, by introducing a granular hydrogel on a 5 mL tube in 3 mL of PBS, over different times points 1, 3,7 days, on each, the PBS was removed and substituted by another 3 mL of PBS. Then, the VEGF was release was evaluated by VEGF ELISA KIT.

#### 4.2.7. Mechanical Characterization

The Young's modulus was evaluated by a mechanical compression assay on a Instron 3343 mechanical analyzer equipped with a 50 N load cell, at RT, for each condition 3 samples with a cylinder-shape with 6 mm of diameter and 3 mm of high were analyzed. With a compression rate of 1.00 mm.min<sup>-1</sup>. The compressive stress and strain were graphed, Young's modulus was calculated by the slope of the initial linear section of the stress-strain curve. In the injectability assays, the HMPs were prepared with ruthenium and sodium periodate as mentioned before, then centrifuged at 500 g for 5 min, and the supernatant was excreted, then was transferred to a 1 mL syringe with and injected through a 21G needle.

#### 4.2.8. Cell culture

The human adipocyte-derived mesenchymal cells (hASC) isolated from human abdominal subcutaneous adipose tissue samples. Between 5-8 passage, human umbilical vein endothelial cells isolated from the umbilical cord (HUVECs) were used between 4 and 7 passage. The cells were cultured at 5 % CO<sub>2</sub>, 95 % atmospheric oxygen, in incubators temperature-controlled at 37°C, they were always manipulated under aseptic conditions. They were maintained in T-75 and T-175 cm<sup>2</sup> cell culture flasks (Sarstedt, S.A. 83.3911.002 and 83.3912.002). The ASCs were cultured on α-MEM supplemented with 10 % (v/v) FBS and 1 % (v/v) ATB, while the HUVECs expiation was on M199

with 10 % (v/v) FBS and 1 % (v/v) ATB and 50  $\mu\text{g}/\text{mL}$  of heparin and 5 $\mu\text{g}/\text{mL}$  endothelial cell growth supplement. The cells were used on the assays after reach the confluence initially of 250 000 cells /200 $\mu\text{L}$  of medium. We used monocultures of ASC, HUVEC, and co-culture of 1:1of HUVECS and ASC. Then HUVECs were used in lowers concentrations of 50 000 cells/mL. For monoculture of hASC, we used  $\alpha$ -MEM, while for HUVECs and co-culture with HUVECs and ASC we used M199 with 1 % of heparin and 0.1% of ECGs.

#### 4.2.9. Cell Viability

The cell viability of the HUVECs, ASC, and co-culture were analyzed at specific time points, 12h, 1 day, t 3 days, and 7 days through different methodologies, explicitly Live/dead assay and no radioactive AlamarBlue<sup>®</sup> cell viability assay. The cell morphology was evaluated by using DAPI for labelling cell nucleus, and Phalloidin-RED for labelling the F-actin filaments.

Alamar Blue<sup>®</sup> was used to measure the cell viability at the days1, 3 and 7, the assays were performed in accordance with the manufacture guidelines, except it was performed in a standard period of 7h30min. The resorufin result of the oxidation of the AlamarBlue<sup>®</sup> was determined by t fluorescence measurements ( $\lambda_{\text{ex}}$ : 540 nm,  $\lambda_{\text{em}}$ : 600 nm). The measurements were performed in a microplate reader by using a 96-well black-clear bottom plate (VWR, CN: CORN3915).

In live dead assays, Calcein- AM (Cal-AM) (3.5  $\mu\text{g}/\text{mL}$ ) and Propidium Iodide (PI) (3.5  $\mu\text{g}/\text{mL}$ ) were incubated in cells for 35 min at 37 °C, then washed 3 times with D-PBS. Samples were then observed by fluorescence microscopy or fixed with 4% formaldehyde(v/v) for posterior observation. To analyze cell morphology after fixation the scaffold with cells was permeabilized with 0.1% Triton X-100, for 10 min, RT. Then washed three times. For the cell staining was used and phalloidin for 1 hour, and DAPI for 10 min. The fluorescence images were acquired on a widefield microscope (Axio Imager M2, Carl, Zeiss, Germany), or in laser scanning confocal microscopes (LSM 510 Meta, and LSM 880.Aryscan, Carl Zeiss, Germany). Analysis of acquired images was performed in Zeiss Zen Blue software (2017).

#### 4.2.10. 3D bioprinting

Extrusion based printing was performed using an Inkredible + 3D bioprinter (CELLINK, Germany). The CAD models were designed in SolidWorks® (Dassault Systems SA). The files were imported into CELLINK Heartware software and post-processed with Slic3r (v 1.3.0) to obtain g-code files with specified layer patterns, for the CELLINK Inkredible + Bioprinter. Previous to any printing, Granular bioinks (0.75 mg/mL of ruthenium, 2.38 mg/mL of sodium peroxide, and  $5.5 \times 10^6$  hASCs /mL) were prepared, by centrifugation and inserted in the cartridge. 3D semi-circular shaped constructs were printed at a speed of  $10 \text{ mm} \cdot \text{s}^{-1}$ , with a 22G nozzle at different pressures. All the printing stages were performed in a printing bead at RT, and the print head temperature was maintained between 19-22 °C, at all times. All the 3D bioprinted structures were posteriorly crosslinked by using a LED light (405 nm), for 5 min, at RT.

#### 4.2.11. Statistical Analysis

All statistical analysis was performed using Graphpad Prism 8 Software (Prism 8™). One-way analysis of variance (One-ANOVA) and Two-way analysis of variance (Two-ANOVA) with Holm-Sidak's post-hoc test.

### 4.3. References

1. Buie, T., McCune, J., and Cosgriff-Hernandez, E. (2020) Gelatin Matrices for Growth Factor Sequestration. *Trends in Biotechnology*, S0167779919303002.
2. Liu, Y., Cheong NG, S., Yu, J., and Tsai, W.-B. (2019) Modification and crosslinking of gelatin-based biomaterials as tissue adhesives. *Colloids and Surfaces B: Biointerfaces*, **174**, 316–323.
3. Al-Abboodi, A., Zhang, S., Al-Saady, M., Ong, J.W., Chan, P.P.Y., and Fu, J. (2019) Printing *in situ* tissue sealant with visible-light-crosslinked porous hydrogel. *Biomed. Mater.*, **14** (4), 045010.
4. Le Thi, P., Lee, Y., Nguyen, D.H., and Park, K.D. (2017) In situ forming gelatin hydrogels by dual-enzymatic cross-linking for enhanced tissue adhesiveness. *J. Mater. Chem. B*, **5** (4), 757–764.
5. Wang, L.-S., Chung, J.E., Pui-Yik Chan, P., and Kurisawa, M. (2010) Injectable biodegradable hydrogels with tunable mechanical properties for the stimulation of neurogenesis differentiation of human mesenchymal stem cells in 3D culture. *Biomaterials*, **31** (6), 1148–1157.
6. Lim, T.C., Toh, W.S., Wang, L.-S., Kurisawa, M., and Spector, M. (2012) The effect of injectable gelatin-hydroxyphenylpropionic acid hydrogel matrices on the proliferation, migration, differentiation and oxidative stress resistance of adult neural stem cells. *Biomaterials*, **33** (12), 3446–3455.
7. Hu, M., Kurisawa, M., Deng, R., Teo, C.-M., Schumacher, A., Thong, Y.-X., Wang, L., Schumacher, K.M., and Ying, J.Y. (2009) Cell immobilization in gelatin–hydroxyphenylpropionic acid hydrogel fibers. *Biomaterials*, **30** (21), 3523–3531.
8. Lavrador, P., Gaspar, V.M., and Mano, J.F. (2020) Mechanochemical Patternable ECM-Mimetic Hydrogels for Programmed Cell Orientation. *Adv. Healthcare Mater.*, **9** (10), 1901860.
9. Lee, B.H., Shirahama, H., Cho, N.-J., and Tan, L.P. (2015) Efficient and controllable synthesis of highly substituted gelatin methacrylamide for mechanically stiff hydrogels. *RSC Adv.*, **5** (128), 106094–106097.
10. Lee, A., Hudson, A.R., Shiwardski, D.J., Tashman, J.W., Hinton, T.J., Yerneni, S., Bliley, J.M., Campbell, P.G., and Feinberg, A.W. (2019) 3D bioprinting of collagen to rebuild components of the human heart. *Science*, **365** (6452), 482–487.

## *MATERIALS AND METHODS*

---

from BioChemica. Sodium chloride provided from Lab Chem. VEGF ELISA KIT and. Flash Phalloidin™ Red 594 from BioLegend (San Diego, CA, EUA) Laminarin 5000 Da, Carbosynth(UK), LOT YL0242. Dialysis bag , Spectra/Por 3, Spectrum Labs.

## **5. Results and Discussion**

This subchapter is based on the review article entitled “Photocrosslinkable Gelatin-Hydroxyphenyl Granular Hydrogel Hierarchic 3D Platforms as Stem Cell Supporting Microenvironments“

Manuscript in preparation

**Photocrosslinkable Gelatin-Hydroxyphenyl Granular Hydrogel Hierarchic 3D Platforms as Stem Cell Supporting Microenvironments**

Ana Fernandes, Vítor M. Gaspar, João F. Mano

Dr. V.M Gaspar

Department of Chemistry

CICECO - Aveiro Institute of Materials, University of Aveiro

Campus Universitário de Santiago 3810-193, Aveiro, Portugal

vm.gaspar@ua.pt

Prof. J.F. Mano

Department of Chemistry

CICECO - Aveiro Institute of Materials, University of Aveiro

Campus Universitário de Santiago 3810-193, Aveiro, Portugal

jmano@ua.pt

**Abstract:** Biomimetic hydrogels are generally engineered to replicate the extracellular matrix (ECM) to improve regeneration. However, hydrogels present several challenges in reproducing the ECM because they do not allow realistic diffusion rates, generally lack the porous architectures required for cells to infiltrate and for nutrients/oxygen exchange, in suitable rates for cells support. Gathering on this scenario, granular hydrogels processing into microporous annealed platforms have been gaining momentum as alternative systems for cell maturation, delivery and recruitment. However, the development of MAPs with suitable and user controlled annealed chemistries is still highly underexplored. Herein, we developed hydroxyphenyl-gelatin (Gel-HPA) based microporous annealed hydrogel microparticles, suitable to be assembled via photo and enzymatic annealing and inherently bearing cell-adhesion motifs. Additional particle-polymer coupling via Schiff-base reactions was also explored as an alternative to create particle-aggregated hierarchic platforms. Gelatin-The resulting photocrosslinked MAPs scaffolds exhibited suitable mechanical properties and stability in biological environments for up to 7 days. The platform is highly biocompatible Photocrosslinked MAP also showed the ability to promote stem cells and vascular progenitor cells adhesion, spreading and cell-cell contacts in monocultures of ASCs and co-cultured ASCs and HUVEC vascular progenitor cells. This granular hydrogel is also injectable and demonstrated suitable properties for being used as fully particle-based bioink ink for extrusion 3D bioprinting, protecting cells from the shear rate exerted during the process.

**Keywords:** Microporous annealed particles, cell-seeding, Hydrogel microparticles, Gelatin hydroxyphenyl propionic acid



## 5.1. Introduction

Hydrogels are frequently used as a scaffold for Tissue Engineering Regenerative Medicine (TERM) due to their biocompatibility, and water content, and their ability to support cell adhesion and proliferation while maintaining a 3D structure. Usually, hydrogels may include cells in their composition to accelerate the cell recruitment and new tissue formation. [1] However, scaffolds with cells encapsulated need to present more safety proofs for FDA due to the risks of excessive proliferation and initiation of an immunologic reaction, prior to clinical translation. [2] In this way, the development of scaffolds that are able to recruit cells from the patient into the damaged area present an interesting opportunity for the TERM. [3]. Usually, bioactive molecules such as growth factors are included in the hydrogels to initiate a cascade that will lead to cell recruitment. [3–6]

Polymeric hydrogels frequently are used as a delivery system, to increase growth factors lifetime, and to proportionate a sustainable release. [7–9] Nevertheless, cells need to degrade the polymeric matrix to infiltrate, reducing the regeneration efficiency. With this, hydrogel microparticles (HMPs) or microgels are frequently used as a delivery system because of their sustainable release and easy application by minimally invasive procedures compatible with *in situ* annealing. [10–12] Growth factors with a short half-life time such as vascular endothelial growth factor VEGF, are commonly encapsulated with the aim to promote their more sustained release. [13–15]

Compacted HMPs, granular hydrogels, offer several advantages in comparison with bulk hydrogels, namely more realistic diffusion rates of oxygen, nutrients and cells through the scaffolds, allowing larger constructs, as well as cell proliferation [16–18], being compatible with minimum invasive procedures. These granular hydrogels can be annealed forming microporous annealed particles (MAPs) scaffolds, and generally the annealing step can occur *in situ*. [18] The investigation on MAPs is gaining more interest, owing to their unique tunable properties crosslinking degrees, the possibility to create gradients or to use microparticles of different origins to assemble the MAPs scaffolds. All of these features make these platforms highly desirable for numerous biomedical applications including bioactive molecules delivery, cell therapies and tissue engineering.

For example, recent studies focusing on developing MAPs with *in vivo* annealing features demonstrated that microporous nature of these platforms increased host cells

infiltration and without any growth factors included in their composition. [19,20]. However, the majority of MAPs developed to date it is also frequently necessary to include motifs for cell adhesion.

Gelatin modification with a tyrosine moiety, gelatin hydroxyphenyl propionic acid (Gelatin-HPA) presents high cytocompatibility and cell adhesion properties conferred by motifs already presented in gelatin, such as RGD. This polymer in bulk hydrogels proved the ability to promote cell recruitment, in comparison to standard gelatin. [22–24] It also showed biodegradability due to the presence of motifs for metalloproteases cleavage. Gelatin-HPA is highly advantageous for administration via minimally invasive procedures owing to its shear thinning properties. Moreover, the chemical reactivity of this derivative also enables *in situ* crosslinking, wither via enzymatic crosslinking, by using tyrosinase or horseradish peroxidase and hydrogen peroxide, or via UV mediated strategy involving the ruthenium-based initiation system  $[\text{RuII}(\text{bpy})_3]^{2+}$ . [25–28] The affordable production and high versatility make Gelatin-HPA an attractive polymer for TERM. [29,30]

Laminarin is a polysaccharide from brown algae. [31–33] It had revealed several therapeutic like anti-inflammatory, anti-tumor, immunostimulatory properties, among other properties. [34,35] Although the benefic properties of laminarin, only recently have been explored by tissue engineering. [36] The low molecular weight of laminarin (between 4-5kDa) facilitates solubilizations in aqueous solutions or organic solvents, as well as facilitate structure modifications. [36] Laminarin can be easily oxidated in aqueous oxidative chemistry, creating aldehydes moiety, allowing bases Schiff reactions with amines, for example on hyaluronic acid or collagen derivatives such as gelatin. [37]

The vast advantages of granular hydrogels lead us to develop a MAP with Gelatin-HPA hydrogel microparticles, suitable not only for being assembled via enzymatic annealing but also as a UV , and a Schiff-based granular hydrogel. To increase the biocompatibility an oil-free emulsion used for HMP production was employed, so as to decrease the organic solvents on HMPs. The HMPs were annealed by using UV light by using ruthenium  $[\text{RuII}(\text{bpy})_3]^{2+}$  and sodium periodate system, once this photoinitiator has an absorbance spectrum in the visible light, as well as tyrosinase. The Schiff-based hydrogels showed self-healing abilities. The larger pores created by the void spaces between of HMPs increased the cell infiltration into the scaffold in the initial days, as well as fast cell recruitment. More importantly light photocrosslinked platforms were

highly stable in biological environment, were inherently cell adhesive and allowed cellular infiltration into the 3D MAP structure thus possessing suitable properties for future TERM applications

## 5.2. Materials and Methods

### 5.2.1. Materials

Gelatin from porcine skin type A, Pluronic-F127, dimethylformamide (DMF) Tyrosinase, phosphate saline buffer (PBS), Albumin-fluorescein isothiocyanate conjugate (BSA-FITC), cell medium M199, fetal bovine serum (FBS), Antibiotic-antimycotic (ATB), ECGS, ethylene glycol, sodium periodate, from Sigma Aldrich (St. Louis, Missouri, EUA). 1-ethyl-3-(3-dimethylaminopropyl) carbodiimide hydrochloride (EDC), Hydroxyphenylpropionic acid (HPA), were acquired from TCI Chemicals (Tokyo, Japan). DAPI (4',6-diamidino-2-phenylindole, dihydrochloride), 2,4,6-trinitrobenzene-sulfonic acid (TNBS),  $\alpha$ -MEM, Alamar Blue, from Thermo Fisher Scientific. Arabic gum supplied by Enzymatic, S.A., Ruthenium kit from Cell Systems, VEGF from STEM CELL Technologies, and heparin from BioChemica. Sodium chloride provided from Lab Chem. VEGF ELISA KIT and. Flash Phalloidin™ Red 594 from BioLegend (San Diego, CA, EUA) Laminarin 5000 Da, Carbosynth (UK), LOT YL0242. Dialysis membrane, Spectra/Por 3, Spectrum Labs.

### 5.2.2. Methods

#### 5.2.2.1. Gelatin-hydroxyphenylpropionic acid synthesis

The conjugated gelatin, Gelatin-HPA, was synthesized as previously described, by a carbodiimide/active ester-mediated coupling reaction, using 3,4-Hydroxyphenylpropionic acid (HPA), in distilled water. [22,30] For the high degree of substitution, HPA (20mmol) was dissolved in 250 ml in a mixture of 3:2 of distilled water and DMF. To this 20mmol of 1 EDC and 27,8 mmol NHS were added. The reaction mixture elapses at room temperature (RT) at pH 4.7 for 5 hours. Then 150 ml aqueous solution of gelatin at 6,25% was added to the mixture and stirred overnight at 40°C. In the low substitution degree, the reaction was the procedure at 20°C instead of 40°C. For that, 20mmol HPA was dissolved, in 250 ml in a mixture of 3:2 of distilled water and DMF and add 20mmol of (EDC) and 27,8 mmol NHS, the reaction also occurs by the 5 hours at a pH of 4,7. Then the solutions were transferred to dialysis tubes of 3.5 kDa.

The tubes were dialyzed against 100 mM sodium chloride solution for 1 day and then against distilled water for 5 days. The purified solutions were lyophilized to obtain gelatin Gelatin-HPA with different degrees.

The structure was determined using  $^1\text{H-NMR}$  at  $37^\circ\text{C}$  at 300 MHz with 512 scans 2 Dummy scans and 15s of relaxation delay. It was confirmed by measuring the absorbance between 200-350nm by a solution of HPA on the water at 0,2mg/mL, as the different degrees of gelatin on a quartz flat bottom plate. It was also used furrier transformed infrared spectra were obtain with the freeze-dried samples, using a Bruker Tensor 27 spectrometer to obtained attenuated total reflectance (ATR-FTIR). The air was used as background control, the samples spectra were recorded at  $4\text{ cm}^{-1}$  resolution in the spectral with of  $4000\text{-}350\text{cm}^{-1}$  in a total of 256 scans.

The substitution degree was calculated by free amines by TNBS which react with primary amino groups. [38] For these, the gelatin-HPA and gelatin, as a control, were separately dissolved in sodium bicarbonate buffer (pH 8.5, 0,1M) at a concentration of  $1,6\text{mg. mL}^{-1}$ . Then 0,5mL of TNBS (0,01% in bicarbonate buffer) was add 0,5mL of each solution in a proportion of 1:1. The sample solutions were incubated at  $37^\circ\text{C}$  for 2 hours. Then, 0,5mL of 10%(w/v) of sodium dodecyl sulfate and, 250 mL were added to stop the creation and the absorbance was measured at 335nm. The molar concentration of primary amino groups in each gelatin solution was determined by comparison with glycol standard solutions at 0, 0.8, 8 16, 32, and  $64\text{ }\mu\text{g. mL}^{-1}$ , that pass for the same procedure.

#### 5.2.2.2. Oxidized laminarin synthesis

The oxidized laminarin was obtained as previously explained and optimized in our group. [37] In a sodium periodate - based oxidation procedure, the hydroxyls in the laminarin structure were remodeled into aldehyde groups. To an intermediate degree of oxidation, the laminarin (500 mg, 0.617 mmol monomer) from *Eisenia Bicyclis* was dissolved in 5 mL of ultra-pure water in 30mL glass vials. Then, was added 440mg (2.06 mmol) of sodium periodate (>99.8%). The resulting mixture was flushed with  $\text{N}_2$  before reacting for 5 h at RT, under moderate magnetic stirring. To stop the reaction, after 5 hours, 120 $\mu\text{L}$  of ethylene glycol (2.2mmol) was added into the solution to quench the oxidation process. This last reagent is in excess to assure the end of the reaction. The reaction mixture was transferred to a dialysis bag (molecular weight cut - off 3500 Da) and dialyzed for a week with distilled water. Then the solution was frozen at  $-80^\circ\text{C}$  and

freeze - dried (LyoQuest Plus, Telstar) for 5 days. The polymer modification was confirmed using  $^1\text{H-NMR}$  at room temperature (RT) at 300 MHz with 512 scans 2 Dummy scans and 15s of relaxation delay.

### 5.2.2.3. Hydrogel microparticles production

In HMPs production, we decided to use an emulsion methodology, once it was fast technique, and allow us to produce a large scale of HMPs and fast methodology. Gelatin-HPA HMPs were produced according to with FRESH methodology with some alterations. [43] Initially 13 mL of ethanol 75% (v/v) and 4.5 mL of water was heated until  $37^\circ\text{C}$ , then 2.5mL of  $10\text{mg mL}^{-1}$  Arabic at  $10\text{mg mL}^{-1}$  was added to solution flowed 2.5 mL by 2mM by Pluronic F-127 over different stirrings. Then 1mL Gelatin-HPA was slowly added over the different stirrings to the previous solution and left at  $37^\circ\text{C}$  for 10 minutes. Then the temperature was slowly dropped to room temperature and added EDC and NHS at a concentration of  $0.025\text{mol mL}^{-1}$ , for 2 hours. The emulsion was centrifuged at 300g for 5 min to separate the HMPs from the supernatant, and washed 3 times on distilled water, to wash the excess Pluronic F-127 and ethanol. To increase hydrogel HMPs were again crosslinked on a 50mM concentration and then washed once then was washed 3 times in PBS maintaining the 300 g for 5 min. Lastly, to compact the HMPs, they were centrifuged for 1000 g for 10 min and stored.

A similar methodology was applied to gelatin HMPs, briefly 0,25% of Pluronic F-127 and 0.1% (w/v) Arabic gum is dissolved in an aqueous solution, to a final concentration of 50/50 water-ethanol. The process was optimized through different stirrings speeds and different gelatin percussor solution concentrations (10% and 20% of gelatin). After 10 minutes the plate temperature was turned off and the solution cool to RT. During this procedure, the beaker was sealed to minimize ethanol evaporation. The resulting emulsion was then separated into Falcons and centrifuged at 300 g for 5 min to separate the gelatin microparticles from the supernatant. Then the microparticles were washed on distilled water three times to remove the ethanol and PluronicF-127 3 times and then washed twice in PBS. In the washing, steps were used 300g for 5 min. Lastly, to remove the excess of PBS the microparticles were centrifuged at 1000g for 10 min, and then the microparticles were stored at  $4^\circ\text{C}$ .

### 5.2.2.4. HMPs annealing

The HMPs annealing was rapidly procedure using photopolymerization by exposition on UV light. With this, 2  $\mu\text{L.mL mL}^{-1}$  a solution of  $[\text{RuII}(\text{bpy})_3]^{2+}$  and sodium peroxide at a concentration of 37,4  $\text{mg. mL}^{-1}$  and 119 $\text{mg. mL}^{-1}$  in PBS was added into the 100 $\mu\text{L}$  of HMPs then the mixture was centrifuged at 300g for 5 min and the supernatant excreted. Then the HMPs were placed on a circular mold and cross-linkable for 2 min under UV light at 3,27  $\text{W.cm}^{-2}$ .

In the enzymatic cross-link, the tyrosinase was added to the solution at a concentration of 2  $\text{kU. mL}^{-1}$ , then the mixture was centrifugated the supernatant removed, and the solution was transferred to a mold and left at 37°C for 4 hours.

The oxLAM solution was prepared at 10% and 5% on PBS. Then, for 1 mL of OxLAM 3 mL of HMPs were added for the granular hydrogel production, to a final concentration of 1,25% of OxLAM (low oxLAM) and 2,5% of oxLAM (high oxLAM). The hydrogel microparticles were suspended for 3 hours under agitation. Then the solution was centrifuged at 300g for 5 min and the excess of laminarin removed with a micropipette. Then, the granular hydrogel was introduced on circular molds of PBS with 6 mm of diameter and 2mm of height and left at 37°C for 1hour, then washed on PBS.

#### 5.2.2.5. Gelatin HPA bulk hydrogel formation

The gelatin-HPA bulk hydrogels were formed by 10% of gelatin-HPA in PBS and crosslinked with 74,8 $\mu\text{g/mL}$  of  $[\text{RuII}(\text{bpy})_3]^{2+}$  and 238 $\mu\text{g.mL}^{-1}$  of sodium peroxide mold and cross-linkable for 2 min under UV light at 3,27  $\text{W.cm}^{-2}$ . Then the bulk hydrogels were immersed on a 50mM of EDC and NHS dissolved in PBS.

#### 5.2.2.6. Characterization of the granular hydrogels

The water uptake rate was calculated according to equation 1, they were incubated into PBS at 37°C. Then the sample masses were measured, with the care to remove wipe with a paper towel any surrounding fluids. The water content the mas determined by measuring the equation 2, to that the samples were incubated at 37°C in PBS, then the weighted and then freeze-dried. In this n=3 samples were used.

Equation (1)

$$\text{water Uptake} = \frac{\text{weight in time 0} - \text{weight of swollen hydrogel}}{\text{weight in time 0}} \times 100$$

Equation (2)

$$\text{Water content} = \frac{\text{weight of swollen hydrogel} - \text{freeze} - \text{dried weight}}{\text{weight of swollen hydrogel}} \times 100$$

In the injectability assays, the HMPs were prepared with ruthenium and sodium periodate as mentioned before, then centrifuged at 500g for 5 min and the supernatant excreted, then was transferred to a 1mL syringe with and injected through a 21G needle.

The area occupied for the HMPs was determined using Acquisition of fluorescence micrographs were performed in a widefield microscope (Axio Imager M2, Carl Zeiss, Germany), or laser scanning confocal microscopes (LSM 510 Meta, and LSM 880Aryscan, Carl Zeiss, Germany), and treated with the function of object analyzer in Huygens Essential.

#### **5.2.2.7. Mechanical assays**

The Young's modulus was evaluated by a mechanical compressions assay on Instron 3343 equipped with a 50 N load cell at room temperature, for each condition 3 samples with a cylinder-shape with 6 mm of diameter and 3 mm of high were analyzed. With a compression rate of 1.00 mm.min<sup>-1</sup>. The compressive stress and strain were graphed, and Young's modulus was calculated by the slope of the initial linear section of the stress-strain curve. For the gelatin-HPA gels were used n= 3 while in gelatin oxLAM were used n=7. The injectability assay was performed in a 21G needle.

#### **5.2.2.8. Encapsulation efficiency and release**

To evaluate the encapsulation ability, through the emulsion we used BSA-FITC to mimic the VEGF, once as the florescence ability so using fluorescence easily confirmed the encapsulation of this protein. With this, a concentration of 1000 µg. mL<sup>-1</sup> was included on gelatin and the emulsion procedure as described above. The efficacy of encapsulation was evaluated by measuring the fluorescence of the supernatant with excitation at λ=485nm and measuring the emission at λ=528nm in a Synergy HTX microplate reader by using a 96-well black-clear bottom plate. To assure that BSA-FITC was encapsulated we observed the HMPs in fluorescence microscopy. A line with different concentrations was used to determine the calibration line to calculate the concentration on a supernatant, and then in the releasing. The efficiency was calculated as presented in the equation:

Encapsulation efficiency = (Protein encapsulated - Protein detected)/(Protein encapsulated)×100. In the BSA-FITC the efficiency of encapsulation decreased to 85%.

The VEGF initially followed the BSA protocol, once BEGF was not detected the VEGF was encapsulated by immersing the HMPs on a concentrated solution ( $2\mu\text{g.mL}^{-1}$ ) of VEGF, for 2 hours, at RT. Then the HMPs were crosslinked with EDC/NHS for 1 hour and lastly annealed with the same conditions mentioned before. The gels were maintained in triplicates in 3 mL of PBS. The release profile was determined using a VEGF ELISA assay.

### 5.2.2.9. 3D bioprinting assays

Extrusion based printing was performed using an Inkredible + 3D bioprinter (CELLINK, Germany). The CAD models were designed in SolidWorks® (Dassault Systems SA). The files were imported into CELLINK Heartware software and post-processed with Slic3r (v 1.3.0) to obtain g-code files with specified layer patterns, for the CELLINK Inkredible + Bioprinter. Before any printing, Granular bioinks ( $0.75\text{ mg.mL}^{-1}$  of ruthenium,  $2.38\text{ mg.mL}^{-1}$  of sodium peroxide, and  $5.5\times 10^6\text{ hASC.mL}^{-1}$ ) were prepared, by centrifugation and inserted in the cartridge. 3D semi-circular shaped constructs were printed at a speed of  $10\text{ mm.s}^{-1}$ , with a 22G nozzle at different pressures. All the printing stages were performed in a printing bead at RT, and the print head temperature was maintained between 19-22 °C, at all timed All the 3D bioprinted structures were posteriorly crosslinked by using a LED light (405 nm), for 5 min, at RT.

### 5.2.2.10. Cell culture

The human adipocyte-derived mesenchymal cells (hASC) isolated from human abdominal subcutaneous adipose tissue samples used between passage 5-8, and human umbilical vein endothelial cells, isolated from the umbilical cord (HUVECs) between 4-7 passage. The cells were used on the assays after reaching the confluence initially 250 000 cells /200 $\mu\text{L}$  of HUVECs and ASC monoculture. We used monocultures of ASC, HUVEC, and co-culture of 1:1of HUVECS and ASC. The low cellular assay was performed with 50 000 cells/gel. For monoculture of hASC,  $\alpha$ -MEM was selected, while for HUVECs and co-culture with HUVECS and ASC M199 with 1% of heparin and 0.1 of ECGs was employed. For cell viability MAPs low gelatin-HPA, with a cylindric shape with 3mm of high and 6 mm of diameter. For each gel was used 200  $\mu\text{L}$  of cells.



#### **5.2.2.11. Cell Viability and morphology**

The cell viability of the HUVECs, ASC, and co-culture were analyzed at specific time points, 12h, 1 day 3 days, and 7 days through different methodologies, explicitly Live/dead assay and no radioactive AlamarBlue<sup>®</sup> cell viability assay. Meanwhile, cells were fixed for fluorescence analyses, with 4% of PFA for 30 min at room temperature, for analysis of cell morphology. Then permeabilized with 0.1% Triton X-100 for 10 min. For the cell staining was used and phalloidin (for F-actin), and 4',6-diamidino-2-phenylindole (DAPI), for nuclei. The fluorescence images were acquired on a widefield microscope (Axio Imager M2, Carl, Zeiss, Germany), or in laser scanning confocal microscopes (LSM 510 Meta, and LSM 880.Aryscan, Carl Zeiss, Germany). Analysis of acquired images was performed in Zeiss Zen Blue software (2017).

#### **5.2.2.12. Statistical Analysis**

All statistical analysis was performed using GraphPad Prism 8 Software (Prism 8TM). One-way analysis of variance (One-ANOVA) and Two-way analysis of variance (Two-ANOVA) with Holm-Sidak's posthoc test.

### 5.3. Results and discussion

#### 5.3.1. Gelatin-HPA synthesizes and characterization

The HMPs were synthesized using Gelatin-HPA. Gelatin was first modified hydroxyphenyl propionic group by carbodiimide/active ester-mediated coupling. The Gelatin-HPA was first were characterized by  $^1\text{H}$  - NMR., where presented peaks higher around  $\delta$  6.8 and 7.13 ppm confirming the conjugation of the presence of a phenolic ring introduced on gelatin, Figure 1. [3,22,28,30,44] The modification was confirmed by analyzing the absorbance spectra at different wavelengths, revealing a peek at 280 nm coincident with the HPA alone, Figure 2. The substitution degree was calculated based on free amines by comparison with gelatin in a TNBS method. The gelatin with high substitution presented a 84 % of modified amines, the low modified gelatin showed a substitution degree of 58 %, Table 1 S1.

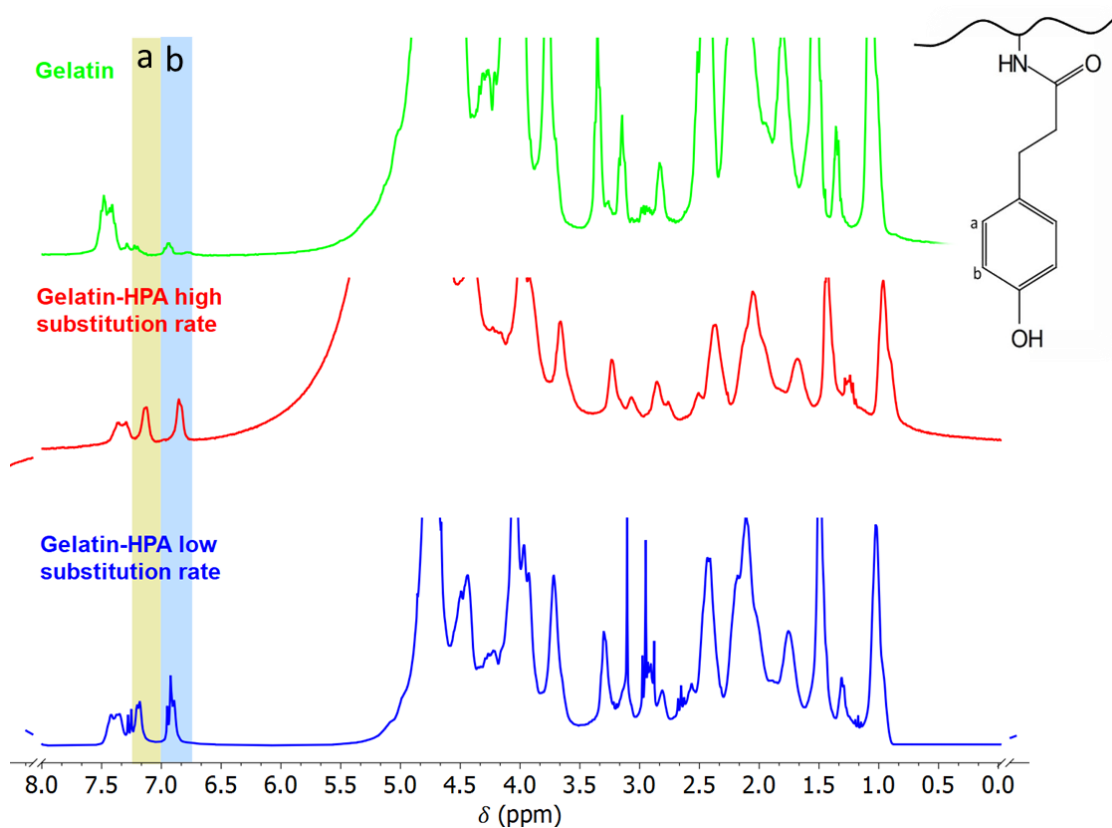


**Figure 1**  $^1\text{H}$ -NMR spectra of gelatin and gelatin-HPA with different degrees of substitution, low (blue) and high (red), and the peak corresponded to each hydrogen on the aromatic ring.

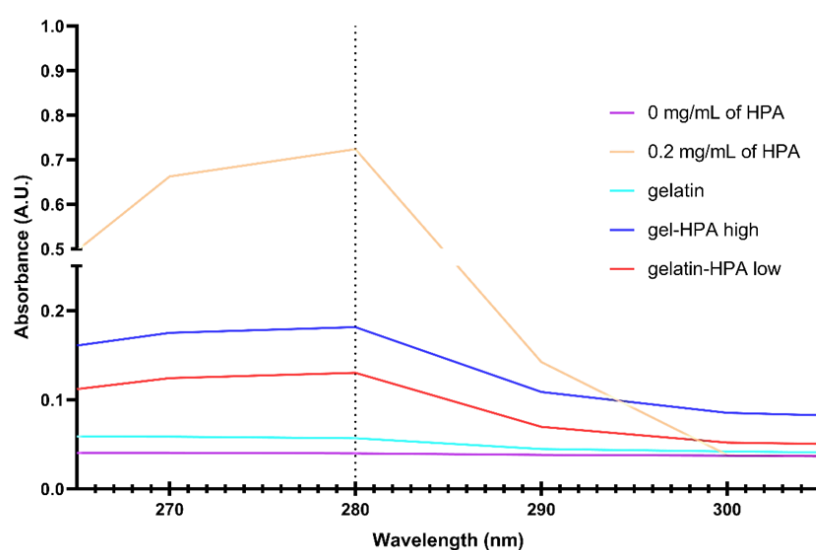


**Figure 2** UV-visible absorption spectrum of gelatin(turquoise) and gelatin-HPA low(red) and high(blue) modified. Positive control of HPA (yellow) and negative control (purple).

ATR-FTIR spectra of gelatin and modified gelatin confirmed the modification of the carboxylic groups. As expected, variations on the wavelengths of characteristic the amide regions, Figure 3. In the amide-A peak, a result of N-H stretching vibration coupled with -OH groups by hydrogen bonds were observed on gelatin at  $3272\text{ cm}^{-1}$ , but this type of vibrations is also verified in water, which can justify the peak amplitude. Nonetheless, in the modified gelatin, the wavelength was on higher wavenumbers, probably indicating new interaction formation created by the alcohol group of HPA and the remaining amines. In the amide I, the peak on the modified gelatin had a higher value number confirming the modification. The amine-II peck representing the bending N-H groups and stretching vibrations of C-N groups was detected at  $1520\text{ cm}^{-1}$  on gelatin and higher values on the modified ones, suggesting a decrease of these intermolecular interactions. [45–47]

**Table 1** Different degrees of substitution of Gelatin-HPA post-synthesis.

Gelatin modification	Temperature	Substitution degree
Gelatin –HPA high	40°C	84 %
Gelatin –HPA low	20°C	58 %

Laminarin, in this turn, is a marine polymer glucan (polysaccharide of glucose) with  $\beta$ -(1-3) and  $\beta$ -(1-6) bonds, in a proportion of 3:1, and numerous  $\beta$ -(1-6)-O-glycosidic branches. [39,40] These structural configurations enable oxidization mediated by

periodate, forming aldehyde groups, but only in the  $\beta$  (1,6) branches. [41] The peaks between  $\delta$  4.9-5.2ppm, Figure 4 - yellow section, are evidence of the hemiacetal groups formed between aldehydes and the neighboring hydroxyls. [34] The peak 4.2 ppm, Figure 4 green section is a characteristic of the  $\beta$ -(1-6) branches reduction, which provides evidence for periodate - mediated aldehyde conversion at this position. [42]

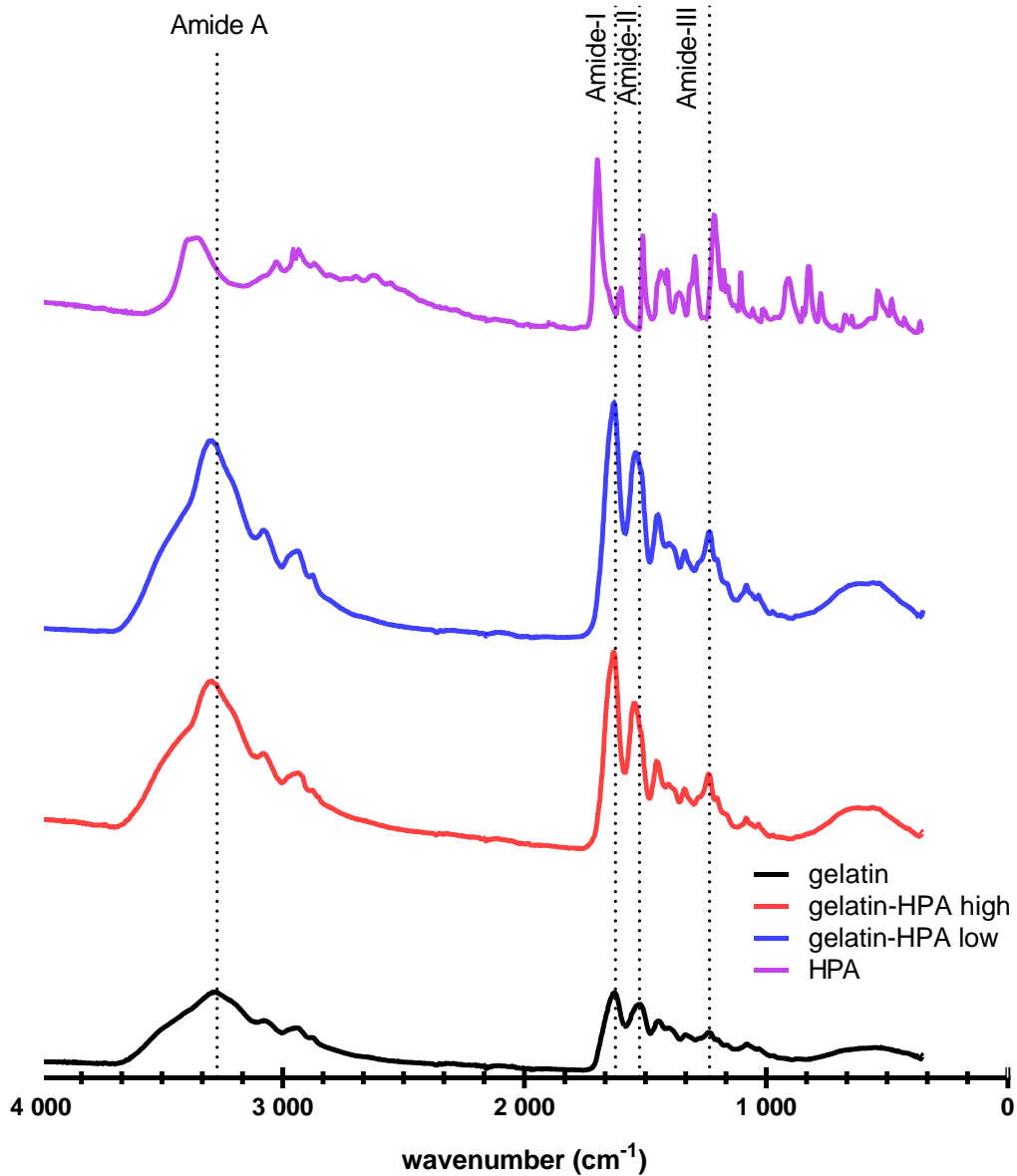


**Figure 3** ATR-FTIR spectra of gelatin (black) and different modifications of freeze dried gelatin-HPA (low in blue, and high in red), and the HPA (purple), at 25°C.

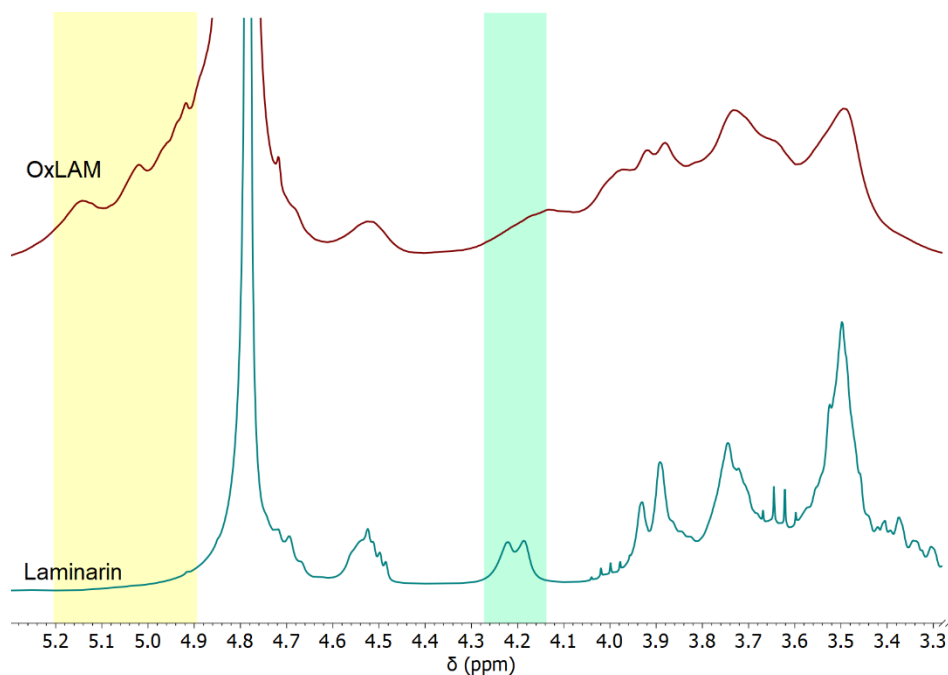


**Figure 4** Oxidized-laminarin(oxLAM) characterization.  $^1\text{H-NMR}$  spectra of native laminarin and modified laminarin, with a decrease in the peaks assigned in the green box. Spectra was acquired in deuterated water at  $25^\circ\text{C}$ . In the yellow section is evidenced the formation of hemiacetal groups. In the green section the reduction of the  $\beta$ -(1-6) branches.

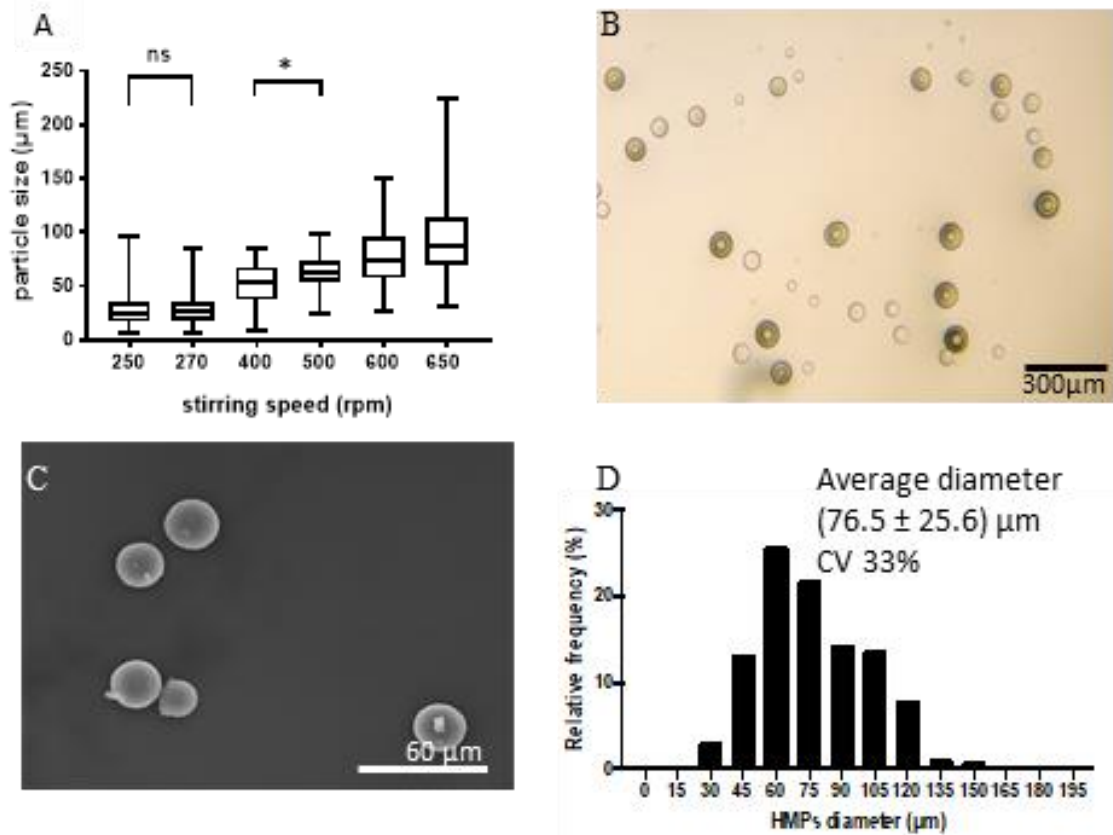
### 5.3.2. Gelatin HMPs size and distribution

In gelatin-HPA hydrogel microparticles production were used emulsion technique once it is a relatively simple technique and does not require special equipment. Usually, emulsions are in oil, though it may lead to some cell toxicity. [48,49] To avoid organic solutions, we adapted the FRESH protocol to produce gelatin-HPA HMPs, and for gelatin HMPs, in an oil-free approach. [43,50] Here, used Pluronic F-127, Arabic gum were employed as emulsion surfactants, in ethanolic dispersion. Opposite to the expected, in Gelatin-HPA, the increase of agitation leads expanded the HMP diameter, Figure 5 a. Nevertheless, it was observed that in higher stirrings, the HMPs became more polydisperse, S2. Oppositely to Gelatin-HPA HMP, in gelatin HMPs with the increase of stirring speed gelatin the HMPs became smaller, and with higher gelatin concentration led to more spherical HMPs, with lower polydispersity, S3.

An advantage of MAP is the high diffusion rates and the rapid cell infiltration, to that is necessary to have pores that cells can pass through, which means that the void's spaces need to be larger than cells. As already described, larger HMPs have larger void spaces, however, in sizes  $60\text{-}100\ \mu\text{m}$  and  $100\text{-}200\ \mu\text{m}$ , the void space between the HMPs is not

statistically different, as well as, cell infiltration, adhesion, and proliferation and growth factors secretion. [51,52] For cellular infiltration is necessary HMPs above 60 $\mu$ m [18,51,52], with this, the formulation that corresponded to these characteristics, with lower polydispersity, was with the 600 rpm where the particles were not aggregated, Figure 5b,c and d. The HMPs demonstrated a spherical shape even when lyophilized, though their size decreased.

**Figure 5** HMPs diameter distribution according to different stirring speeds, A) Gelatin-



HPA B) HMPs sample of the formulation at 600rpm; C) SEM image of the HMPs, D) histogram of the HMPs diameter distribution.

Based on analyzes of the formulations of gelatin HMPs, we used the hydrogels microparticles produced with 560 rpm, once was the higher diameter hydrogel microparticles produced and, and 20% of gelatin due to the low dispersion when compared with 10% gelatin, S3.MAP formation and mechanical characterization

In bulk gelatin-HPA hydrogels cross-linking was reported peroxidase or tyrosinase or UV cross-linking associated with a photoinitiator. [24,26,27,29] For the HMPs annealing, we used ruthenium and sodium periodate, Figure 6A, once they present a spectrum of

## RESULTS AND DISCUSSION

absorption on the UV light lower wavelengths, and several studies had revealed no cytotoxicity. Later we used tyrosinase to compare the mechanical properties and demonstrate the annealing adaptability, Figure 6B. After the HMPs annealing, the construct remains stable even in an aqueous solution or in a cell medium, Figure 6C. In the lyophilized structure, the HMPs proved that the annealing did not change the spherical format of the HMPs and is possible to see the empty spaces between the HMPs.

Contrary to gelatin hydrogels, which can swell 300 % of their size, MAPs have limited water uptake ability. The water uptake is limited to the swell of each particle. The gelatin-HPA MAP showed a limited swelling ability. The water uptake stopped after three days, around 25%, Figure 6D, revealing high stability through time, without large variations. [18,20,48,53] The water content of the granular hydrogels revealed slightly increases until day 3, Figure 6H. However, at the end of the 7 days, the granular hydrogel has 82% of water, which is relatable with a bulk hydrogel water composition.

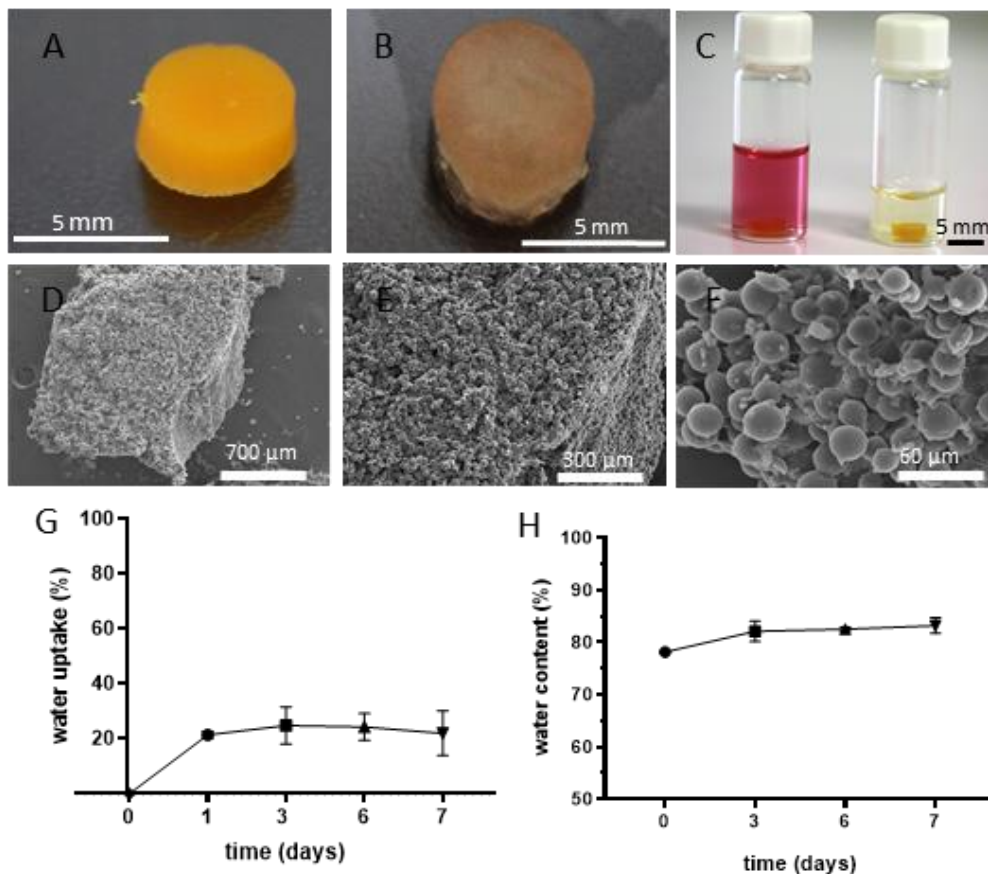


**Figure 6** A )Low gelatin MAP scaffold annealed by UV light B) enzymatic annealed MAP scaffold; C) MAP stability in the medium and PBS. D; E; F) images acquired SEM MAP with the magnification of D) 40 times; E) 100 times F) and 500 times. G) graphic representation of the swelling ability, through 7 days; H) graphic representation of water content through 7 days.

The gelatin oxLAM MAP produced was revealed to be stable with the medium as well as with other aqueous solutions, with a water content similar to the ones observed on hydrogels, Figure 7A. [37] Young's modulus of the granular hydrogels did not present statistically significant differences between the high oxLAM ( $23.73 \pm 2.63$  kPa) and low oxLAM ( $22.03 \pm 2.77$  kPa), Figure 7B and presented much higher than other MAPs, comparable with the bulk hydrogel of Gelatin-HPA. However, only high oxLAM hydrogel revealed self-healing ability, this characteristic is very interesting, especially for patient injection. The granular hydrogel proved to be injectable, forming a continuous filament Figure 7D, without crushing the gelatin particles, Figure 7E.

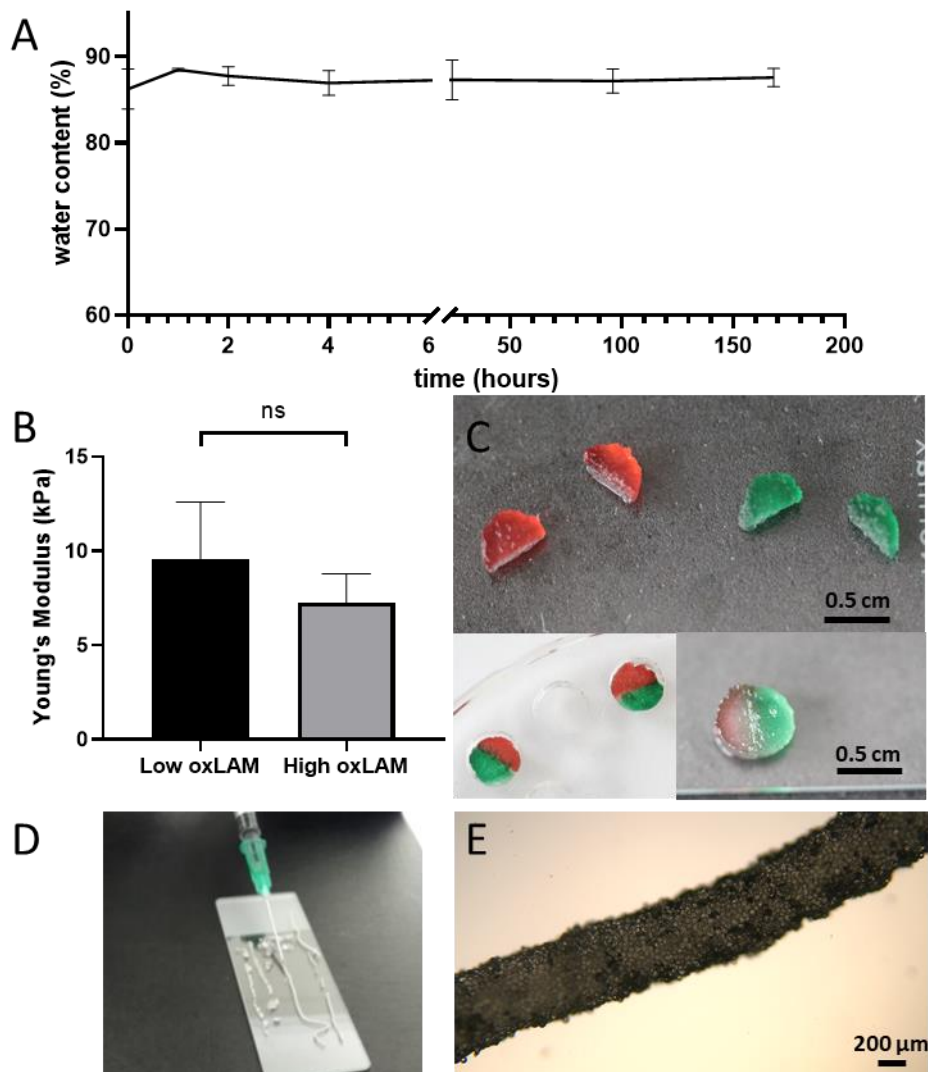


**Figure 7** A) Water content of low oxLAM granular hydrogels over 7 days. B) Young's modulus of the granular hydrogels produced, without statistical significance difference C) Self-healing ability of the high granular hydrogel. D) Injectability of the granular hydrogel, and E) the filament created.



It was observed on the mechanical assays performed, where all the MAPs had a lower Young's Modulus than a bulk hydrogel ( $19.2 \pm 2.6$  kPa). However, Young's modulus is comparable with other porous gelatin hydrogels. After The compression, the MAP also exhibits a more liquid behavior than the bulk hydrogel, which shows some breaks, Figure 6B.

In the gelatin-HPA MAPs, different types of annealing in the developed MAP did not confer distinct rheologic properties, as verified in UV-mediated annealed granular hydrogels ( $5.1 \pm 0.9$  kPa) and enzymatic annealing ( $6.6 \pm 0.9$  kPa), Figure 8A. The time of annealing need on enzymatic annealing did not lead to high compaction rates. The gelatin-HPA substitution degree presented with a higher Young's modulus probably due to the increase of HPA groups available for the annealing. However, this difference was no significant difference between the granular hydrogels with the highly modified gelatin with Young's modulus of  $9.6 \pm 1.4$  kPa. Usually, increasing the packing ratio leads to a higher Young's modulus. [54,55] Comparing with other MAPs, the MAPs developed presented a higher Young's Modulus. [52,56] The same occurs by comparing with others as gelatin porous scaffolds. [57] The granular hydrogel showed the injectability through

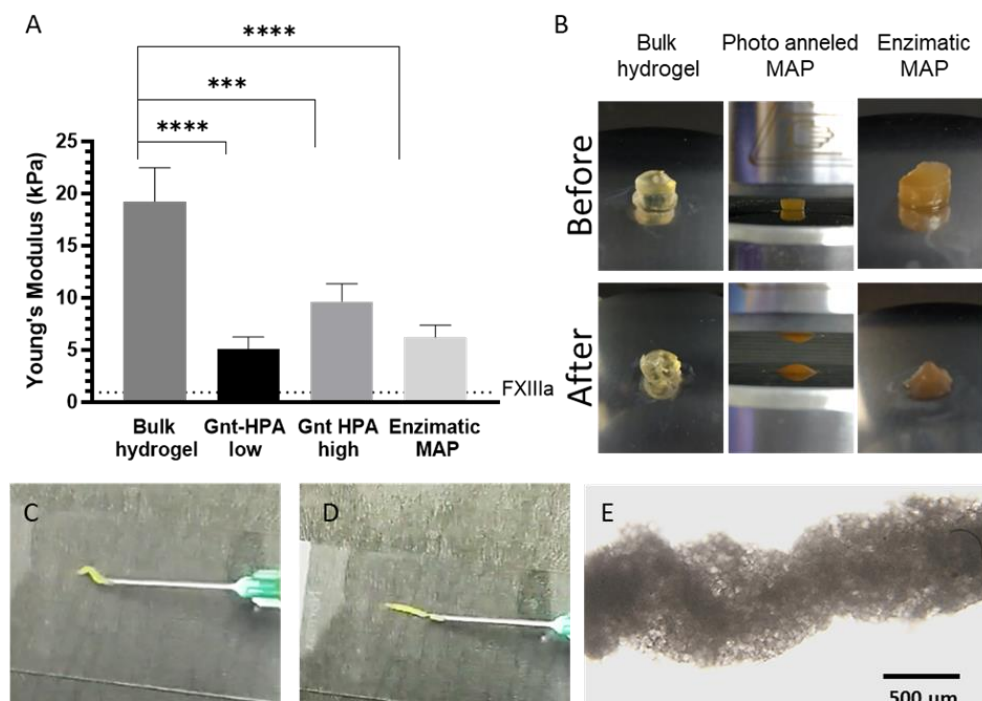


**Figure 8** A) Young's Modulus determined under compressive assays, of a Gelatin-HPA, end MAP scaffolds. Error bars represent standard deviation; \*\*\*\* $p \leq 0.0001$ . B) Scaffolds before and after the compression. C) Granular hydrogel injection; D) formation of a continuous filament of the granular hydrogel; E) continuous filament in microscopic analysis.

a needle, forming a continuous filament, Figure 8C, D. The HMPs in the filament maintained the spherical form, Figure 6E.

The biggest advantages of MAPs are conferred by the void spaces between the particles. [18,48] This characteristic allows diffusion rates similar to the ones founded in tissues. Figure 9 presents confocal images of the produced Gelatin-HPA MAPs. It is notorious empty spaces between the particles, Figure 9B. However, in a closer approximation is smaller HMPS can be between larger HMPS which will reduce the void space area, Figure 0A. The area occupied for the HMPs of 33,3% compared with a bulk hydrogel with the same dimensions.

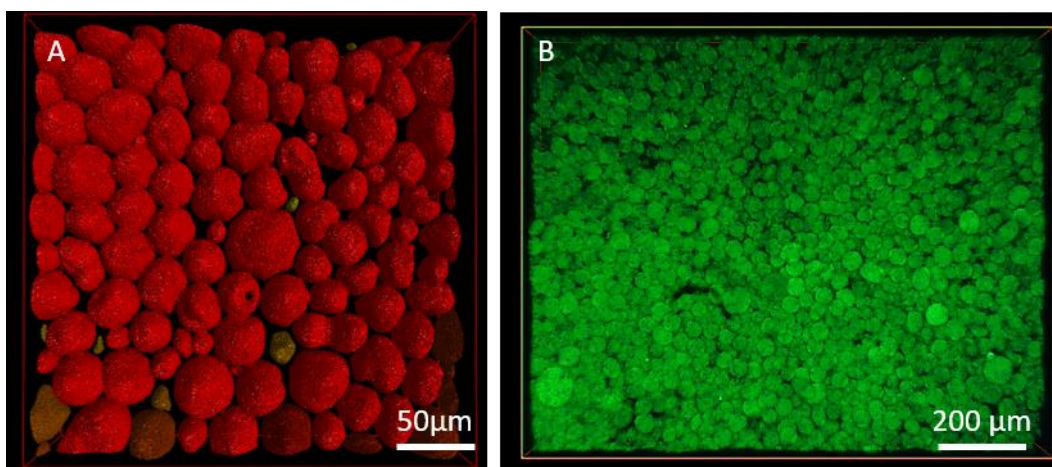


**Figure 9** MAP analysis of the area occupied by the HMPs A) surface reconstruction of a MAP; B) confocal image of a MAP.

### 5.3.3. Release profile

Initially, to test if the emulsions were stable for encapsulation, a model protein was encapsulated into the Gelatin-HPA particles. Namely, BSA-FITC was encapsulated at final concentration of  $1000 \mu\text{g.mL}^{-1}$ , presenting an  $\sim 85\%$  encapsulation efficiency. To confirm if the BSA-FITC was encapsulated, the HMPs were observed by fluorescence microscopy, which confirmed the encapsulation in Figure 11. However, testing the same methodology for VEGF encapsulation, it was not possible to detect the VEGF. With this in mind, HMPs were emersed on a VEGF solution for 2 hours for the VEGF to migrate by diffusion. The release of these HMPs had burst on the first day, with no VEGF detected on the other days, with high variability between results S4.

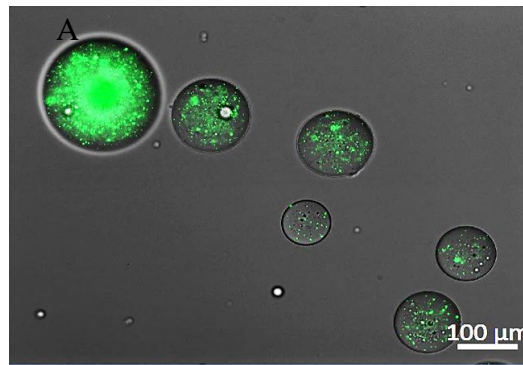


**Figure 10** Encapsulation in the HMPs a) HMPs with BSA-FITC, with the FITC groups encapsulated with fluorescence in green.

### 5.3.4. MAPs biological performance - Cell Compatibility and Support

Regarding cell biocompatibility and non-toxicity the developed MAP scaffold showed clear cells adhesion when cells were seeded on top, with low levels of cell death, as demonstrated by live/Dead analysis, Figure 11. After 12 hours, hASC only infiltrated a few layers of the scaffold remaining on the surface. Interestingly, as early as 12 hours the hASC already presented a fully extended morphology on the granular hydrogel surface, with the F-actin fibers from the seeded cells clearly surrounding the annealed HMPs. Smaller cells, such as HUVECs, showed a higher ability to move into the scaffold. However, these cells have not presented a fully spread morphology, which is expected at these early time points and in these more confined conditions. [19,20,52,58–60]

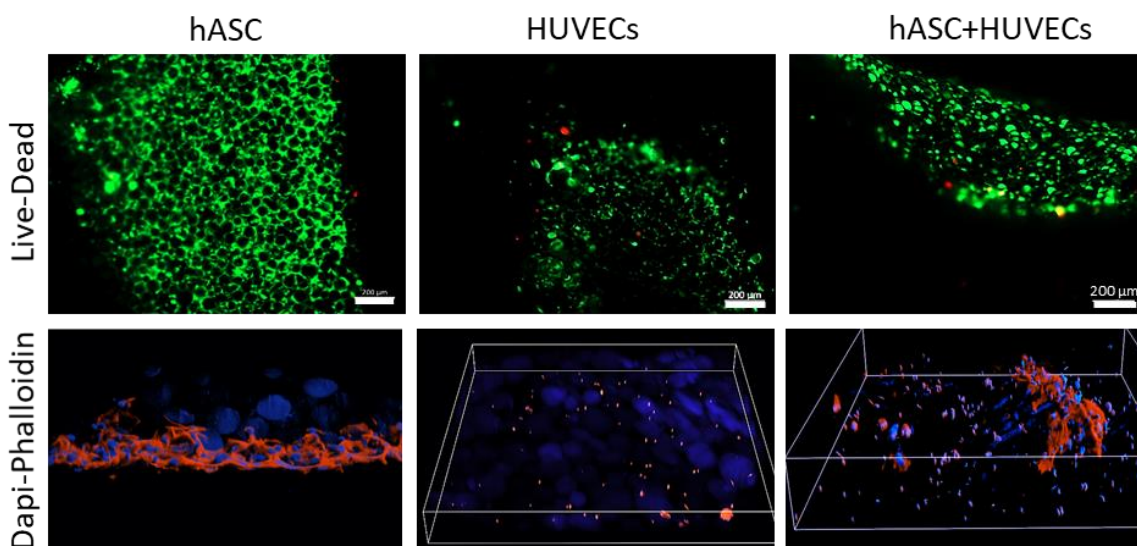


**Figure 11** Live- dead assay, where alive cells are stained with green calcein, while dead cells are stained with red PI. Image hAS and HUVECs monocultures and a co-culture of both cell types. DAPI-phalloidin 3D images staining cells, the F-actin is stained in red by the phalloidin, and the nucleus with DAPI( in blue).

In the co-culture assays, it was visible that cells adhered to the MAPs surface. Based on the monoculture assays, we can speculate that ASCs represent the majority of surface bound cells, while the cells inside the MAP are HUVECs. Nevertheless, it is still necessary to use specific cell markers to prove this hypothesis.

In assays performed along seven days, hASC monoculture, cell viability starts to slightly decrease, in bulk hydrogels and MAP, however the AlamarBlue® data is not significant and these results should be further complemented with DNA analysis assays. On the other hand, in live-death staining it is notorious that the bulk hydrogel presents a higher fraction of dead cells, on the contrary to what happens in MAPs scaffolds. Importantly, in the MAP scaffold, hASCs showed active fibers surrounding the HMPs, Figure 11. The metabolic activity was lower on MAP bulk hydrogels, but these results were contradicted with the fluorescence images. It would be interesting to analyze if the cells are changing the phenotype to one that is less metabolic active, to better understand this difference.

As already shown in Figure 11, after 12h, HUVECs showed the ability to move through the microporous scaffold structure, and the same seems to happen along time. However, on day 7, only a few cells were visible on the scaffolds. After one day, it is possible to see that HUVECs are attached and located around the gelatin-HPA HMPs, Figure 13. The cell viability also decreased along the time, Figure 13. Similarly, to what might take place in ASCs, the high cellular density used may cause the decrease the cell viability, with this new cell assays were performed with lower cell amount, cell assays with 50 000 cells/gel were performed, S5. As previously described, cells seem to interpenetrate into the MAP scaffold, and as expected, cell viability was better maintained in lower cell density. And in comparison to the previous results with higher cell density, the MAP scaffold had considerably higher cell viability than the bulk hydrogel, as expected,S5.

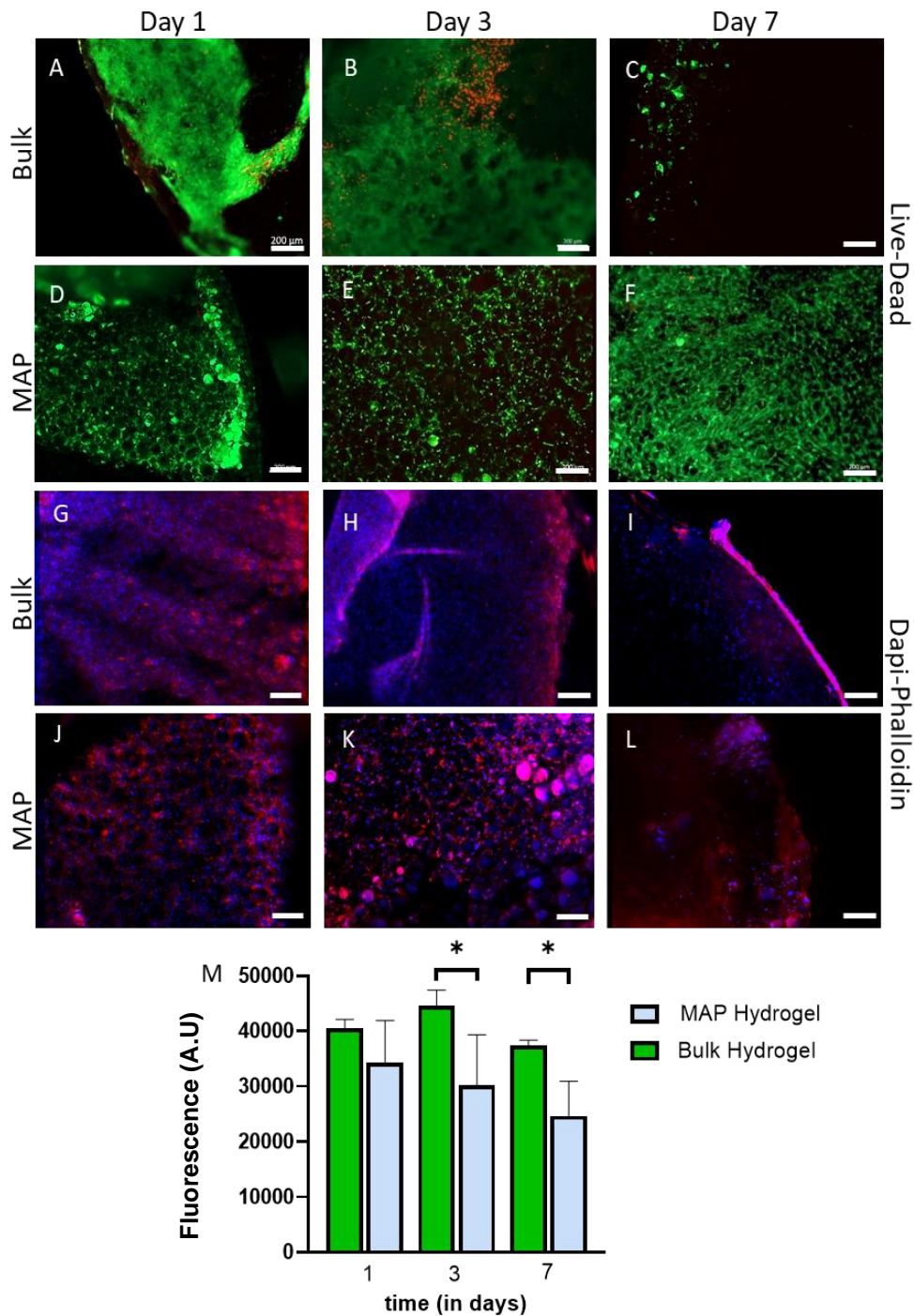


**Figure 12** Live- dead staining, with hASC, where live cells are stained with calcein – green channel, while dead cells are with PI – red channel. A - C) Bulk hydrogels; D - F) MAPs scaffold, at day 1, 3 and 7. DAPI-phalloidin 3D confocal laser scanning reconstruction of stained cells of: (G - I) Bulk and (J – L) MAPs scaffolds. F-actin- red channel, DAPI cell nucleus – Blue channel, at days 1, 3 and 7. M) cell viability assay through the 7 days with bulk hydrogel in green and MAP in blue. scale bar: 200 $\mu$ m. Data is presented as mean  $\pm$  s.d., n=3, \*p<0.05.

In co-cultures, metabolic activity decreased over time Figure 14, as showed on the monoculture assays. However, on the first day and the seventh day the cell viability was

higher in granular hydrogels. It was proved by the live-dead assay, where more cells could be founded alive. The cells seem to start to infiltrate the MAP. Evaluating cell extension, on the 7<sup>th</sup> day, the MAP scaffold proportionated more elongation of the actin fibers Figure 14. As in the others, more cells were presented alive however they showed a decrease in their viability by Alamar Blue.

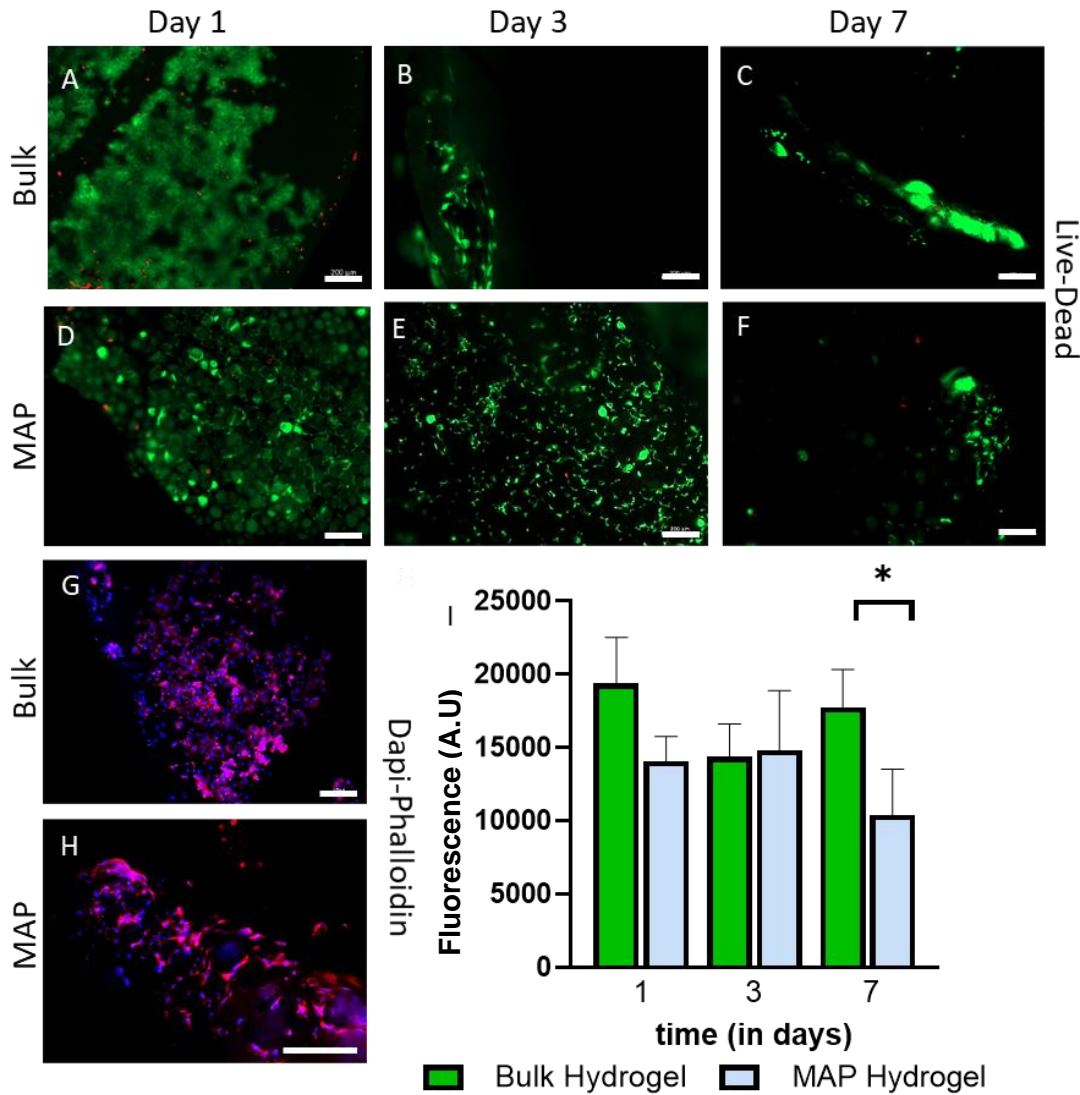


**Figure 13** Live- dead staining, with HUVECs, where live cells are stained with calcein-green channel, while dead cells are stained with PI- red channel. A-C) Bulk hydrogel, D-F) Gelatin-HPA MAPs scaffolds. DAPI-phalloidin 3D confocal laser scanning microscopy reconstruction of G) Bulk hydrogel and H) MAP, at day 1. F-actin- red channel, DAPI nuclear staining- blue channel. scale bar: 200  $\mu$ m. I) AlamarBlue<sup>®</sup> Cell viability assay with bulk hydrogel in green and MAP in blue, at the course of seven days (Data is represented as mean  $\pm$  s.d., n=3, \*p<0.05).

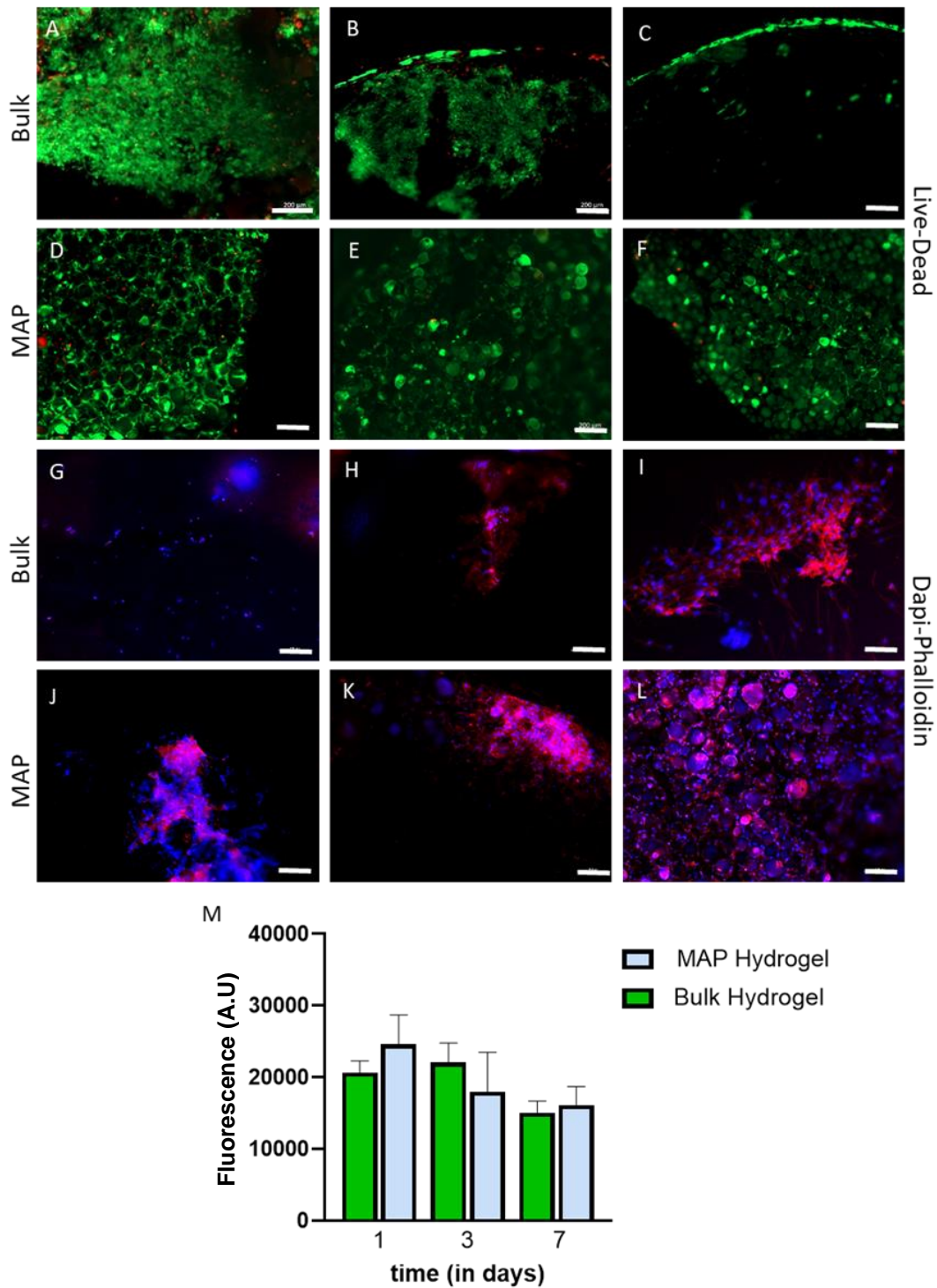


**Figure 14** Live- dead staining, with co-culture, where live cells are stained with Calcein – green channel, while dead cells are stained with PI – red channel. A - C) Bulk hydrogels, D-F ) MAPs scaffolds, at days 1, 3 and 7. G-L) DAPI-phalloidin 3D confocal laser scanning reconstructed micrographs.

The cells were seed-on-top of the MAP scaffold, showing that cell dimensions influence the ability to infiltrate into the scaffold. Smaller cells like HUVECs showed a

higher scaffold infiltration in reduced time (12h), while hASC only infiltrate a few layers of the MAP. In all the cell types used, the F-actin fibers encircle the particles, this could increase the stiffness of the scaffold by increasing the particle's connection. The MAP produced proved to be biocompatible and enable cell proliferation. These results show the MAP a higher penetration in a reduced time than the bulk hydrogel which is essential in tissue regeneration.

### 5.3.5. 3D bioprinting

Recently granular hydrogels are being started to be explored as multi-component bioinks for 3D bioprinting due to their suitable rheological features including shear thinning and viscosity. [61–64] It was possible to print in a continuous filament. The shear rate between the HMPs did not cause cell damage, leading to the dead, Figure 16. After 3D Bioprinting the majority of the extruded cells were viable, including 1 day after printing. The structure was printed with fidelity. Nevertheless, this process remains some optimizations. The HMPs approach allows a higher control of the cell environment and allows new approaches for fabrications of bioinks with heterogeneity similar to the ones founded in tissues.

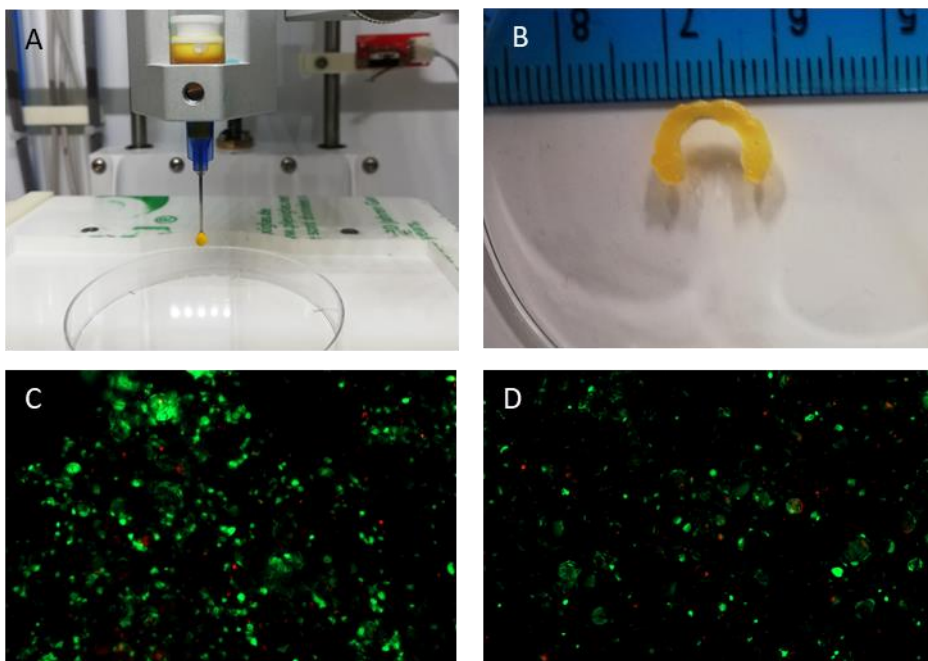


**Figure 15** Live- dead staining, with hASC, where alive cells are stained with green calcein, while dead cells are stained with red PI. C) live dead after the printing, D) live dead on day one. where alive cells are stained with green calcein, while dead cells are stained with red. The scale bar corresponds to 200 $\mu$ m.



## 5.4. Conclusions

In summary, here a gelatin-HPA based photocrosslinkable MAP suitable for annealing on-demand was developed. The hydrogel microparticle components of the MAP, as well as the entire hierarchic structure, was stable, presented suitable mechanical properties for application in soft Tissue engineering applications (elastic modulus ca~10kPa). The gelatin-HPA MAP showed the ability to encapsulate a model protein which may lead to the encapsulation of different molecules, while also successfully functioning as a cell adhesive and cell supporting platform. Moreover, the gelatin-HPA MAPs scaffold was also suitable for 3D bioprinting as a bioink containing stem cells. The overall results indicate that cells are maintained viable after printing a key fact which opens the possibility to process such HMPs for personalized tissue engineering applications that benefit from CAD designed 3D granular constructs.

## 5.5. References

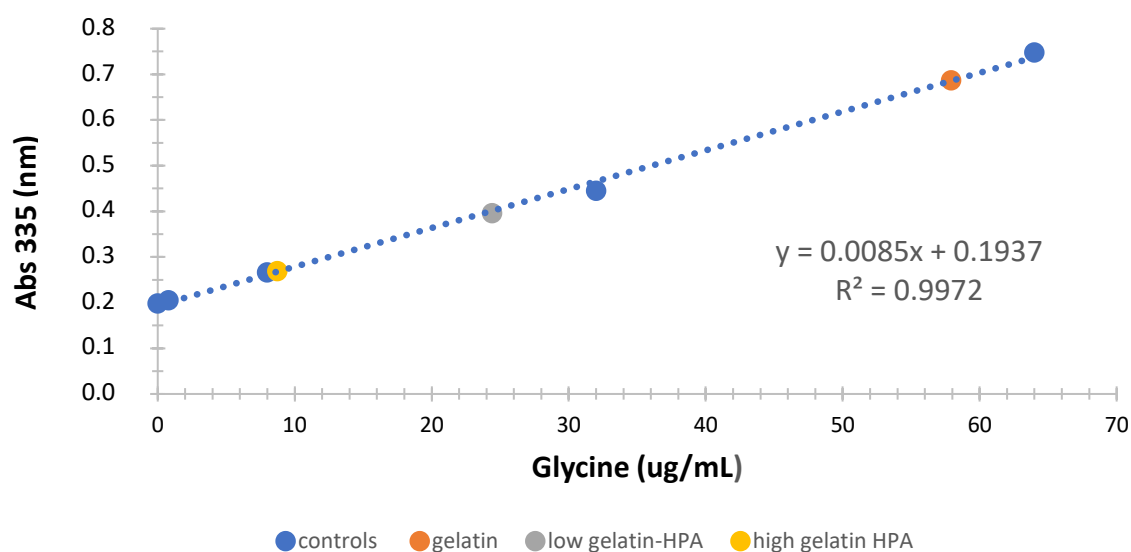
1. Moysidou, C.-M., Barberio, C., and Owens, R.M. (2021) Advances in Engineering Human Tissue Models. *Front. Bioeng. Biotechnol.*, **8**, 620962.
2. Golchin, A., and Farahany, T.Z. (2019) Biological Products: Cellular Therapy and FDA Approved Products. *Stem Cell Rev and Rep*, **15** (2), 166–175.
3. Yoon, D.S., Lee, Y., Ryu, H.A., Jang, Y., Lee, K.-M., Choi, Y., Choi, W.J., Lee, M., Park, K.M., Park, K.D., and Lee, J.W. (2016) Cell recruiting chemokine-loaded sprayable gelatin hydrogel dressings for diabetic wound healing. *Acta Biomaterialia*, **38**, 59–68.
4. Wang, Q., Tang, Y., Ke, Q., Yin, W., Zhang, C., Guo, Y., and Guan, J. (2020) Magnetic lanthanum-doped hydroxyapatite/chitosan scaffolds with endogenous stem cell-recruiting and immunomodulatory properties for bone regeneration. *J. Mater. Chem. B*, **8** (24), 5280–5292.
5. Shafiq, M., Zhang, Y., Zhu, D., Zhao, Z., Kim, D.-H., Kim, S.H., and Kong, D. (2018) In situ cardiac regeneration by using neuropeptide substance P and IGF-1C peptide eluting heart patches. *Regenerative Biomaterials*, **5** (5), 303–316.
6. Karamysheva, A.F. (2008) Mechanisms of angiogenesis. *Biochemistry Moscow*, **73** (7), 751–762.
7. Rufaihah, A.J., Johari, N.A., Vaibavi, S.R., Plotkin, M., Di Thien, D.T., Kofidis, T., and Seliktar, D. (2017) Dual delivery of VEGF and ANG-1 in ischemic hearts using an injectable hydrogel. *Acta Biomaterialia*, **48**, 58–67.
8. Ma, H., Caldwell, A.S., Azagarsamy, M.A., Gonzalez Rodriguez, A., and Anseth, K.S. (2020) Bioorthogonal click chemistries enable simultaneous spatial patterning of multiple proteins to probe synergistic protein effects on fibroblast function. *Biomaterials*, **255**, 120205.
9. Yu, Y., Lin, X., Wang, Q., He, M., and Chau, Y. (2019) Long-term therapeutic effect in nonhuman primate eye from a single injection of anti-VEGF controlled release hydrogel. *Bioengineering & Translational Medicine*, **4** (2).
10. Chen, M.H., Chung, J.J., Mealy, J.E., Zaman, S., Li, E.C., Arisi, M.F., Atluri, P., and Burdick, J.A. (2019) Injectable Supramolecular Hydrogel/Microgel Composites for Therapeutic Delivery. *Macromol. Biosci.*, **19** (1), 1800248.
11. Jeon, O., Wolfson, D.W., and Alsberg, E. (2015) In-Situ Formation of Growth-Factor-Loaded Coacervate Microparticle-Embedded Hydrogels for Directing Encapsulated Stem Cell Fate. *Adv. Mater.*, **27** (13), 2216–2223.
12. Solorio, L.D., Phillips, L.M., McMillan, A., Cheng, C.W., Dang, P.N., Samorezov, J.E., Yu, X., Murphy, W.L., and Alsberg, E. (2015) Spatially Organized Differentiation of Mesenchymal Stem Cells within Biphasic Microparticle-Incorporated High Cell Density Osteochondral Tissues. *Adv. Healthcare Mater.*, **4** (15), 2306–2313.

13. Nourbakhsh, M., Zarrintaj, P., Jafari, S.H., Hosseini, S.M., Aliakbari, S., Pourbadie, H.G., Naderi, N., Zibaii, M.I., Gholizadeh, S.S., Ramsey, J.D., Thomas, S., Farokhi, M., and Saeb, M.R. (2020) Fabricating an electroactive injectable hydrogel based on pluronic-chitosan/aniline-pentamer containing angiogenic factor for functional repair of the hippocampus ischemia rat model. *Materials Science and Engineering: C*, **117**, 111328.
14. Nih, L.R. (2020) Engineered Biomaterials for Tissue Regeneration of Innervated and Vascularized Tissues: Lessons Learned from the Brain. *Journal of Endodontics*, **46** (9), S101–S104.
15. Patel, Z.S., Ueda, H., Yamamoto, M., Tabata, Y., and Mikos, A.G. (2008) In Vitro and In Vivo Release of Vascular Endothelial Growth Factor from Gelatin Microparticles and Biodegradable Composite Scaffolds. *Pharm Res*, **25** (10), 2370–2378.
16. Griffin, D.R., Weaver, W.M., Scumpia, P.O., Di Carlo, D., and Segura, T. (2015) Accelerated wound healing by injectable microporous gel scaffolds assembled from annealed building blocks. *Nature Mater*, **14** (7), 737–744.
17. Dimatteo, R., Darling, N.J., and Segura, T. (2018) In situ forming injectable hydrogels for drug delivery and wound repair. *Advanced Drug Delivery Reviews*, **127**, 167–184.
18. Riley, L., Schirmer, L., and Segura, T. (2019) Granular hydrogels: emergent properties of jammed hydrogel microparticles and their applications in tissue repair and regeneration. *Current Opinion in Biotechnology*, **60**, 1–8.
19. Darling, N.J., Sideris, E., Hamada, N., Carmichael, S.T., and Segura, T. (2018) Injectable and Spatially Patterned Microporous Annealed Particle (MAP) Hydrogels for Tissue Repair Applications. *Adv. Sci.*, **5** (11), 1801046.
20. Nih, L.R., Sideris, E., Carmichael, S.T., and Segura, T. (2017) Injection of Microporous Annealing Particle (MAP) Hydrogels in the Stroke Cavity Reduces Gliosis and Inflammation and Promotes NPC Migration to the Lesion. *Adv. Mater.*, **29** (32), 1606471.
21. Fang, J., Koh, J., Fang, Q., Qiu, H., Archang, M.M., Hasani-Sadrabadi, M.M., Miwa, H., Zhong, X., Sievers, R., Gao, D., Lee, R., Di Carlo, D., and Li, S. (2020) Injectable Drug-Releasing Microporous Annealed Particle Scaffolds for Treating Myocardial Infarction. *Adv. Funct. Mater.*, 2004307.
22. Wang, L.-S., Chung, J.E., Pui-Yik Chan, P., and Kurisawa, M. (2010) Injectable biodegradable hydrogels with tunable mechanical properties for the stimulation of neurogenic differentiation of human mesenchymal stem cells in 3D culture. *Biomaterials*, **31** (6), 1148–1157.
23. Hu, M., Kurisawa, M., Deng, R., Teo, C.-M., Schumacher, A., Thong, Y.-X., Wang, L., Schumacher, K.M., and Ying, J.Y. (2009) Cell immobilization in gelatin–hydroxyphenylpropionic acid hydrogel fibers. *Biomaterials*, **30** (21), 3523–3531.
24. Liu, Y., Cheong NG, S., Yu, J., and Tsai, W.-B. (2019) Modification and crosslinking of gelatin-based biomaterials as tissue adhesives. *Colloids and Surfaces B: Biointerfaces*, **174**, 316–323.
25. Le Thi, P., Lee, Y., Nguyen, D.H., and Park, K.D. (2017) In situ forming gelatin hydrogels by dual-enzymatic cross-linking for enhanced tissue adhesiveness. *J. Mater. Chem. B*, **5** (4), 757–764.
26. Al-Abboodi, A., Zhang, S., Al-Saady, M., Ong, J.W., Chan, P.P.Y., and Fu, J. (2019) Printing *in situ* tissue sealant with visible-light-crosslinked porous hydrogel. *Biomed. Mater.*, **14** (4), 045010.
27. Lim, T.C., Toh, W.S., Wang, L.-S., Kurisawa, M., and Spector, M. (2012) The effect of injectable gelatin-hydroxyphenylpropionic acid hydrogel matrices on the proliferation, migration, differentiation and oxidative stress resistance of adult neural stem cells. *Biomaterials*, **33** (12), 3446–3455.
28. Hoang Thi, T.T., Lee, Y., Ryu, S.B., Nguyen, D.H., and Park, K.D. (2018) Enhanced tissue adhesiveness of injectable gelatin hydrogels through dual catalytic activity of horseradish peroxidase. *Biopolymers*, **109** (1), e23077.
29. Liu, H.-Y., Korc, M., and Lin, C.-C. (2018) Biomimetic and enzyme-responsive dynamic hydrogels for studying cell-matrix interactions in pancreatic ductal adenocarcinoma. *Biomaterials*, **160**, 24–36.
30. Wang, L.-S., Du, C., Chung, J.E., and Kurisawa, M. (2012) Enzymatically cross-linked gelatin-phenol hydrogels with a broader stiffness range for osteogenic differentiation of human mesenchymal stem cells. *Acta Biomaterialia*, **8** (5), 1826–1837.
31. Rioux, L.-E., and Turgeon, S.L. (2015) Chapter 7 - Seaweed carbohydrates, in *Seaweed Sustainability* (eds. Tiwari, B.K., and Troy, D.J.), Academic Press, San Diego, pp. 141–192.
32. Lee, Y.-E., Kim, H., Seo, C., Park, T., Lee, K.B., Yoo, S.-Y., Hong, S.-C., Kim, J.T., and Lee, J. (2017) Marine polysaccharides: therapeutic efficacy and biomedical applications. *Arch. Pharm. Res.*, **40** (9), 1006–1020.
33. Lee, K.Y., and Mooney, D.J. (2012) Alginate: Properties and biomedical applications. *Progress in Polymer Science*, **37** (1), 106–126.

34. Custódio, C.A., Reis, R.L., and Mano, J.F. (2016) Photo-Cross-Linked Laminarin-Based Hydrogels for Biomedical Applications. *Biomacromolecules*, **17** (5), 1602–1609.
35. Martins, C.R., Custódio, C.A., and Mano, J.F. (2018) Multifunctional laminarin microparticles for cell adhesion and expansion. *Carbohydr Polym*, **202**, 91–98.
36. Zargarzadeh, M., Amaral, A.J.R., Custódio, C.A., and Mano, J.F. (2020) Biomedical applications of laminarin. *Carbohydr Polym*, **232**, 115774.
37. Lavrador, P., Gaspar, V.M., and Mano, J.F. (2020) Mechanochemical Patternable ECM-Mimetic Hydrogels for Programmed Cell Orientation. *Adv. Healthcare Mater.*, **9** (10), 1901860.
38. Lee, B.H., Shirahama, H., Cho, N.-J., and Tan, L.P. (2015) Efficient and controllable synthesis of highly substituted gelatin methacrylamide for mechanically stiff hydrogels. *RSC Adv.*, **5** (128), 106094–106097.
39. Menshova, R.V., Ermakova, S.P., Anastuyk, S.D., Isakov, V.V., Dubrovskaya, Y.V., Kusaykin, M.I., Um, B.-H., and Zvyagintseva, T.N. (2014) Structure, enzymatic transformation and anticancer activity of branched high molecular weight laminaran from brown alga *Eisenia bicyclis*. *Carbohydrate Polymers*, **99**, 101–109.
40. Usui, T., Toriyama, T., and Mizuno, T. (1979) Structural investigation of laminaran of *Eisenia bicyclis*. *Agricultural and Biological Chemistry*, **43** (3), 603–611.
41. Synytsya, A., and Novak, M. (2014) Structural analysis of glucans. *Ann Transl Med*, **2** (2), 17.
42. Torosantucci, A., Bromuro, C., Chiani, P., De Bernardis, F., Berti, F., Galli, C., Norelli, F., Bellucci, C., Polonelli, L., Costantino, P., Rappuoli, R., and Cassone, A. (2005) A novel glyco-conjugate vaccine against fungal pathogens. *Journal of Experimental Medicine*, **202** (5), 597–606.
43. Lee, A., Hudson, A.R., Shiwarski, D.J., Tashman, J.W., Hinton, T.J., Yerneni, S., Bliley, J.M., Campbell, P.G., and Feinberg, A.W. (2019) 3D bioprinting of collagen to rebuild components of the human heart. *Science*, **365** (6452), 482–487.
44. Lim, T.C., Toh, W.S., Wang, L.-S., Kurisawa, M., and Spector, M. (2012) The effect of injectable gelatin-hydroxyphenylpropionic acid hydrogel matrices on the proliferation, migration, differentiation and oxidative stress resistance of adult neural stem cells. *Biomaterials*, **33** (12), 3446–3455.
45. Benbettaieb, N., Karbowski, T., Brachais, C.-H., and Debeaufort, F. (2015) Coupling tyrosol, quercetin or ferulic acid and electron beam irradiation to cross-link chitosan–gelatin films: A structure–function approach. *European Polymer Journal*, **67**, 113–127.
46. Benbettaieb, N., Kurek, M., Bornaz, S., and Debeaufort, F. (2014) Barrier, structural and mechanical properties of bovine gelatin-chitosan blend films related to biopolymer interactions: Properties of gelatin-chitosan films. *J. Sci. Food Agric.*, **94** (12), 2409–2419.
47. Nur Hanani, Z.A., McNamara, J., Roos, Y.H., and Kerry, J.P. (2013) Effect of plasticizer content on the functional properties of extruded gelatin-based composite films. *Food Hydrocolloids*, **31** (2), 264–269.
48. Daly, A.C., Riley, L., Segura, T., e Burdick, J.A. (2019) Hydrogel microparticles for biomedical applications. *Nat Rev Mater*, **5**, 20–43.
49. Nasiri, R., Shamloo, A., Ahadian, S., Amirifar, L., Akbari, J., Goudie, M.J., Lee, K., Ashammakhi, N., Dokmeci, M.R., Di Carlo, D., and Khademhosseini, A. (2020) Microfluidic-Based Approaches in Targeted Cell/Particle Separation Based on Physical Properties: Fundamentals and Applications. *Small*, **16** (29), 2000171.
50. Hinton, T.J., Jallerat, Q., Palchesko, R.N., Park, J.H., Grodzicki, M.S., Shue, H.-J., Ramadan, M.H., Hudson, A.R., and Feinberg, A.W. (2015) Three-dimensional printing of complex biological structures by freeform reversible embedding of suspended hydrogels. *Sci. Adv.*, **1** (9), e1500758.
51. Caldwell, A.S., Rao, V.V., Golden, A.C., and Anseth, K.S. (2020) Porous bio-click microgel scaffolds control hMSC interactions and promote their secretory properties. *Biomaterials*, **232**, 119725.
52. Truong, N.F., Kurt, E., Tahmizyan, N., Leshner-Pérez, S.C., Chen, M., Darling, N.J., Xi, W., and Segura, T. (2019) Microporous annealed particle hydrogel stiffness, void space size, and adhesion properties impact cell proliferation, cell spreading, and gene transfer. *Acta Biomaterialia*, **94**, 160–172.
53. Alzanbaki, H., Moretti, M., and Hauser, C.A.E. (2021) Engineered Microgels—Their Manufacturing and Biomedical Applications. *Micromachines*, **12** (1), 45.
54. Holt, S.E., Rakoski, A., Jivan, F., Pérez, L.M., and Alge, D.L. (2020) Hydrogel Synthesis and Stabilization via Tetrazine Click-Induced Secondary Interactions. *Macromol. Rapid Commun.*, 2000287.
55. Xin, S., Dai, J., Gregory, C.A., Han, A., and Alge, D.L. (2020) Creating Physicochemical Gradients in Modular Microporous Annealed Particle Hydrogels via a Microfluidic Method. *Adv. Funct. Mater.*, **30** (6), 1907102.
56. Sideris, E., Griffin, D.R., Ding, Y., Li, S., Weaver, M., Carlo, D.D., Hsiai, T., and Segura, T. (2016) Particle hydrogels based on hyaluronic acid building blocks, **2**, 23.

57. Puckert, C., Tomaskovic-Crook, E., Gambhir, S., Wallace, G.G., Crook, J.M., and Higgins, M.J. (2017) Electro-mechano responsive properties of gelatin methacrylate (GelMA) hydrogel on conducting polymer electrodes quantified using atomic force microscopy. *Soft Matter*, **13** (27), 4761–4772.
58. Zoratto, N., Di Lisa, D., Rutte, J., Sakib, M.N., Alves e Silva, A.R., Tamayol, A., Di Carlo, D., Khademhosseini, A., and Sheikhi, A. (2020) In situ forming microporous gelatin methacryloyl hydrogel scaffolds from thermostable microgels for tissue engineering. *Bioeng Transl Med*, **5** (3).
59. Griffin, D.R., Archang, M.M., Kuan, C.-H., Weaver, W.M., Weinstein, J.S., Feng, A.C., Ruccia, A., Sideris, E., Ragkousis, V., Koh, J., Plikus, M.V., Di Carlo, D., Segura, T., and Scumpia, P.O. (2020) Activating an adaptive immune response from a hydrogel scaffold imparts regenerative wound healing. *Nat. Mater*, 1-20.
60. Mendes, B.B., Daly, A.C., Reis, R.L., Domingues, R.M.A., Gomes, M.E., and Burdick, J.A. (2020) Injectable hyaluronic acid and platelet lysate-derived granular hydrogels for biomedical applications. *Acta Biomaterialia*, S1742706120306383.
61. Cheng, W., Zhang, J., Liu, J., and Yu, Z. (2020) Granular hydrogels for 3D bioprinting applications. *View*, 20200060.
62. Zhang, H., Cong, Y., Osi, A.R., Zhou, Y., Huang, F., Zaccaria, R.P., Chen, J., Wang, R., and Fu, J. (2020) Direct 3D Printed Biomimetic Scaffolds Based on Hydrogel Microparticles for Cell Spheroid Growth. *Adv. Funct. Mater.*, **30** (13), 1910573.
63. Highley, C.B., Song, K.H., Daly, A.C., and Burdick, J.A. (2019) Jammed Microgel Inks for 3D Printing Applications. *Adv. Sci.*, **6** (1), 1801076.
64. Highley, C.B., Rodell, C.B., and Burdick, J.A. (2015) Direct 3D Printing of Shear-Thinning Hydrogels into Self-Healing Hydrogels. *Adv. Mater.*, **27** (34), 5075–5079.

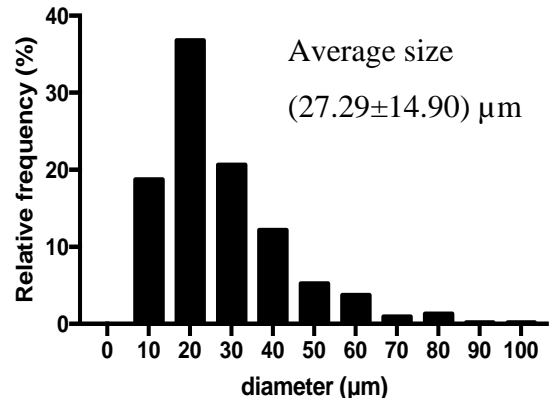
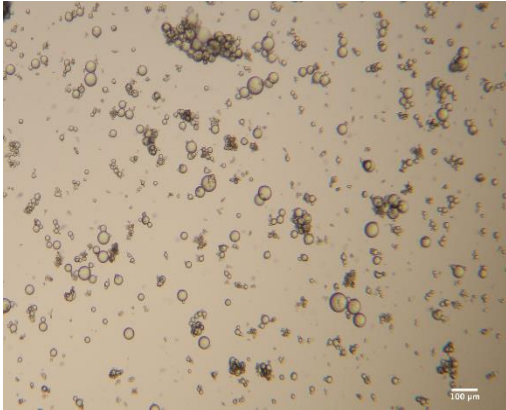
## 5.6. Supplementary information



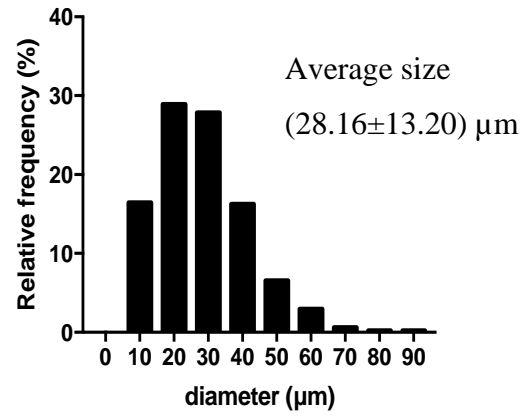
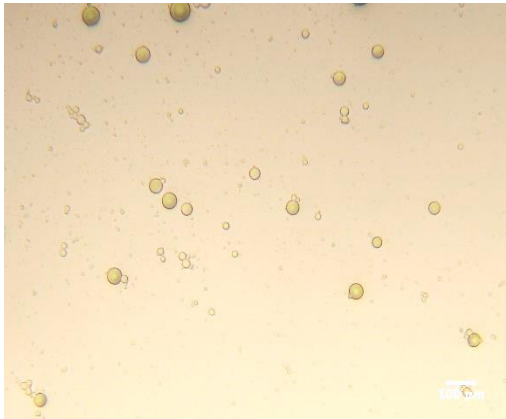
**S 1** TNBS assay. Calibration curve (blue dots), the low modified gelatin (grey dots), high modified gelatin (yellow dots) were compared to gelatin (orange dots).

RESULTS AND DISCUSSION

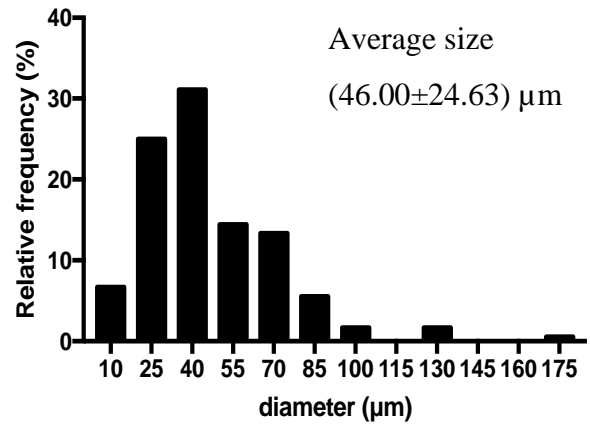
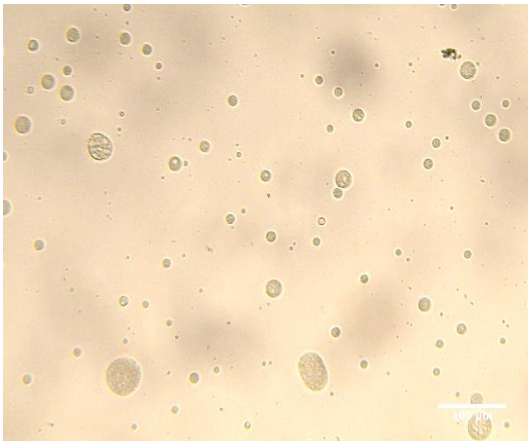
250 rpm



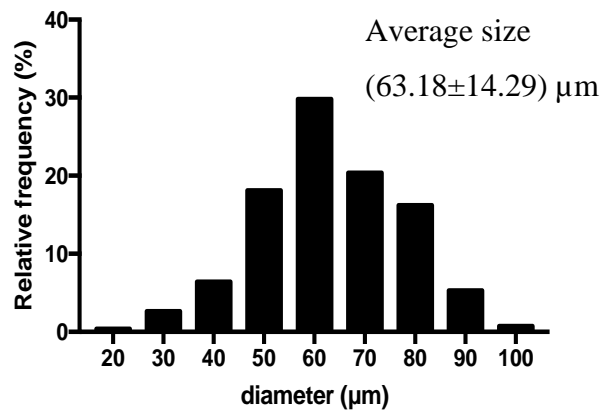
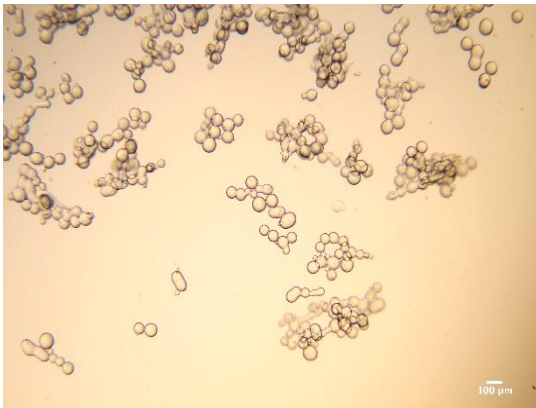
270 rpm

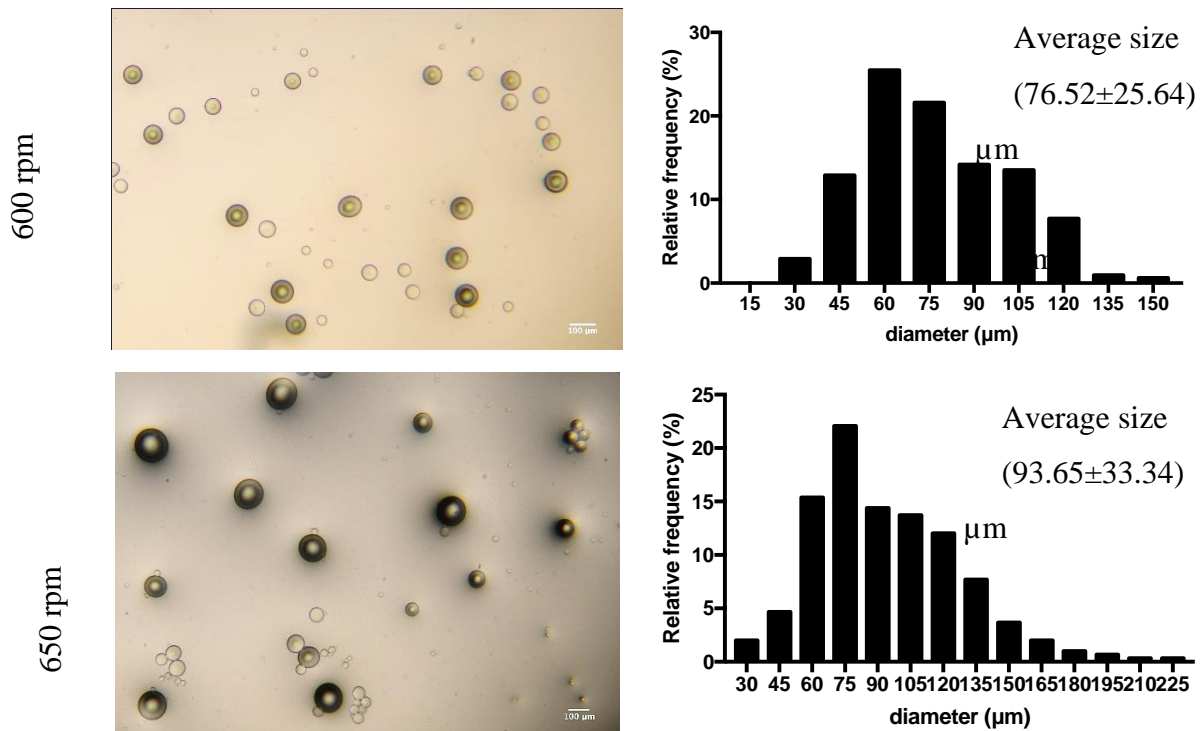


395 rpm

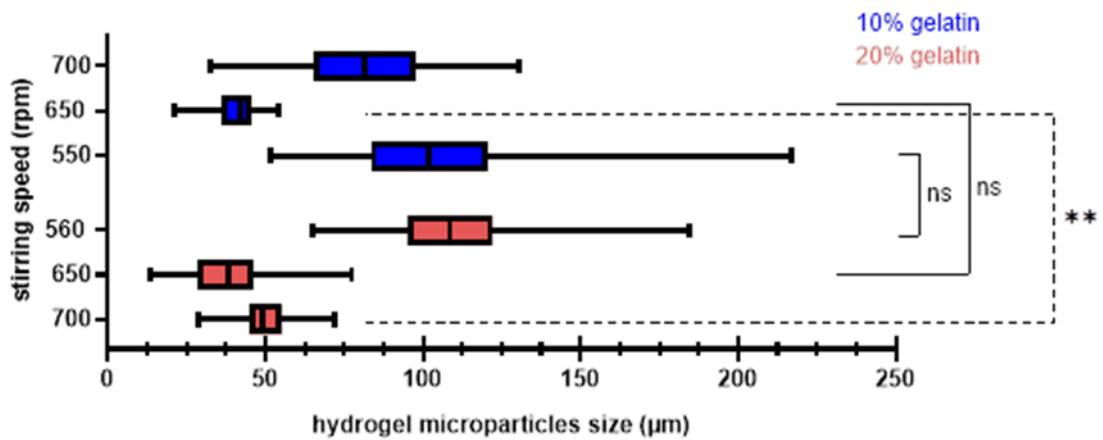


510 rpm

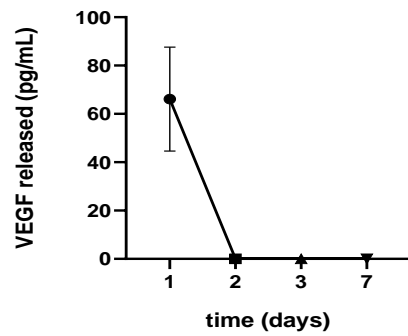




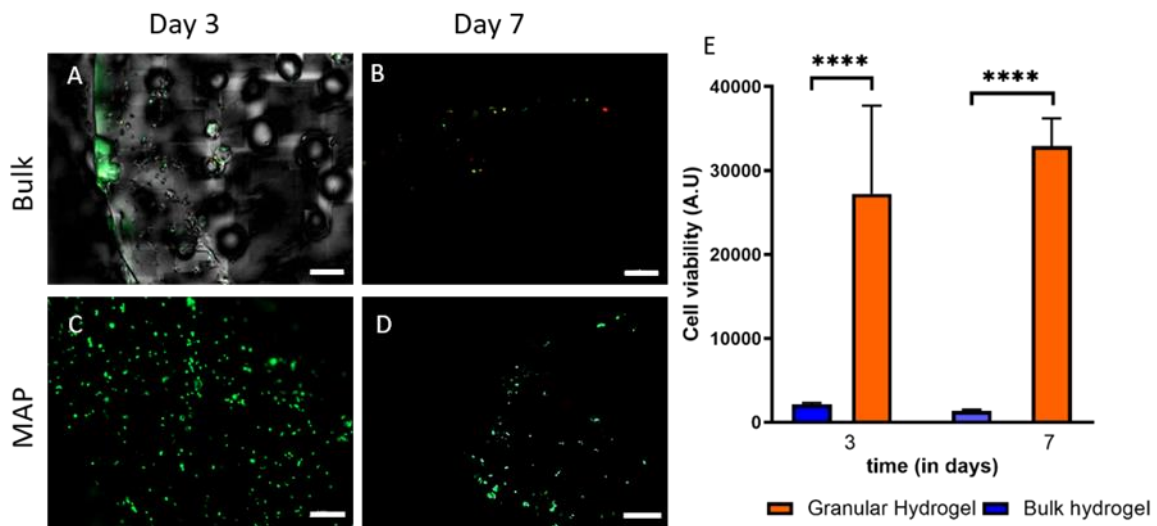
S 2 HMPs distribution through the different stirrings speed, and respective histograms of HMPs diameters distribution.



S 3 Distribution of the hydrogels microparticles through different concentrations and speeds. All the groups were statistically different with  $p < 0.0001$  with exception from the ones presented with, ns non statistically different and \*\*  $p < 0.01$ . Data is presented as at least 200 particles.



**S 4** ELISA-based quantification of VEGF release along time. Data is presented as mean  $\pm$  s.d., n=2.



**S 5** Live- dead staining, with a low cell density of HUVECs, where live cells are stained with calcein -channel, while dead cells are stained with PI – red chanel. A-B) Bulk hdyrogel and C-D) Gelatin-HPA Maps scaffolds at day 1 and 3. Scale bar : 200 $\mu$ m. E) AlamarBlue®-based cell viability with bulk hydrogel and MAPs scaffolds, at day 7. Data is presented as mean  $\pm$  s.d., n=3, \*\*\*\*p<0.0001.

## 6. Conclusion and future perspectives

Recently granular hydrogels are being proposed as an alternative to bridge key limitations of standard bulk hydrogels. Granular hydrogels are injectable scaffolds, able to mold to small defects, and the resulting the voids spaces between the HMPs present in MAPs scaffolds allows nutrients/metabolites diffusion rates similar those observed in tissues. There is no doubt that granular hydrogels and microporous annealed particles present significant advantages for future biomedical applications either in the context of biomolecules delivery and/or Tissue Engineering.

MAPs generally exhibit a high regenerative ability based on the facilitated cell infiltration into the microporous structure of these scaffolds. In addition, the possibility of being used as delivery vehicles for promoting bioactive molecules release, such as growth factors or small drugs, provides HMP and granular hydrogels with a vast range of applications. The ability to create new and more complex scaffolds by easily integrating different HMPs in their characteristics leads to an optimistic view for future endeavors. MAPs and granular hydrogels are also highly versatile, not only in the sense of introducing key chemical modifications to their building blocks, but also on the very nature of HMPs. The ability to inject via minimally invasive procedures and then assemble the MAPs scaffolds *in situ* provides an added degree of functionality and is of high value for TERM applications. The utilization of granular hydrogels as bioink in the context of extrusion-based 3D bioprinting also provides advantages in the sense that such HMPS have shown to protect cells from shear stress during extrusion which causes cell membrane damage. The ability to produce a single filament solely comprised by HMPs and cells, with high viability, also provides new opportunities for exploring the manufacture of advanced scaffolds based on MAPs.

However, until now no MAP was described to be suitable for annealing via different chemistries, in this case, enzymatic or photo-mediated annealing using the same chemical functionality. Here the HMPs production technologies were also adapted to use oil-free methodology, decreasing the environmental impact and reducing the possible cytotoxicity for cells. The MAP of gelatin-HPA developed also presented better mechanical characteristics than the others developed to date in the literature, particularly comparing with enzymatic annealing. The Gelatin-HPA MAP has shown potential for encapsulating bioactive molecules that may lead to a faster vascularization of the scaffold and



## CONCLUSION

---

consequently a fast tissue regeneration. The granular hydrogel annealing also showed to be suitable for 3D bioprinting without cell damage, maintaining cell survival.

The results obtained in the gelatin-HPA MAP are thus very promising, however, it would be interesting to analyze if HMPs triggers stem cells differentiation, and evaluate the cell behavior through time in an extended time frame. It would also be relevant to optimize the VEGF incorporation release, and later verify the pro-angiogenic potential of this scaffold by using chorioallantoic membrane (CAM) assays, to prove the ability to recruit blood vessels and fast penetration. Lastly it would be important to perform an *in vivo* assay to verify if the regenerative properties are like the other MAPs already developed.

The granular hydrogel of gelatin-OxLAM remains with several optimizations. This platform revealed a self-healing ability which is a very desirable feature for TERM. Nevertheless, this granular hydrogel appears to present good characteristics for 3D bioprinting. Lastly, it would be necessary to analyze the cytocompatibility of the granular hydrogel. Granular hydrogels, present several advantages for TERM and it is clear that they will have a key role in tissue regeneration.